Neurodegeneration induced by ß-synuclein in the context of the neurotransmitter dopamine

Dissertation

for the award of the degree

Doctor of Philosophy (Ph.D.)

Faculty of Biology

of the Georg-August-Universität Göttingen

submitted by

Anupam Raina

Born in

New Delhi, India

Göttingen 2019

Supervisor:

Dr. Sebastian Kügler	Department of Neurology University Medical Center Göttingen

Thesis committee:

Prof. Dr. Mathias Bähr	Department of Neurology University Medical Center Göttingen
Prof. Dr. Gerhard Braus	Department of Molecular Biology and Genetics Georg August University Göttingen
Prof. Dr. Tiago Fleming Outeiro	Department of Experimental Neurodegeneration University Medical Center Göttingen

Examination committee:

Prof. Dr. Thomas Dresbach	Department of Anatomy and Embryology University Medical Center Göttingen
Prof. Dr. Lutz Walter	Department of Primate Genetics German Primate Center

Date of disputation: April 8, 2019

Declaration

Hereby, I declare that this thesis entitled:

“Neurodegeneration induced by ß-synuclein in the context of the neurotransmitter dopamine”

has been written independently and with no other sources and aids than quoted.

Anupam Raina

Göttingen, February 2019

Dedicated to my loved one

Table of contents

List of figures

1. Abstract

Objective: α-synuclein and degeneration of dopaminergic neurons have been closely associated to Parkinson´s disease. The interaction of α-synuclein with the neurotransmitter dopamine has been connected to neurodegeneration, and suggested to be causatively involved in Parkinson´s disease (PD). Like α-synuclein, ß-synuclein is extensively expressed in the central nervous system. Recent findings in rodent models of PD suggest that ß-synuclein can aggregate and induce degeneration of dopaminergic neurons (Taschenberger et al. 2013). This suggests a link between ß-synuclein and the dopaminergic neurotransmitter phenotype that has not been investigated so far. Therefore, the objective of this thesis is to generate a robust cell-based model with dopaminergic neurotransmitter phenotype, and to study the neurodegeneration induced by ß-synuclein in the context of dopamine.

Methods: Primary cortical neurons, isolated from rat pups during embryonic development day 18, were used to develop the cell-based model with dopaminergic neurotransmitter phenotype. Two approaches were employed. In a transdifferentiation approach, transcription factors known to induce the dopaminergic neurotransmitter phenotype were expressed in cortical neurons. In the second approach, enzymes, substrates, and transporter proteins necessary to mimic the dopaminergic neurotransmitter phenotype, were introduced into cortical neurons. Neurotoxicity of α-synuclein, ß-synuclein, and γ-synuclein were comparatively elucidated in the developed cell-model.

Results: In the first approach to develop the cell-model by transdifferentiation, transcription factors Ascl1, Nurr1, and Lmx1a (“ANL”) induced the expression of classical dopaminergic neurotransmitter markers tyrosine hydroxylase (TH), aromatic

L-amino acid decarboxylase (AADC), vesicular monoamine transferase 2 (VMAT2), and dopamine transporter (DAT) in 15-22% of total cortical neurons. Results further revealed that “ANL” induced the dopaminergic neurotransmitter phenotype only in cortical GABAergic neurons. GABAergic neurons lost their GABA neurotransmitter-determining marker GAD65 by DIV 21, suggesting a true neuronal phenotype switch. However, “ANL” caused degeneration of glutamatergic neurons. Moreover, “ANL” was unable to transdifferentiate midbrain GABAergic neurons in culture. In conclusion, neuronal transdifferentiation was achieved in principle. However, due to low yield of desired neurons, and due to the profound loss of cells, the second approach was employed.

In the second approach to develop the cell-based model, AADC, VMAT2 and multiple doses of extracellular L-3,4-dihydroxyphenylalanine (L-DOPA) were introduced into the cortical neurons. This resulted in robust dopamine production. Results suggested that most of the dopamine was incorporated into and presumably released by glutamatergic vesicles in the cell culture supernatant due to endogenous electrical activity of cortical neurons. Similarly, the introduction of DAT, VMAT2, and multiple doses of extracellular dopamine dramatically enhanced the intracellular dopamine levels. In conclusion, a cell-model based on AADC-VMAT2-L-DOPA, and another cell-model based on DAT-VMAT2-dopamine were established.

Using the developed cell-models, it was found for the first time that dopamine aggravates neurotoxic properties of ß-synuclein, and to a similar extent, of α-synuclein. It has been reported that α-synuclein impairs endogenous network activity by decreasing the action potential frequency (Tolo et al. 2018). However, in this study, it was found that dopamine production in α-synuclein and ß-synuclein overexpressing cells does not impair the endogenous network activity *in vitro*. Furthermore, NMR

studies revealed that the binding affinity of dopamine with ß-synuclein is 10-100 fold less in comparison to the binding affinity of dopamine with α-synuclein, suggesting that ß-synuclein-dopamine binding might not be directly responsible for aggravated neurodegeneration.

Conclusion: The results in this study provide new perspectives on the neurodegeneration induced by ß-synuclein in the context of the neurotransmitter dopamine.

Introduction

2. Introduction

2.1 Parkinson´s disease: A neurodegenerative disorder

Parkinson´s disease (PD) is one of the most fast growing neurological disorders of the central nervous system. The number of people affected by PD is expected to double to a staggering 14.2 million by 2040 (Dorsey and Bloem 2018). PD affects 1-2% of all individuals over 65 years of age. There are no curative treatments available. The etiology of PD is not clear. Further understanding of biological mechanisms of PD at the cellular and molecular level is essential, and a need of the hour, to develop effective therapeutics.

2.2 Characteristics of Parkinson´s disease

2.2.1 Clinical features

Dr. James Parkinson first described the clinical symptoms of PD in 1817. Typical motor symptoms of PD include tremor at rest, bradykinesia, akinesia, postural instability, and rigidity and non-motor symptoms include mainly sleep disturbances, depression, constipation, anosmia (Barker and Williams-Gray 2016).

2.2.2 Pathophysiological features

Two major pathophysiological hallmarks are known for PD. In 1912, Frederik Lewy discovered protein aggregates in the cell bodies of neurons. These aggregates were named after him as Lewy bodies and Lewy neurites. Formation of Lewy bodies and Lewy neurites are the first pathophysiological hallmark. Konstantin Tretiakoff in 1919 suggested that the pathological feature of PD could be the loss of mostly dopaminergic neurons from the substantia nigra. This theory was accepted after decades and is

considered as one of the pathological hallmarks of PD (Drew 2016). In 1997, Spillantini and colleagues reported for the first time that the primary constituent of Lewy bodies is the misfolded protein α-synuclein (Spillantini et al. 1997). Therefore, the two major pathophysiological hallmarks of PD are the progressive loss of mostly dopaminergic neurons in the substantia nigra, and the formation of Lewy bodies and Lewy neurites majorly composed of the protein α-synuclein.

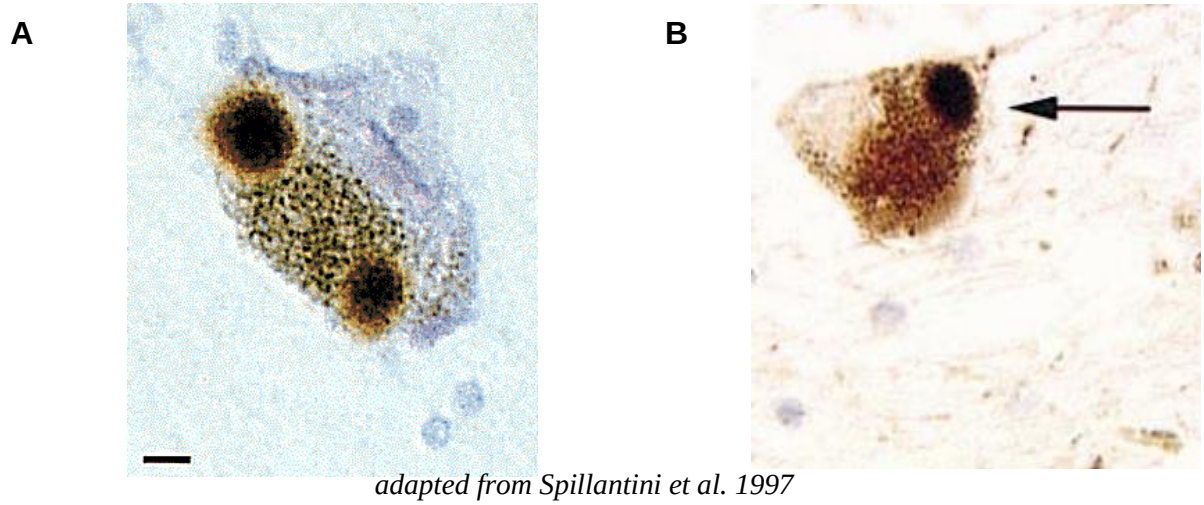

adapted from Spillantini et al. 1997

Figure 2.1. Lewy bodies in neurons.

(A) Pigmented neuron with two Lewy bodies immunopositive for α-synuclein.

(B) Lewy body in pigmented neurons of substantia nigra immunopositive for α-synuclein.

In addition to α-synuclein, Lewy bodies and Lewy neurites are comprised of 14-3-3 chaperon-like protein (Kawamoto et al. 2002), synphilin-1 (Wakabayashi et al. 2000), ubiquitin (Uryu et al. 2006).

2.3 The synuclein protein family

Synucleins are natively unfolded proteins that possess very little or no ordered structure under physiological conditions (Uversky 2008). The synuclein family consists of three proteins: α-synuclein, ß-synuclein, and γ-synuclein.

SNCA gene lies on chromosome 4 and encodes α-synuclein that is a 140 aminoacid protein (Campion et al. 1995). Three missense mutations (A30P, A53T, E46K) of SNCA gene with high penetrance had been identified as the first genetic evidence of the involvement of α-synuclein gene in PD (Kruger et al. 1998; Polymeropoulos et al. 1997; Zarranz et al. 2004). SNCB gene lies on chromosome 5 and codes for ß-synuclein that is a 134 aminoacid protein (Spillantini, Divane, and Goedert 1995). Two ß-synuclein mutations, V70M and P123H, were identified in highly conserved regions of ß-synuclein (Ohtake et al. 2004). These mutations were suggested to be linked to dementia with Lewy bodies. SNCG gene lies on chromosome 10 and codes for γ-synuclein that is a 127 aminoacid protein (Lavedan et al. 1998). The overexpression of γ-synuclein in transgenic mice is linked to degeneration of motor neurons (Ninkina et al. 2009). Mutated forms of γ-synuclein are not reported so far.

The proteins consist of three regions: N-terminal region, non-amyloid ß component domain (NAC), and C-terminal region. The highly conserved N-terminal region is amphipathic and rich in lysines, and contains 5 - 7 imperfect motif repeats of KTKEGV that is known to bind to membranes to form α-helices (Ulmer et al. 2005). NAC domain is rich in hydrophobic residues, and is supposed to be responsible for α-synuclein aggregation (Hashimoto et al. 2000; Spillantini et al. 1997; Ueda et al. 1993). In ß-synuclein, NAC domain lacks 11 residues (71-82) that are known to be crucial for α-synuclein oligomerization. In γ-synuclein, the NAC domain is not identical to α-synuclein as it is less hydrophobic than the NAC domain of α-synuclein (Surguchov

2013). C-terminal region is negatively charged, highly disordered, and is known to bind metals, small molecules, and proteins (Ulmer et al. 2005).

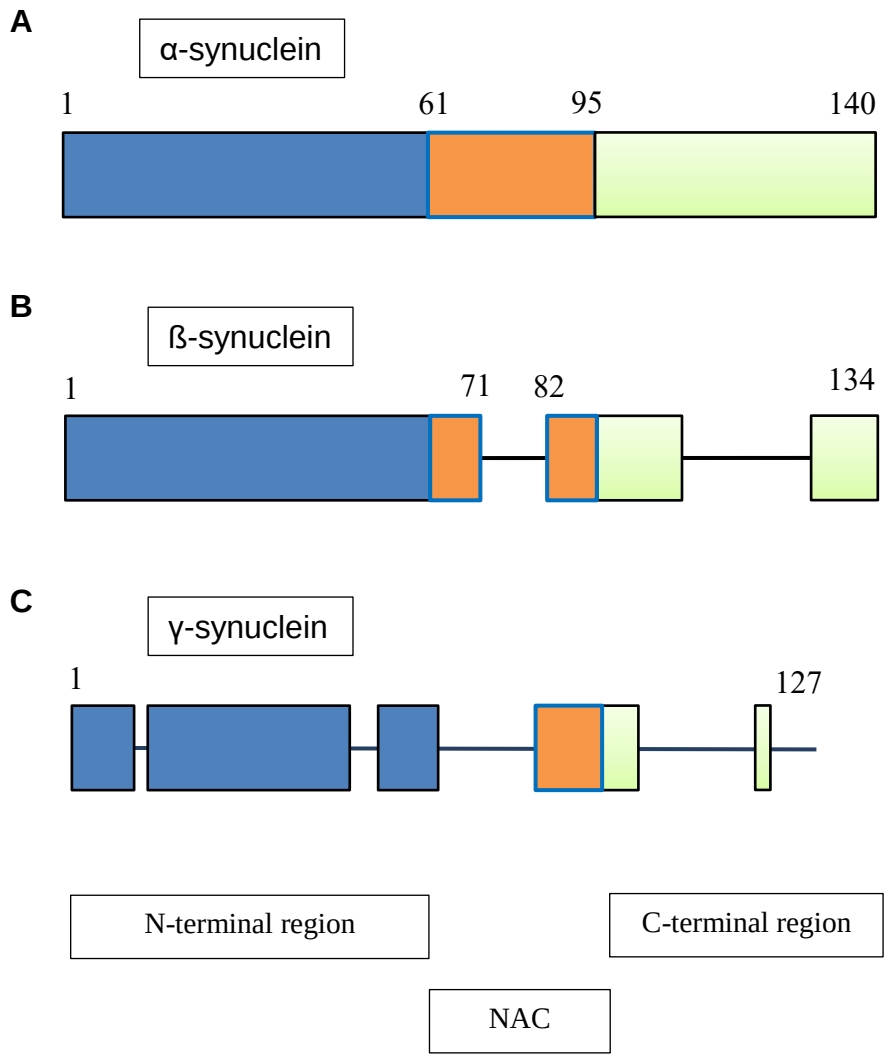

Figure 2.2. The synuclein protein family.

(A) *α-synuclein:* 140 amino acids long, highly conserved N-terminal region (1-61), NAC domain (61-95), and C-terminal region (95-140).

(B) *ß-synuclein:* 134 amino acids long, highly conserved N-terminal region, lacks 11 residues in the NAC domain, and least conserved C-terminal region.

(C) *γ-synuclein:* 127 amino acids long, less conserved N-terminal region, less hydrophobic NAC domain, and least conserved C-terminal region.

2.3.1. Physiological roles of synucleins

α-synuclein and ß-synuclein are mainly expressed in the central nervous system and γ-synuclein is mainly expressed in the peripheral nervous system. The physiological roles of synucleins are not clearly defined. There are studies performed which suggest their role in different cellular processes. α-synuclein and ß-synuclein are presynaptic proteins that suggests their association with synaptic vesicles (Kahle et al. 2000; Lee, Jeon, and Kandror 2008; Zhang et al. 2008; Chandra et al. 2004). α-synuclein controls vesicles exocytosis by directly interacting with phospholipase D2 (Payton et al. 2004). It is reported that α-synuclein can act as a chaperone protein for presynaptic SNARE protein, which is involved in the neurotransmitter dopamine release (Burre et al. 2010). α-synuclein interacts with target membrane- and vesicle-associated SNARE proteins, and therefore affects vesicle recycling, stability of target membrane-associated SNARE complexes, and the neurotransmitter release, like dopamine (Lashuel et al. 2013; Scott et al. 2010).

2.3.2. α-synuclein and neurodegeneration

The reason for progressive degeneration of dopaminergic neurons is not clear. After 21 years of research, the precise mechanism of action of α-synuclein mediated neurodegeneration is not fully understood.

α-synuclein is an unfolded monomer which tends to aggregate. In the process of α-synuclein aggregation and fibrillogenesis, the α-synuclein oligomers and amyloid fibrils are known to be toxic and may induce mitochondrial dysfunction, disrupt ER-Golgi trafficking, inhibit autophagy and proteasome pathways, and disrupt synaptic transmission (Lashuel et al. 2013). The toxic cytosolic ring-like α-synuclein oligomers may also disrupt membrane integrity and disturb intracellular calcium homeostasis

(Danzer et al. 2007). The toxic α-synuclein oligomeric forms cause toxicity by causing insults on mitochondria (Hsu et al. 2000), lysosome (Hashimoto, Kawahara, et al. 2004), and microtubules (Alim et al. 2004). The α-synuclein oligomers are also known to affect axonal transport of synapsin 1, resulting in non-functional synapses (Scott et al. 2010). Furthermore, our group reported that overexpression of α-synuclein in cultured cortical neurons lead to cell death by increase in mitochondrial thiol oxidation, outer mitochondrial membrane permeabilization, and activation of caspases (Tolo et al. 2018). It is interesting to learn new mechanisms of neurodegeneration. However, the question why mostly dopaminergic neurons are degenerated in Parkinson´s disease remains to be answered.

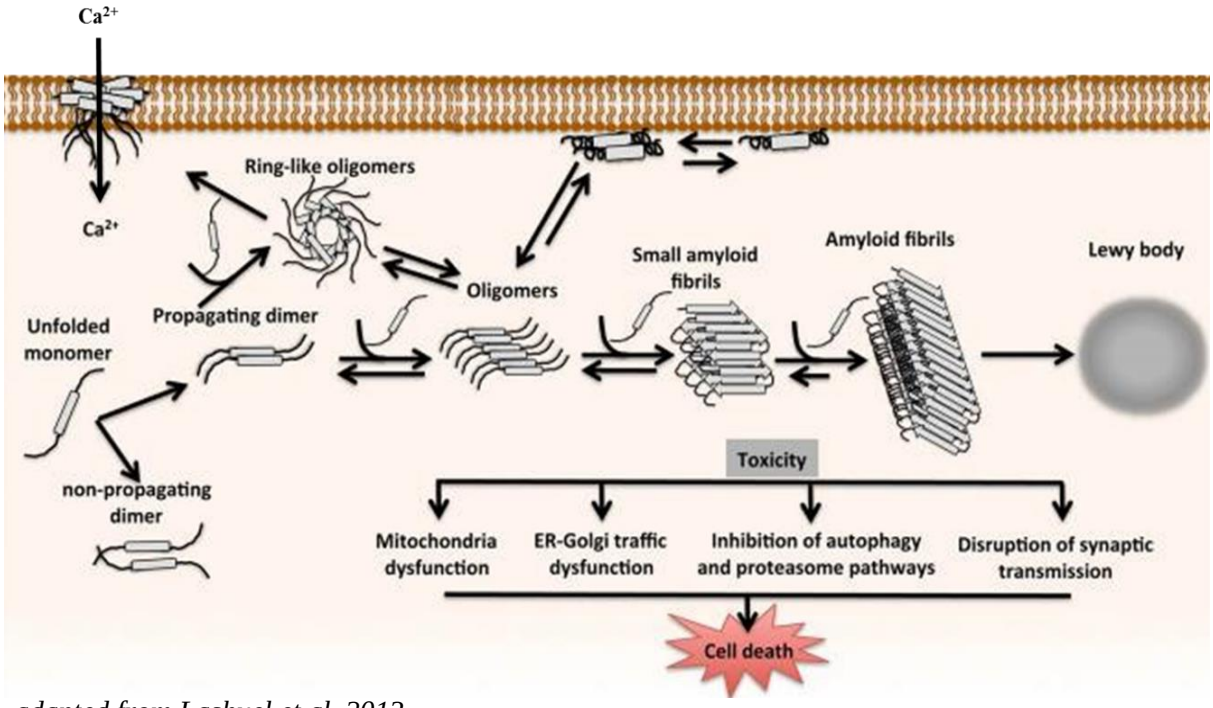

adapted from Lashuel et al. 2013

Figure 2.3. Mechanisms through which α-synuclein aggregates and causes toxicity (Lashuel et al. 2013)

The unfolded α-synuclein monomer dimerizes to form ring-like oligomers that may form pore-like structures resulting in the influx of Ca^{2+} ions. The propagating dimer might oligomerize with α-synuclein monomer forming oligomers. Small oligomers further oligomerize to form amyloid fibrils that aggregate to form Lewy body. The intermediate α-synuclein oligomeric forms are known to be toxic to neurons.

α-synuclein has been intimately linked to Parkinson´s disease because α-synuclein rich Lewy bodies and Lewy neurites are also detected in dopaminergic neurons in substantia nigra. Although the mechanism of degeneration of mostly dopaminergic neurons is not clear so far, dopaminergic neurons exhibiting Lewy body pathology suggests a strong link between α-synuclein and the neurotransmitter dopamine.

2.4 Dopamine and α-synuclein

The interaction of dopamine to α-synuclein is known to affect the structural organization and aggregation propensities of α-synuclein. Dopamine can readily oxidize to dopamine quinone species, hydrogen peroxide, and other electrophiles at cytosolic pH (Graham 1978; Jenner and Olanow 1996; Sulzer and Zecca 2000). Conway and colleagues were the first to show in cell-free solution that oxidized dopamine can interact with α-synuclein oligomers and kinetically stabilize them resulting in the accumulation of protofibrils (Conway et al. 2001). 4 years later, Norris and colleagues showed that oxidized form of dopamine (dopaminochrome) interacts with the C-terminal region of α-synuclein ^{125}YEMPS^{129}, which inhibits α-synuclein fibrillization (Norris et al. 2005). This interaction was found to be non-covalent and reversible. Mutation or deletion of ^{125}YEMPS^{129} motif restores the ability of α-synuclein to fibrillize (Norris et al. 2005). 4 years later, Herrera and colleagues demonstrated that a point mutation, E83A, in the NAC domain prevents dopamine to inhibit α-synuclein fibrillization (Herrera et al. 2008). These reports strongly suggest that dopamine oxidation is required for kinetic arrest of α-synuclein protofibrils. The mechanism, through which dopamine-α-synuclein adducts cause toxicity in a neuronal cell, is unexplored. Some *in vitro* studies revealed that dopamine-α-synuclein adducts inhibit the formation of SNARE, neurotransmitter release (Choi et al. 2013), and prevent degradation by chaperone-mediated autophagy (Martinez-Vicente et al. 2008).

With increasing *in vitro* evidences that dopamine inhibits α-synuclein fibrillization, very few groups have explained if this mechanism also takes place *in vivo*. To study this mechanism *in vivo*, Mor and colleagues, targeted a Lentiviral vector to substantia nigra expressing a mutated (R37E and R38E) form of tyrosine hydroxylase. Tyrosine hydroxylase is a rate-limiting enzyme for dopamine biosynthesis. The mutated form (TH-RREE) of tyrosine hydroxylase is devoid of feedback inhibition by dopamine. As a result, there was increased (up to 50% more) dopamine biosynthesis in substantia nigra. When TH-RREE was expressed in non-transgenic mice, 5 months post injection (5 mpi) there was no neurotoxicity observed. Interestingly, dopamine transporter was found to be upregulated, which suggests that cells protect themselves by tweaking the dopamine metabolic systems (Mor et al. 2017).

Next, they increased dopamine levels in mice expressing human α-synuclein with A53T familial PD mutation. By 5 mpi, 62% of dopaminergic synapses were lost, and there was 25% decrease in the cell bodies in substantia nigra as compared with control vector-injected A53T mice. This indicated that the increased dopamine biosynthesis aggravated α-synuclein neurotoxicity in cells (Mor et al. 2017). It was suspected that oxidized dopamine might interact with α-synuclein motif ^{125}YEMPS^{129}, as this was observed *in vitro* (Conway et al. 2001; Herrera et al. 2008; Norris et al. 2005).

In an attempt to understand the mechanism of neurotoxicity, Mor and colleagues used model organism *Caenorhabditis elegans*. The ^{125}YEMPS^{129} motif of A53T α-synuclein was mutated to ^{125}FAAFA^{129} and expressed along with increased dopamine levels in dopaminergic neurons. Interestingly, they found that enhanced dopamine production in A53T α-synuclein expressing worms did not result in neurotoxicity. This suggested that the interaction of dopamine with the ^{125}YEMPS^{129} motif on C-terminal region of α-synuclein was responsible to induce neurodegeneration *in vivo* (Mor et al. 2017).

After confirming that dopamine interacts with the ^{125}YEMPS^{129} motif on C-terminal region of α-synuclein, Mor and colleagues extracted substantia nigra from increased dopamine producing A53T mice and control A53T mice and characterized α-synuclein species using size-exclusion chromatography and sodium dodecyl sulfate polyacrylamide gel electrophoresis. Results suggested that dopamine increased the steady-state level of α-synuclein oligomers (Mor et al. 2017). These reports confirm that dopamine induces neurodegeneration *in vivo* by directly interacting with ^{125}YEMPS^{129} motif in α-synuclein, thereby stabilizing the α-synuclein oligomeric species, and providing a link between dopamine toxicity and α-synuclein aggregation (Mor et al. 2017).

2.5. Dopamine and ß-synuclein

There is no genetic link between ß-synuclein and PD described so far, and ß-synuclein is not detected in Lewy bodies and Lewy neurites. ß-synuclein is present in similar levels as α-synuclein in the presynaptic nerve termini in the central nervous system (Mori et al. 2002).

ß-synuclein and α-synuclein share a 78% sequence homology. There are more negatively charged residues in the C-terminus of ß-synuclein than α-synuclein, but ß-synuclein lacks 11 residues in the NAC domain that are known to promote oligomerization in α-synuclein.

ß-synuclein has been shown to have a potential to confer neuroprotection against α-synuclein in different experimental set-ups *in vitro* and *in vivo*. The α-ß-synuclein bigenic mice had reduced neurodegenerative effects as compared to α-synuclein mice (Hashimoto et al. 2001). Furthermore, Hashimoto and colleagues demonstrated that ß-synuclein coimmunoprecipitates with α-synuclein and inhibits α-synuclein

aggregation in dose-dependent manner *in vitro*. The mechanism of neuroprotection is being widely studied. Recent studies in cell-free solution by Leitao and colleagues suggest that ß-synuclein inhibits α-synuclein aggregation by incorporating into α-synuclein oligomers (Leitao et al. 2018). The α-synuclein oligomers can act as a template to seed the nucleation of free monomers through surface interaction between oligomers and free α-synuclein monomers. This process is called as autocatalytic surface interactions. Brown and colleagues determined that ß-synuclein competes for the binding of α-synuclein monomers to α-synuclein oligomers, thereby inhibiting the autocatalytic surface interactions (Brown et al. 2016).

Until 2012, ß-synuclein was considered as nonamyloidogenic. In 2013, our group reported that *in vivo* ß-synuclein forms proteinase K resistant aggregates, similar to α-synuclein, suggesting that ß-synuclein is amyloidogenic (Taschenberger et al. 2013). Recently it was reported that the fibrillation propensity of ß-synuclein also depends on the pH. Moriarty and colleagues found that ß-synuclein fibrillates at acidic pH 5.8, but not at pH 7.3. The N-terminal domain of ß-synuclein is 90% identical to α-synuclein. When ß-synuclein contained the N-terminal domain of α-synuclein, ß-synuclein lost its ability to fibrillate, even at pH 5.8 (Moriarty et al. 2017), suggesting that N-terminal domain of ß-synuclein is important for fibrillation of ß-synuclein. The NAC domain of ß-synuclein lacks 11 residues found in the NAC domain of α-synuclein. When α-synuclein contained the NAC domain of ß-synuclein, the chimeric (α-synuclein + NAC domain of ß-synuclein) synuclein fibrillated only at acidic pH 5.8 (Moriarty et al. 2017), suggesting that ß-synuclein fibrillates at pH 5.8 due to its NAC domain. Interestingly, Moriarty and colleagues also showed that a point mutation of glutamic acid to alanine (E61A) resulted in robust and rapid fibrillation of ß-synuclein and α-synuclein at both pH 5.8 and 7.3, suggesting that residue glutamic acid at 61 position in ß-synuclein is crucial for its fibrillation. The C-terminal domain, which has the lowest sequence

similarity to α-synuclein, was not found to be involved in ß-synuclein fibrillation (Moriarty et al. 2017).

ß-synuclein is known as a component of axonal lesions in hippocampus associated with DLB and PD (Galvin et al. 1999). The DLB-linked P123H mutation of ß-synuclein causes progressive neurodegeneration in transgenic mice, which is aggravated when crossed with α-synuclein transgenic mice (Fujita et al. 2010). The bigenic mice (α-synuclein/P123H ß-synuclein) showed enhanced loss of tyrosine hydroxylase, L-DOPA decarboxylase (AADC), dopamine transporter (DAT), and 40% reduction in dopamine concentration (Fujita et al. 2010). P123H mutation in ß-synuclein may disturb the polyproline II helix making the C-terminal region of mutant ß-synuclein more flexible like in α-synuclein (Bertoncini et al. 2007), causing it to misfold and aggregate α-synuclein (Fujita et al. 2010). In 2013, our group, Taschenberger and colleagues, reported that ß-synuclein degenerated nigral dopaminergic neurons, similar to α-synuclein, in rodent models of PD (Taschenberger et al. 2013). α-synuclein, ß-synuclein, γ-synuclein, and enhanced green fluorescent protein (EGFP) were expressed by adeno-associated viral vectors in rat substantia nigra. Vesicular monoamine transporter 2 (VMAT2) positive cells were counted. At 8th week after injection, ß-synuclein induced neurodegeneration in 45% of dopaminergic neurons, which was found to be similar to α-synuclein induced neurodegeneration (Taschenberger et al. 2013). Dopaminergic neurons were not lost in EGFP and γ-synuclein expressing cells. The results suggested that not only α-synuclein, but also ß-synuclein should be considered as a toxic molecule in PD, DLB, and other synucleinopathies (Taschenberger et al. 2013).

As ß-synuclein induced neurodegeneration of nigral dopaminergic neurons, it strongly indicated to a connection between ß-synuclein and the neurotransmitter dopamine,

which has not been investigated so far. Therefore, the aim of this thesis is to investigate the neurotoxicity of ß-synuclein in the context of the neurotransmitter dopamine.

In order to study the neurodegeneration induced by ß-synuclein in the context of dopamine, a robust dopamine producing cell-based model is very essential. There are few *in vitro* cell-based models developed for Parkinson´s disease.

2.6. Cell-based models for PD

Phaeochromacytoma (PC12) cells are derived from rat adrenal medulla (Greene and Tischler 1976). PC12 cells do not originate from the CNS. Although PC12 cells can be differentiated into non-dividing cells, they still have cancerogenous properties, and have a physiology that is very different from normal cells in tissue (Hyman and Simons 2011). MN9D is another cell-line in use. It is derived from mice by the fusion of ventral mesencephalic cells and neuroblastoma cells. MN9D cells expressed TH, voltage-dependent sodium channels, and synthesized dopamine (Choi et al. 1992). However, they were reported to lack electrical activity of “dopaminergic neuron-like cells” (Rick et al. 2006). Another cell-line commonly used is SH-SY5Y that mimics dopaminergic neurons. This cell-line is a sub-clone of a clone isolated from a neuroblastoma bone marrow biopsy (Biedler, Helson, and Spengler 1973). It is difficult to differentiate into dopaminergic cells and they originate from a cancerogenous tissue. However, it is reported that TH and AADC could not be detected in this cell-line, and cannot be used as a cell-based model for PD research (Xie, Hu, and Li 2010).

Primary midbrain cells isolated from ventral mesencephalon of mouse or rat pups at embryonal development day 12-15 are used. These cultures contain only 5 – 10% of dopaminergic neurons in a pool of GABAergic cells, and are short-lived (Yan, Studer, and McKay 2001; Prasad et al. 1994).

Another dopaminergic cell-model widely used for PD research is Lund Human Mesencephalic cells (LUHMES). LUHMES cell-line was developed when *v-myc* was introduced to immortalize 2-month-old fetal human ventral mesencephalic cells (Scholz et al. 2011; Lotharius et al. 2005). It was shown that human-derived LUHMES cells could be differentiated to post-mitotic neurons within 5 days in the presence of tetracycline that turns off *myc* oncogene (Scholz et al. 2011). It is reported that during the process of differentiation of LUHMES cells, dopaminergic markers TH, AADC, receptor tyrosine kinase, and DAT were expressed (Scholz et al. 2011). The expression required the presence of dibutryl cyclic adenosine monophosphate (cAMP) and glial cell derived neurotrophic factor (GDNF) in the cell culture medium. LUHMES were also demonstrated to have electrophysiological properties. The intracellular dopamine was detected to be less than 0.2 nanograms (per 10,000 cells) (Scholz et al. 2011). Even though LUHMES differentiate into “dopaminergic neuron-like cells”, they are originated from non-neuronal cells immortalized by *v-myc* oncogene and they are difficult to maintain *in vitro* for longer duration.

The discovery that forced expression of transcription factors to reprogram human fibroblasts into induced pluripotent stem cells (iPSCs) revolutionized regenerative medicine (Takahashi and Yamanaka 2006). Human derived induced pluripotent stem cells (hiPSCs) are used widely in PD research in recent years as they carry the genetic make-up of the patients. Human iPSCs can be differentiated into dopaminergic neurons using different protocols (Arenas, Denham, and Villaescusa 2015). Interestingly, forced expression of transcription factors converted fibroblasts (Caiazzo et al. 2011) and hiPSCs (Theka et al. 2013) into dopaminergic neurons (iDA). The transcription factors used were Ascl1: *Achaete-scute homolog 1;* Lmx1a: *LIM homeobox transcription factor 1, alpha;* Nurr1: *Nuclear Receptor Related 1.* The iDA neurons were also generated by ectopic expression of Nurr1 and Pitx3: *Pituitary*

homeobox 3 in mouse iPSCs (Salemi et al. 2016). It was interesting to learn that dopaminergic neurotransmitter phenotype determining transcription factors involved Lmx1a, Nurr1, and Pitx3. It is reported that Lmx1a is central and acts as a core component for determining dopaminergic phenotype by forming an Lmx1a-Wnt1-ß-catenin autoregulatory loop (Chung et al. 2009; Andersson et al. 2006). Additionally, Lmx1a upregulates Nurr1 and Pitx3, and Nurr1 and Pitx3 in turn regulate the expression of dopaminergic neurotransmitter battery of genes (Arenas, Denham, and Villaescusa 2015). In contrast, Ascl1 is a pan-neuronal marker that is not involved in dopaminergic fate determination. Ascl1 is known to play a pivotal role in transdifferentiation, that is, to convert mouse fibroblasts into induced neurons (Vierbuchen et al. 2010) by acting as a pioneer transcription factor (Wapinski et al. 2013). In spite of the recent advances, the number of dopaminergic neurons obtained *in vitro* by transdifferentiation or patterning and differentiation vary from 7 – 70%, and the dopamine production reported from different protocols is also variable (Marton and Ioannidis 2018; Arenas, Denham, and Villaescusa 2015).

In contrast, the cortical neurons from rodent embryos can be readily isolated in very large amounts. These neurons survive in culture for several weeks, show endogenous non-stimulated neuronal network activity, and are a reliable and valuable cellular model for neurobiological studies. It has not been investigated so far, if postnatal cortical neurons can be experimentally prompted to switch their neurotransmitter phenotype to another neurotransmitter phenotype of interest. Using the knowledge gained from the existing cell-based models, and the recent progresses made in the field of regenerative medicine, a transdifferentiation strategy was devised to induce the dopaminergic neurotransmitter phenotype in readily available rat cortical neurons with an objective to generate a large number of neurons with the dopaminergic neurotransmitter phenotype.

To develop a dopaminergic cell-based model through transdifferentiation strategy, the transcription factors Ascl1, Nurr1, Lmx1a, and Pitx3 were introduced into rat cortical neurons at embryonal development day 18. Results suggested that Ascl1, Nurr1, and Lmx1a transdifferentiated only cortical GABAergic neurons to dopaminergic neurons with the upregulation of classical dopaminergic markers TH, AADC, VMAT2, and DAT. Due to low yield of dopaminergic neurons and profound loss of cells that were unable to transdifferentiate, an alternate experimental paradigm was exploited. In this approach AADC, VMAT2, L-3,4-dihydroxyphenylalanine (L-DOPA) or DAT, VMAT2, dopamine were introduced into cortical neurons to mimic the dopaminergic neurotransmitter phenotype. As a result, robust dopamine production and enhanced intracellular dopamine levels were achieved. Using the cell-based model, which mimics the dopaminergic neurotransmitter phenotype, it was found for the first time that dopamine aggravated the neurotoxic properties of ß-synuclein, and to a similar extent, of α-synuclein. NMR studies revealed that dopamine might not be directly involved in aggravating neurotoxicity of ß-synuclein. Taken all together, the results of this thesis provide new perspectives on the neurodegeneration induced by ß-synuclein in the context of the neurotransmitter dopamine.

2.7. Aim of the thesis

To generate a robust cell-based model with dopaminergic neurotransmitter phenotype, and to study the neurodegeneration induced by ß-synuclein in the context of dopamine.

2.7.1. Objectives

- To generate a dopaminergic cell-based model by inducing dopaminergic neurotransmitter phenotype using a transdifferentiation approach: introduction of transcription factors Ascl1, Lmx1a, Nurr1, and Pitx3 into rat cortical neurons isolated at embryonal day of development 18.

- To generate a dopaminergic cell-based model by mimicking the dopaminergic neurotransmitter phenotype: introduction of AADC, VMAT2, and extracellular L-DOPA or DAT, VMAT2, and extracellular dopamine into rat cortical neurons isolated at embryonal day of development 18.

- To study the neurotoxicity induced by ß-synuclein in a cell-based model with dopaminergic neurotransmitter phenotype.

Results

3. Results

3.1 Primary approach to develop a dopaminergic cell-model by transdifferentiating primary cortical neurons using transcription factors

Transcription factors, Ascl1: *Achaete-scute homolog 1,* Lmx1a: *LIM homeobox transcription factor 1, alpha,* Nurr1: *Nuclear Receptor Related 1 and* Pitx3: *Pituitary homeobox 3,* were employed to transdifferentiate primary cortical neurons isolated at day 18 (E18) from rat embryos.

3.1.1 Endogenous levels and overexpression of transcription factors in primary cortical neurons

In order to determine the time-point of the introduction of transcription factors into cortical neurons, the endogenous levels of Nurr1, Ascl1, Lmx1a, and Pitx3 were analyzed.

Cortical neurons were isolated from E18 rat embryos and plated on poly-L-ornithine and laminin-coated wells (150,000 cells/well). Western blot of the cell lysates was performed at day *in vitro* (DIV) 0, 2, 4, 7, 9, 11, 14.

Results indicated that Nurr1 peaked at DIV 4 and Lmx1a peaked at DIV 7 (**Fig.3.1.A**). The endogenous Ascl1 was sparingly detected until DIV 9 in primary cortical neurons (**Fig.3.1.A**). Furthermore, Pitx3 was endogenously expressed (**Fig.3.1.A**) consistently until DIV 14. The results indicated that at DIV 0, the endogenous levels of Ascl1, Nurr1, and Lmx1a were low; however, Pitx3 expressed consistently until DIV 14. It was hypothesized that an early introduction of transcription factors will allow efficient transdifferentiation of cortical neurons. Therefore, DIV 0 was determined to be an ideal

time-point to introduce Nurr1, Ascl1, Lmx1a, and Pitx3. In order to determine if the introduced transcription factors can be detected in cortical neurons, the next objective was to establish the overexpression pattern of Nurr1, Ascl1, Lmx1a, and Pitx3.

Monocistronic adeno-associated virus vectors with neuron-specific human synapsin 1 gene promoter (Kugler et al. 2003) drove the overexpression of transcription factors Ascl1, Nurr1, Lmx1a, and Pitx3 in rat E18 primary cortical neurons (**Fig.3.1.B**). AAV serotype 6 (AAV-6) was used. Primary cortical neurons were isolated from E18 rat embryo and plated on poly-L-ornithine and laminin-coated wells on a 24-well plate. AAV-6 vectors expressing Ascl1, Nurr1, Lmx1a, and Pitx3 were introduced into primary cortical neurons at day *in vitro* (DIV) 0.

Western blot analysis revealed that anti-Nurr1, anti-Ascl1, and anti-Lmx1a antibody detected a robust overexpression of Nurr1 (**Fig.3.1.C**), Ascl1 (**Fig.3.1.D**), and Lmx1a (**Fig.3.1.E**) respectively, in cultured cortical neurons. Overexpression of Pitx3 was not achieved in cortical neurons because Pitx3 was endogenously expressed (**Fig.3.1.A**) consistently until DIV 14. When Pitx3 was tagged with an AU1 tag at the N-terminus of Pitx3, anti-AU1 antibody detected the expression levels of AU1-Pitx3 achieved by the transgene (**Fig.3.1.F**).

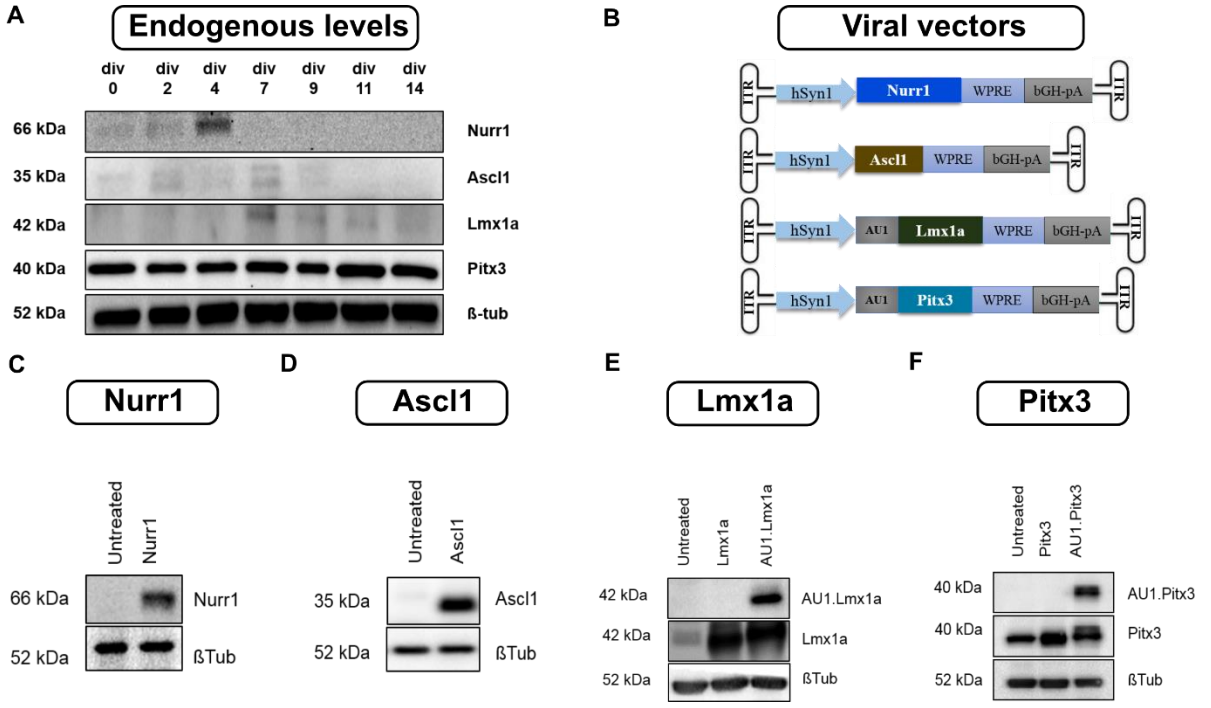

Figure 3.1. Endogenous levels and overexpression of transcription factors in rat primary cortical neurons.

(A) *Endogenous levels of Nurr1, Ascl1, Lmx1a, and Pitx3.* The endogenous levels of Nurr1, Ascl1, Lmx1a, and Pitx3 in cortical neurons were detected by anti-Nurr1, anti-Ascl1, anti-Lmx1a, and anti-Pitx3 antibody using Western blot.

(B) *Monocistronic AAV vector genomes encoding Nurr1, Ascl1, Lmx1a, and Pitx3.* The expression of Nurr1, Ascl1, Lmx1a, and Pitx3 was driven by human synapsin 1 promoter. WPRE: woodchuck hepatitis virus post-transcriptional control element, bGH-pA: bovine growth hormone fused to poly adenylation site, AU1: AU1 epitope tag, hSyn1: human synapsin 1 gene promoter, ITR: inverted terminal repeat.

(C, D, E, F) *Overexpression of transcription factors after 7 days post-transduction (dpt), DIV 7:* **(C)** The anti-Nurr1 antibody detected the overexpression of Nurr1; **(D)** the anti-Ascl1 antibody detected the overexpression of Ascl1. **(E)** the anti-AU1 and anti-Lmx1a antibody detected the overexpression of AU1.Lmx1a and Lmx1a respectively; **(F)** the anti-AU1 and anti-Pitx3 antibody detected the expression of AU1.Pitx3 and Pitx3, respectively. Western blots were normalized to ß-tubulin expression at the respective time-points.

Dr. Sebastian Kügler, Monika Zebski and Sonja Heyroth produced viruses (AAVs). Monika Zebski cloned the AAV vector genomes with AU1 tagged transcription factors. Department of Neurology, University Medical Center Goettingen (UMG).

Summary: Primary cortical neurons at DIV 0 was determined to be an ideal time-point to introduce Nurr1, Ascl1, and Lmx1a. AAV-6 vectors robustly overexpressed Ascl1, Nurr1, and Lmx1a in primary neurons. The anti-AU1 antibody detected the expression of AU1-Pitx3; however, the Pitx3 overexpression was not achieved due to endogenously expressed Pitx3 in primary cortical neurons. If the overexpression of Ascl1, Nurr1, Lmx1a ("ANL") induced dopaminergic phenotype in cortical neurons, remained to be elucidated.

3.1.2. Ascl1, Nurr1, and Lmx1a ("ANL") induce the expression of tyrosine hydroxylase in cortical neurons

After it was clear that "ANL" overexpressed in cortical neurons, the next objective was to overexpress transcription factors in different combinations to determine which combination induced the expression of dopaminergic marker, tyrosine hydroxylase (TH), in primary cortical neurons.

Primary cortical neurons were isolated from E18 rat embryos and plated on coverslips coated with poly-L-ornithine and laminin on a 24-well plate (150,000 cells/well). AAV-6 vectors with neuron-specific hSyn1 gene promoter (Kugler et al. 2003) expressing Ascl1, Nurr1, Lmx1a, and Pitx3 (22.5×10^8 vector genomes (vg)/150,000 cells) were introduced into cortical neurons at DIV 0 in different combinations (**Fig.3.2.A**).

ICC results suggested that the combination of transcription factors Ascl1, Nurr1, and Lmx1a ("ANL") induced the expression of TH (**Fig.3.2.B**). At DIV 7 (**Fig.3.2.C**), the combination of "ANL" resulted in 3-8% of TH positive neurons. Nurr1 alone was able to induce TH expression in 1-2% of cortical neurons unlike other transcription factors expressing alone. At DIV 14 (**Fig.3.2.C**), the combination of Ascl1 and Nurr1 (AN) was sufficient to induce the expression of TH. The expression of "ANL" resulted in 10-18% of TH positive neurons. At DIV 21 (**Fig.3.2.C**), the combination of AN resulted in 5-20% and "ANL" resulted in 15-24% of TH positive neurons. Furthermore, "ANL" overexpressing neurons were less in number as compared to the untreated neurons (**Fig. 3.2.B**). Overall, the results suggested that the yield of TH positive neurons after Ascl1 and Nurr1 overexpression was less than 25%. The introduction of Pitx3 alone and in combinations with "ANL" did not induce TH expression (data not shown).

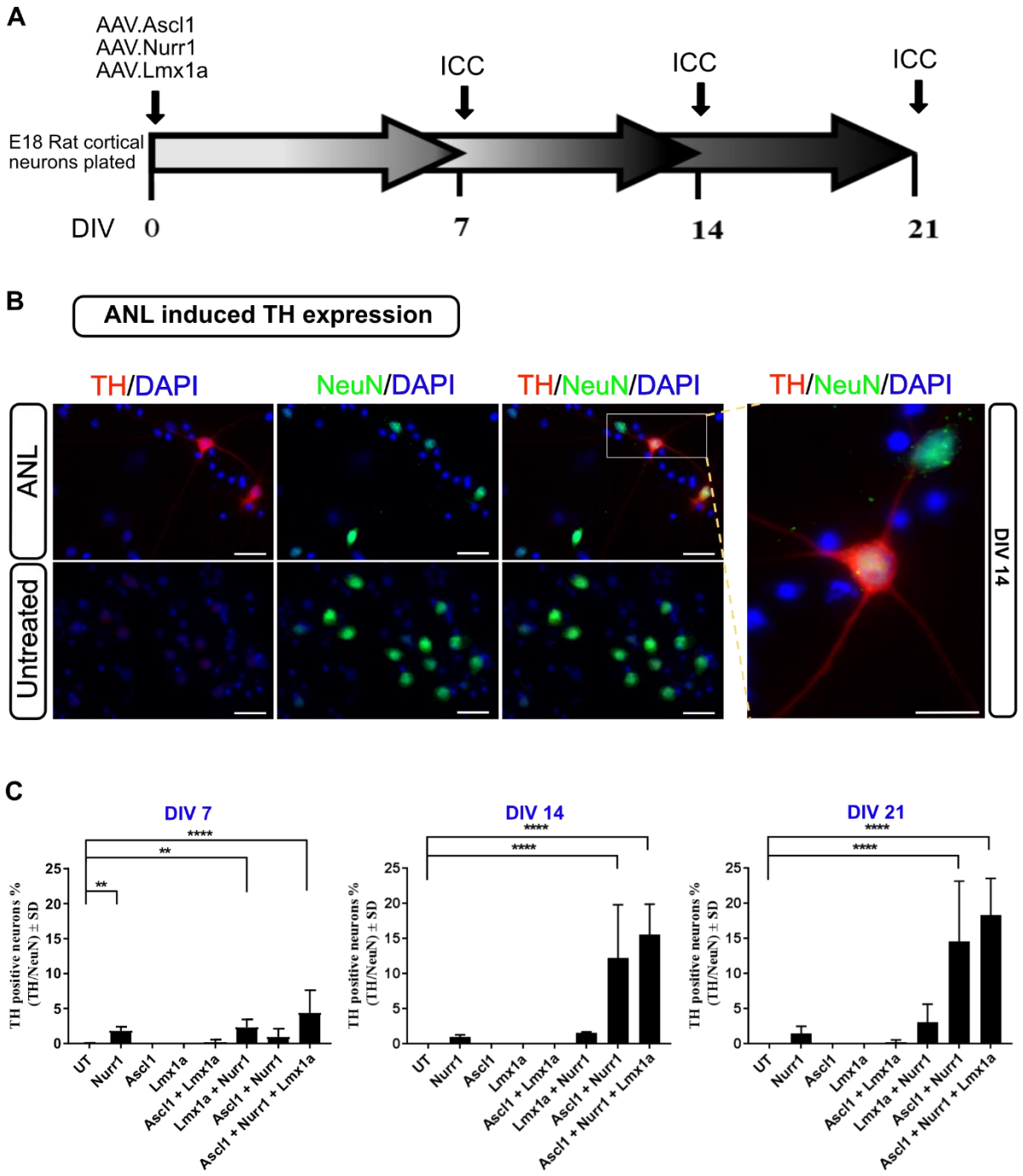

Figure 3.2. Ascl1, Nurr1, and Lmx1a ("ANL") induce the expression of TH in cortical neurons.

Figure 3.2. Ascl1, Nurr1, and Lmx1a ("ANL") induce the expression of TH in cortical neurons.

(A) *Experimental schematic to detect the expression of dopaminergic neuronal marker, tyrosine hydroxylase (TH).* Cortical neurons were isolated from E18 rat embryo and plated on poly-L-ornithine and laminin-coated wells (150,000 cells). AAV vectors expressing Ascl1, Nurr1, Lmx1a, and Pitx3 were introduced into cortical neurons at DIV 0 in different combinations.

(B) *Expression of Ascl1, Nurr1, and Lmx1a ("ANL") induced the expression of TH.* Representative immunofluorescence images of "ANL" treated cortical neurons immunopositive for neuronal marker NeuN (green) and dopaminergic neuronal marker TH (red), and images of untreated cortical neurons immunonegative for TH at DIV 14. Nuclei were counterstained with DAPI (blue). Scale bars: 10 µm, 20µm (magnified image).

(C) *Quantification of TH positive neurons.* Different percentages of TH positive neurons resulted from different combinations of transcription factors at DIV 7, DIV 14, and DIV 21. 1-way ANOVA with Dunnet's test calculated statistical significances by comparison with untreated neurons. **p=0.0021, ****p<0.0001. Bars show mean ± standard deviation and represent the percentage of TH positive cells normalized to NeuN. N = 4-6 independent experiments. Statistical power > 0.85.

Summary: Overexpression of Ascl1, Nurr1, and Lmx1a ("ANL") induced TH expression in 15-24% of cortical neurons by DIV 21. The combination of Ascl1 and Nurr1 was sufficient to induce TH expression, and the Ascl1, Nurr1, together with Lmx1a did not significantly increase TH positive (TH+) neurons. The overall number of neurons in "ANL" overexpressing group were less in comparison to the group of untreated neurons. Furthermore, the introduction of Pitx3 alone and in combinations with "ANL" did not induce TH expression.

3.1.3 Dopaminergic neuron-like cells express dopaminergic neuronal markers

As “ANL” overexpression induced TH in cortical neurons, the next objective was to determine if “ANL” also induced the expression of dopaminergic markers in dopaminergic neuron-like cells.

Neuron-specific AAV-6 vectors expressing Ascl1, Nurr1, and Lmx1a (“ANL”, total viral load 75 x 10^8 vector genomes (vg)/150,000 cells) were introduced into cortical neurons at DIV 0. Untreated neurons and “ANL” overexpressing neurons were stained for TH, and individually counter-stained for aromatic L-amino acid decarboxylase (AADC), vesicular monoamine transferase 2 (VMAT2), and dopamine transporter (DAT).

ICC results indicated that TH expressing neurons co-expressed AADC (**Fig.3.3.A**), VMAT2 (**Fig.3.3.B**), and DAT (**Fig.3.3.C**). Furthermore, unspecific signal was observed in untreated neurons. The pattern of the unspecific signal was different from the pattern observed in “ANL” overexpressing neurons, and it appears that the unspecific signal was observed due to the different secondary antibodies used.

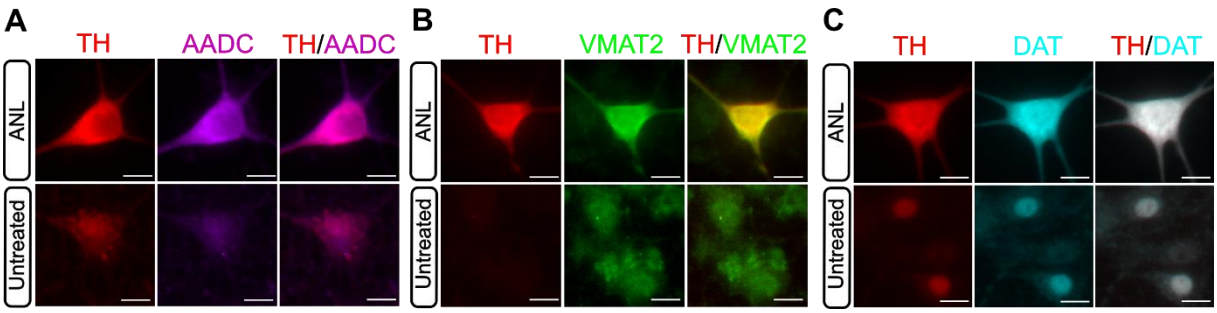

Figure 3.3. Dopaminergic neuron-like cells express dopaminergic neuronal markers at DIV 21.

(A, B, C) *Induction of dopaminergic markers.* Representative immunofluorescence images of untreated and Ascl1, Nurr1, and Lmx1a ("ANL") overexpressing cortical neurons at DIV 21, stained for tyrosine hydroxylase (TH; red) and counter-stained for **(A)** aromatic L-amino acid decarboxylase (AADC; magenta), **(B)** vesicular monoamine transferase 2 (VMAT2; green), and **(C)** dopamine transporter (DAT; cyan). Scale bar: 10µm.

Summary: "ANL" induced TH expression along with the expression of other dopaminergic markers, AADC, VMAT2, and DAT, which are necessary for a functional dopaminergic neuron. Unspecific signal was observed in untreated neurons. The pattern of the unspecific signal was different from the pattern observed in "ANL" overexpressing neurons, and it appears that the unspecific signal was observed due to the different secondary antibodies used.

3.1.4 Cortical GABAergic neurons, a subpopulation of cortical neurons, transdifferentiate to dopaminergic neuron-like cells

"ANL" induced dopaminergic neurotransmitter phenotype in 15 – 24% of total cortical neurons, which suggests that not all cortical neurons do transdifferentiate. The transduction efficacy of AAV6 vectors in cortical neuron culture is sufficient to reach > 90% of all neurons (Taschenberger et al. 2013; Tolo et al. 2018). Therefore, I wondered why the percentage of transdifferentiated cortical neurons was limited to 15%.

To understand the reason behind the low yield of dopaminergic neuron-like cells (cDNs) after "ANL" overexpression, untreated neurons and "ANL" overexpressing neurons were stained for TH and counter-stained with Ascl1 and Nurr1 at DIV 14. Immunocytochemistry results suggested that even though the majority of cortical neurons overexpressed Ascl1 and Nurr1, TH was induced only in a subpopulation of Ascl1 and Nurr1 overexpressing cortical neurons (**Fig.3.4.A**).

The majority of cortical neurons are glutamatergic and only 5-20% are GABAergic (Dichter 1980; Herrero et al. 1998; Stichel and Muller 1991). Immunocytochemical analyses of cDNs (identified as TH), GABAergic neurons (identified as GAD 65), and glutamatergic neurons (identified as CaMKIIß) revealed that TH expression was induced in GABAergic neurons because TH and GAD65 colocalize (**Fig. 3.4.B**). TH expression was not induced in glutamatergic neurons because TH and CaMKIIß did not colocalize (**Fig.3.4.C**).

Quantification of neuronal cell numbers revealed that the percentage of TH+ cells increased significantly by DIV 14 and DIV 21, and the percentage of GAD+ cells dropped significantly by DIV 21 in "ANL" overexpressing cortical neurons (**Fig.3.4.D**), Interestingly, the results indicated that out of the pool of cortical GABAergic neurons,

55% of neurons co-expressed TH and GAD65 at DIV 7, which significantly dropped (15%) at DIV 14. Intriguingly, none of the neurons coexpressed TH and GAD65 markers at DIV 21 (**Fig.3.4.D**).

Next, absolute number of TH+, GAD+, and CaMKIIß+ cells were plotted. 68% of "ANL" overexpressing CaMKIIß+ cells already degenerate at DIV 7 (**Fig.3.5.A**). Even though there was a significant drop in the cortical neuronal cell counts at DIV 14 and at DIV 21 due to the age of the culture, the "ANL" overexpressing CaMKIIß+ cell counts further dropped by 80% at DIV 14 and DIV 21 in comparison to the untreated neurons. There was a significant rise in the number of "ANL" overexpressing TH+ cell counts at DIV 7, DIV 14, and DIV 21 in comparison to the untreated cells at the same time-points (**Fig.3.5.B**). The rise in the TH+ cell counts can be attributed to the previous results, which revealed that TH was induced in "ANL" overexpressing GAD+ cells (**Fig.3.4.B**). This suggests that the source of TH+ cells are basically GAD+ cells. The number of "ANL" overexpressing GAD+ do not change significantly in comparison to the untreated neurons at DIV 7 (**Fig.3.5.C**). There was a significant drop observed in the GAD+ cell counts at DIV 14 and DIV 21 in comparison to the untreated neurons, because majority of GAD+ cells transdifferentiated to TH+ cells (**Fig.3.5.B.C**). However, the GAD+ cell counts actually drop or the expression of GAD65 was lost in the process of transdifferentiation, was not clear. To conclude, "ANL" overexpression aggravated degeneration of cortical glutamatergic neurons (identified as CaMKIIß), but not GABAergic neurons (identified as GAD 65), and increased the yield of dopaminergic neuron-like cell (identified as TH+).

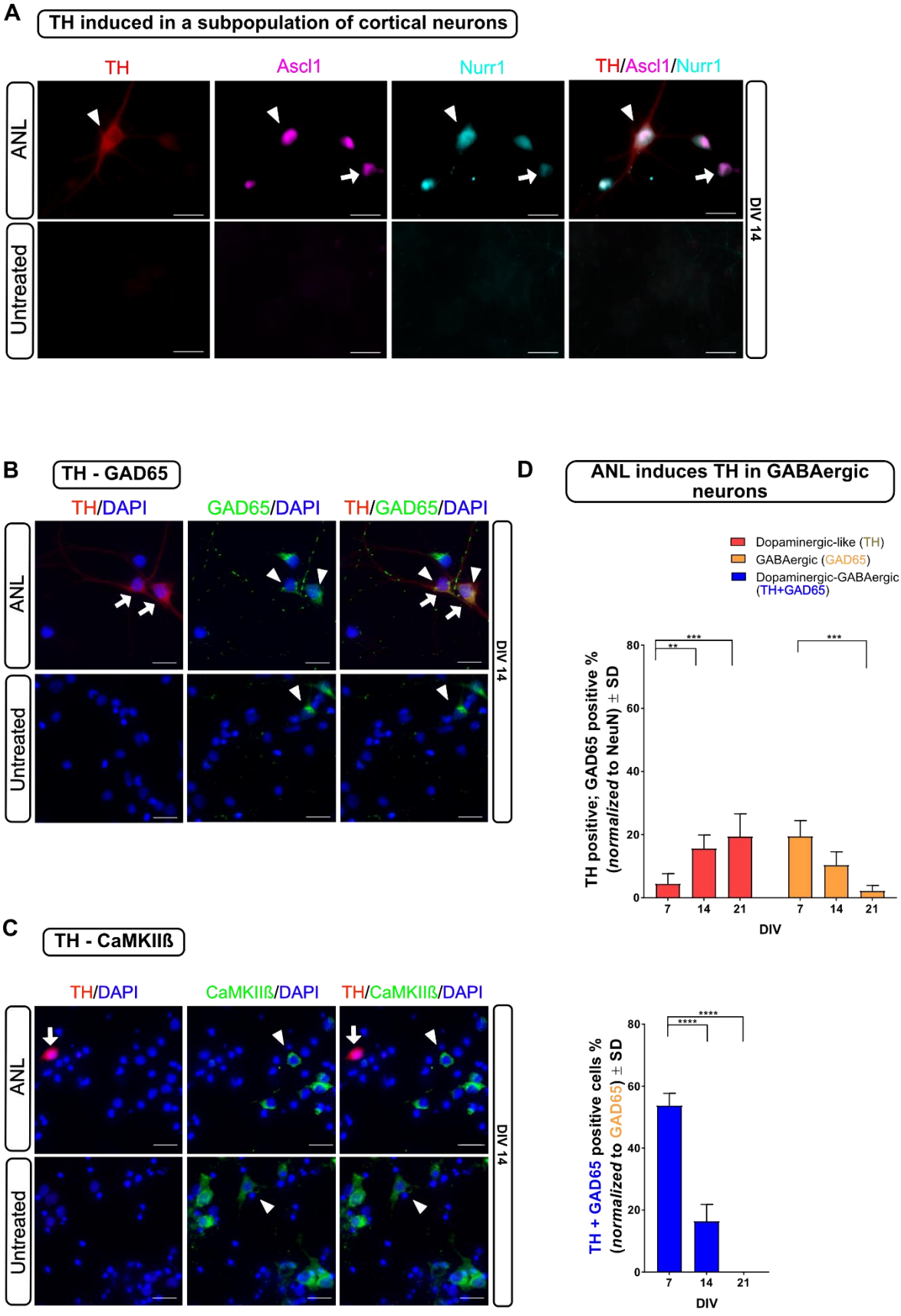

Figure 3.4. Cortical GABAergic neurons, a subpopulation of cortical neurons, transdifferentiate to dopaminergic neuron-like cells.

Figure 3.4. Cortical GABAergic neurons, a subpopulation of cortical neurons, transdifferentiate to dopaminergic neuron-like cells.

(A) *TH expression was induced in a subpopulation of cortical neurons.* Representative immunofluorescence images of "ANL" treated cortical neurons immunopositive for dopaminergic neuronal marker TH (red), and transcription factors Ascl1 (magenta) and Nurr1 (cyan) at DIV 14. Untreated cortical neurons were immunonegative for TH, Ascl1, and Nurr1. White arrowhead indicates neurons expressing TH, Ascl1, and Nurr1, whereas white arrow indicates neurons expressing only Ascl1 and Nurr1, but not TH. Scale bar: 10 µm.

(B) *TH and GAD65 colocalize*. Representative immunofluorescence images of Ascl1, Nurr1, and Lmx1a ("ANL") treated cortical neurons. "ANL" overexpressing cells immunopositive for dopaminergic marker TH (red) and GABAergic marker GAD65 (green), whereas untreated neurons immunonegative for TH, but immunopositive for GAD65. TH and GAD65 colocalized at DIV 14 in "ANL" expressing neurons. Nuclei were counterstained with DAPI (blue). White arrow indicates cDN and white arrowhead indicates GABAergic neuron. Scale bar: 10 µm.

(C) *TH and CaMKIIß do not colocalize.* Representative immunofluorescence images of "ANL" treated cortical neurons immunopositive for TH (red) and glutamatergic marker CaMKIIß (green), whereas untreated cortical neurons immunonegative for TH, but immunopositive for CaMKIIß. TH and CaMKIIß did not colocalize at DIV 14 in "ANL" expressing neurons. Nuclei were counterstained with DAPI (blue). White arrow indicates cDN and white arrowhead indicates glutamatergic neuron. Scale bar: 10 µm.

(D) *Quantification of different neuronal cell-types in "ANL" expressing neurons:* Quantification of percentages of dopaminergic-like neurons (red bars), GABAergic neurons (green bars), and neurons coexpressing TH and GAD65 (blue bars) in "ANL" expressing neurons. 1-way ANOVA with Dunnet´s test calculated statistical significances by comparison with DIV 7. **p=0.0021, ***p=0.0002, ****p<0.0001. Bars show mean ± standard deviation and represent the percentage of dopaminergic-like, GABAergic, normalized to NeuN; TH and GAD65 coexpressing neurons were normalized to GAD65. Statistical power for all conditions > 0.95.

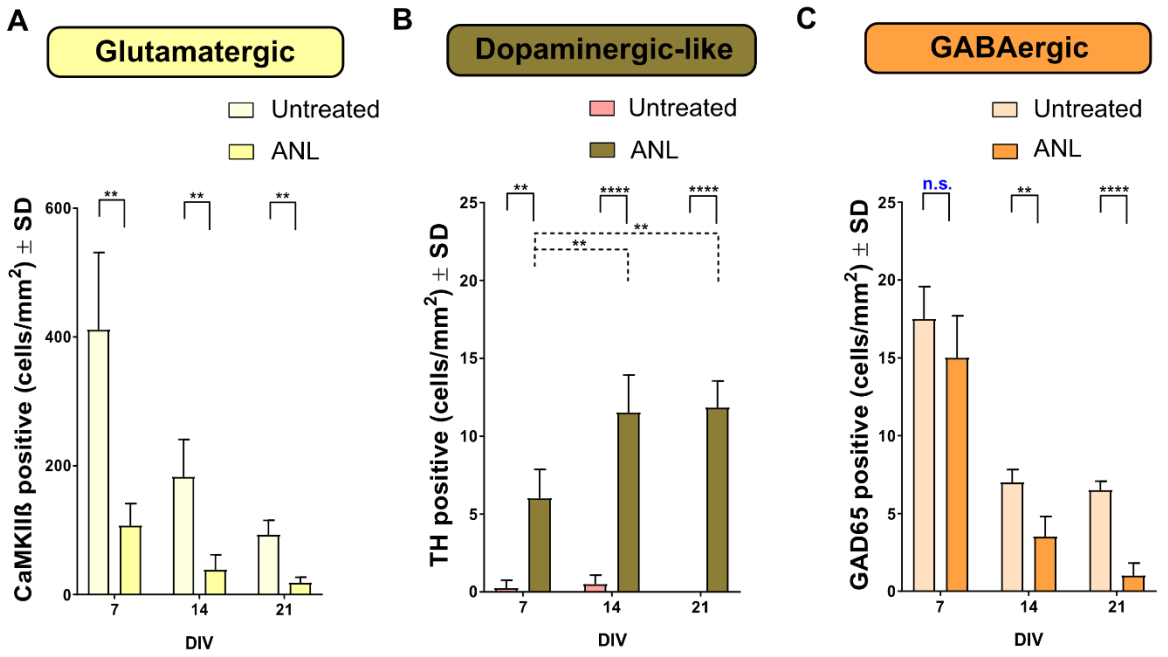

Figure 3.5. "ANL" cause degeneration of glutamatergic neurons.

(A) *Quantification of absolute cell counts of glutamatergic neurons (identified as CaMKIIß).* 68% of "ANL" overexpressing CaMKIIß+ cells already degenerated at DIV 7. There were significantly less CaMKIIß+ cells in comparison to untreated cells at DIV 14 and DIV 21. The age of the culture also affected the total cell counts; however, "ANL" overexpression aggravated degeneration of glutamatergic neurons.

(B) *Quantification of absolute cell counts of dopaminergic neuron-like cells (identified as TH+).* There was a significant rise in the number of "ANL" overexpressing TH+ cell counts at DIV 7, DIV 14, and DIV 21 in comparison to untreated cells at the same time-points.

(C) *Quantification of absolute cell counts of GABAergic neurons (identified as GAD65+).* There was no significant drop in GAD65+ cell counts at DIV 7; however, the cell counts dropped significantly at DIV 14 and DIV 21. This might be due to the results explained in figure 2.4.B that GAD+ cells undergo transdifferentiation to TH+ cells.

Student´s unpaired two-tailed t-test with Welch´s correction calculated statistical significances by comparison with untreated. **p=0.0021, ****p<0.0001. Bars show mean ± standard deviation and represent the absolute cell counts per square millimeter. N = 4-5 independent experiments. Statistical power for all conditions > 0.95.

3.1.5 "ANL" overexpression diminishes the expression of GAD65 marker in cortical GABAergic neurons

In order to understand if GABAergic neurons deplete in number during transdifferentiation, the next objective was to determine if the GABAergic neurons lose their phenotype in the process of fate switch.

ICC results indicated that GAD65 marker in untreated and "ANL" expressing neurons was intact at DIV 7 (**Fig.3.6**); however, GAD65 was diminished in "ANL" expressing neurons at DIV 14 and DIV 21 (**Fig.3.6**). It appears that there is some residual GAD65 staining still present in the neurites. "ANL" overexpressing neurons were positive for Ascl1 and Nurr1, and untreated neurons were negative for Ascl1 and Nurr1, suggesting that the concerted overexpression of both Ascl1 and Nurr1 diminishes GAD65. Overall, these results suggest that the "ANL" diminishes the cytoplasmic GAD65, while some residual GAD65 staining still persists in the neurites of GABAergic neurons.

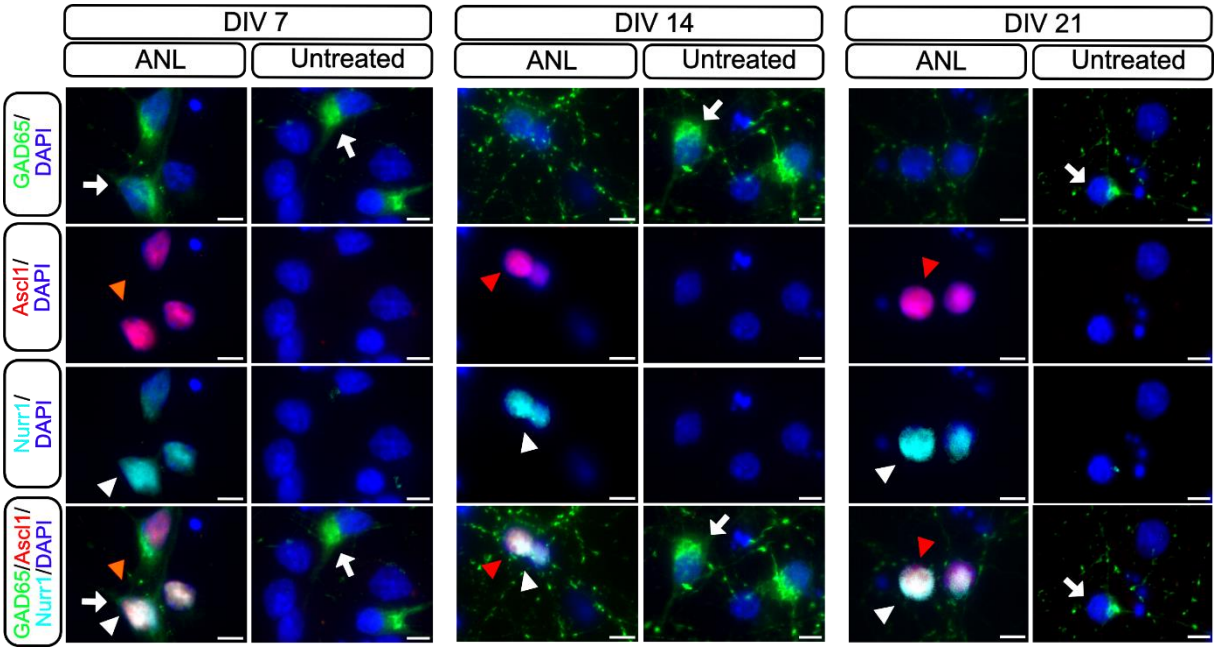

Figure 3.6. Ascl1, Nurr1, and Lmx1a ("ANL") overexpression diminishes the expression of GAD65 marker in cortical GABAergic neurons.

Figure 3.6. Ascl1, Nurr1, and Lmx1a ("ANL") overexpression diminishes the expression of GAD65 marker in cortical GABAergic neurons.

"ANL" expression altered the expression pattern of GAD65 in GABAergic neurons. Representative immunofluorescence images of "ANL" treated cortical neurons immunopositive for GAD65 (green) at DIV 7, but not at DIV14 and DIV 21, whereas GAD65 expression was maintained in untreated cortical neurons until DIV 21. "ANL" treated cortical neurons were immunopositive for Ascl1 (red) and Nurr1 (cyan) until DIV 21, whereas untreated cortical neurons were immunonegative for Ascl1 and Nurr1. White arrow indicates GABAergic neuron, red arrowhead indicates Ascl1 and white arrowhead indicates Nurr1 overexpressing neurons. Nuclei were counterstained with DAPI (blue). Scale bar: 10µm.

Summary: "ANL" induces dopaminergic neurotransmitter phenotype only in cortical GABAergic neurons (GAD+ cells), but not cortical glutamatergic neurons (CaMKIIß+ cells). As a result, TH+ neurons significantly increase from DIV 7 to DIV 14 and DIV 21, while GAD+ cells significantly decrease from DIV 7 to DIV 21. Furthermore, "ANL" diminished GAD65 expression in GABAergic neurons, suggesting a neuronal phenotype switch. "ANL" aggravated the degeneration of glutamatergic neurons; however, "ANL" induced dopaminergic neurotransmitter phenotype in GABAergic neurons, thereby increasing the number of dopaminergic neuron-like cells (TH+ cells) in cortical culture.

3.1.6 Rat primary midbrain GABAergic neurons do not transdifferentiate towards dopaminergic neurotransmitter phenotype

Given the fact that GABAergic neurons transdifferentiated to TH+ neurons, it was hypothesized this effect can be boosted in a neuronal culture that consists of a majority of GABAergic neurons. It is reported that the GABAergic neurons (GAD+ cells) are predominantly present in a midbrain culture along with a minority of TH+ neurons (Gaven, Marin, and Claeysen 2014). I thus overexpressed “ANL” in neurons isolated from rat E14.5 midbrain.

Primary midbrain neurons were isolated from E14 rat embryo and plated on coverslips coated with poly-L-ornithine and laminin on a 24-well plate (500,000 neurons/well). AAV-6 vectors expressing Ascl1, Nurr1, and Lmx1a (total viral load 75 x 10^8 vg/500,000 cells) were introduced into midbrain neurons at DIV 0 (**Fig.3.7.A**).

Untreated neurons and “ANL” overexpressing neurons were stained for dopaminergic marker, TH, and a pan-neuronal marker, NeuN (**Fig.3.7.B**). ICC results indicated that “ANL” overexpression did not increase the percentage of TH positive neurons significantly in comparison to the untreated neurons (**Fig.3.7.C**). Unexpectedly, there were significantly less TH+ cells in “ANL” treated cells in comparison to the untreated cells at DIV 14 and DIV 21. TH+ cells were observed in the untreated midbrain neurons, because the midbrain culture consists of a minority (< 5%) of TH+ cells (Gaven, Marin, and Claeysen 2014). Furthermore, cells were stained with TH, and counter-stained with GABAergic marker, GAD65. The ICC results indicated that TH and GAD65 do not colocalize in a midbrain GABAergic neuronal cell (**Fig.3.7.D**) suggesting that midbrain GABAergic neurons cannot be transdifferentiated into dopaminergic neurotransmitter phenotype.

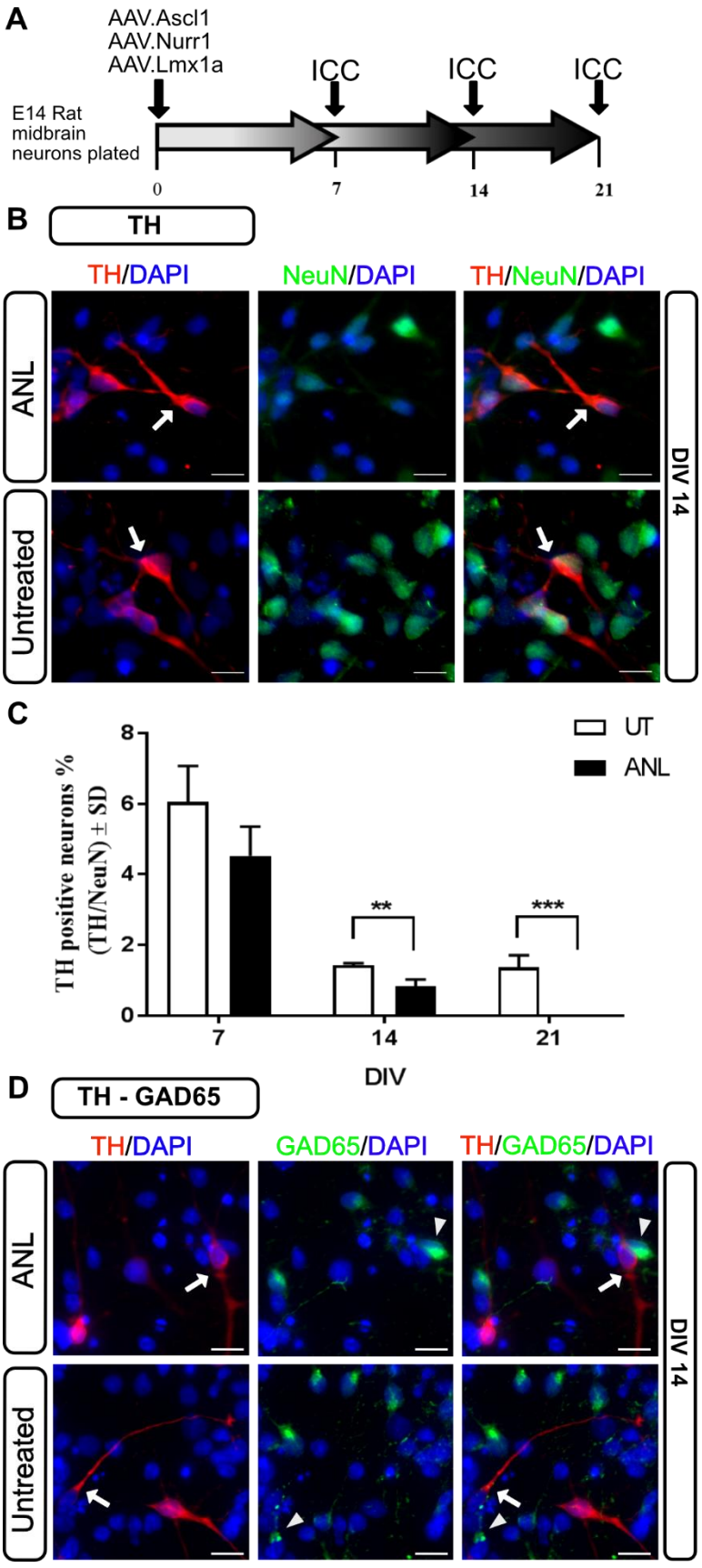

Figure 3.7. Rat primary midbrain GABAergic neurons do not transdifferentiate towards dopaminergic neurotransmitter phenotype

Figure 3.7. Rat primary midbrain GABAergic neurons do not transdifferentiate towards dopaminergic neurotransmitter phenotype

(A) *Experimental schematic to detect the expression of dopaminergic cell marker, tyrosine hydroxylase (TH).* Midbrain neurons were isolated from E14 rat embryo and plated on poly-L-ornithine and laminin-coated wells. Adeno-associated viral vectors expressing Ascl1, Nurr1, and Lmx1a (total viral load 75 x 10^8 viral genomes/500,000 cells) were introduced into midbrain neurons at DIV 0.

(B) *Expression of Ascl1, Nurr1, and Lmx1a ("ANL") did not induce the expression of TH.* Representative immunofluorescence images of untreated and "ANL" treated midbrain neurons immunopositive for neuronal marker NeuN (green) and dopaminergic neuronal marker TH (red, white arrow) at DIV 14. Nuclei were counterstained with DAPI (blue). White arrow indicate dopaminergic neurons. Scale bars: 10 µm.

(C) *Quantification of TH positive neurons.* The quantification of TH positive neurons in untreated group of neurons (white bar), and "ANL" overexpressing neurons (black bar) at DIV 7, DIV 14, and DIV 21. Bars show mean ± standard deviation and represent the percentage of surviving neurons normalized to NeuN. Student´s unpaired two-tailed t-test with Welch´s correction calculated statistical significances by comparison between the two groups. **p=0.0021, ***p<0.0002. N=2 independent experiments. Statistical power > 0.80

(F) *TH and GAD65 did not colocalize*. Representative immunofluorescence images of untreated and "ANL" treated midbrain neurons immunopositive for dopaminergic marker TH (red) and GABAergic marker GAD65 (green) at DIV 14. TH and GAD65 did not colocalize in "ANL" overexpressing midbrain neurons. Nuclei were counterstained with DAPI (blue). White arrow indicates dopaminergic neuron and white arrowhead indicates GABAergic neuron. White arrow indicate dopaminergic neurons, and white arrowhead indicates GABAergic neurons. Scale bars: 10 µm.

Elisabeth Barski performed the primary midbrain culture. Claudia Fokken stained the coverslips. Anupam Raina captured images, generated data, analyzed trends statistically, and derived conclusion. Department of Neurology, UMG.

Summary: “ANL” overexpression could not transdifferentiate the midbrain GABAergic neurons towards dopaminergic neurotransmitter phenotype; however, “ANL” transdifferentiated cortical GABAergic neurons towards dopaminergic neurotransmitter phenotype (**Fig.3.4.B**) suggesting that the region of the rat embryo, from where the GABAergic postnatal cells are isolated, plays an important role in determining the chances of neurotransmitter phenotype switch. However, the mechanism remains to be elucidated.

3.1.7 Summary of results – I

Transcription factors Ascl1, Nurr1, and Lmx1a transdifferentiated rat cortical GABAergic neurons, but not rat midbrain GABAergic and not rat cortical glutamatergic neurons, to dopaminergic neuron-like cells, thereby, providing evidence that neuronal transdifferentiation could be achieved in principle. Intriguingly, the induction of another neurotransmitter phenotype is dependent on the region of embryo used for isolating cells to induce transdifferentiation *in vitro*; suggesting that microenvironment of different embryonal regions might be a limiting factor for triggering transdifferentiation of postnatal neuronal cells.

Due to an insufficient yield of dopaminergic neurons, and the profound loss of neurons, the cell-model developed by transdifferentiation of cortical neurons cannot be used to study neurodegeneration induced by ß-Synuclein in the context of dopamine production.

In order to circumvent this challenge, an alternate approach was employed in which specific proteins necessary for dopamine production in a dopaminergic neuron, were introduced into cortical neurons.

3.2. Alternate approach to develop a dopaminergic cell-model by mimicking the dopaminergic neurotransmitter phenotype in cortical neurons

As the primary approach to generate dopaminergic neurons did not develop as desired, an alternate experimental paradigm was exploited. It was hypothesized that the introduction of specific enzymes, transporter proteins, and substrates, which are necessary for dopamine production, may produce dopamine in cortical neurons. Aromatic L-amino acid decarboxylase (AADC), vesicular monoamine transferase 2 (VMAT2), and L-3,4-dihydroxyphenylalanine (levodopa; L-DOPA) or dopamine transporter (DAT), VMAT2, and dopamine were introduced into cortical neurons (**Fig.3.8**).

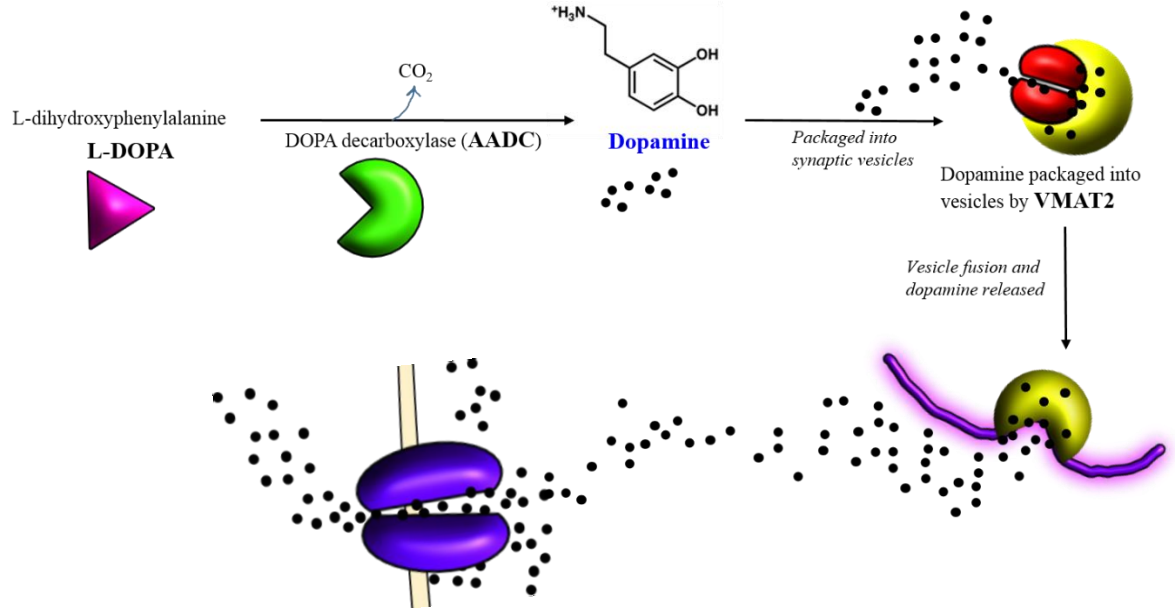

Figure 3.8. Mimicking the dopaminergic neurotransmitter phenotype in cortical neurons

AADC decarboxylates L-DOPA to produce dopamine. Cytosolic dopamine is sequestered into synaptic vesicles by VMAT2. Synaptic vesicles fuse to the cell membrane to release dopamine into synaptic cleft when neurons depolarize. DAT pumps dopamine from the synaptic cleft back into the cytosol.

3.2.1 Introduction of AADC, VMAT2, and extracellular L-DOPA or DAT, VMAT2, and extracellular dopamine into cortical neurons

The cortical neurons isolated from rat pups on embryonic day of development 18 (E18) consist of a majority (80-95%) of glutamatergic neurons and a minority (5-20%) of GABAergic neurons (Dichter 1980; Herrero et al. 1998; Stichel and Muller 1991). Cortical neurons are maintained with glial cells that grow up to 40-50% of all cells in later stages.

Adeno-associated viruses of serotype 6 (AAV6) were applied to the culture medium with cells (250,000 cells) at the time of preparation before seeding. Monocistronic AAV6 vectors expressed AADC and VMAT2 (AD-VM) or DAT and VMAT2 (DT-VM) in the transduced cells (**Fig.3.9**). AD-VM or DT-VM expression was driven by hSyn1 promoter that restricts the expression of AD-VM or DT-VM strictly to neurons (Kugler et al. 2003).

10µM L-DOPA was applied to the culture medium of AD-VM expressing cells from DIV 3 onwards every alternate days. L-DOPA was uptaken into cortical neurons presumably by L-type amino acid transporter (Sampaio-Maia, Serrao, and Soares-da-Silva 2001). In the control condition, the cells were transduced with AAV6 vectors expressing AADC and VMAT2, but L-DOPA was not applied to the culture medium of control cells. This system was named as cell-based model 1 (**Fig.3.10.A**).

12.5µM dopamine was applied to the culture medium of DT-VM expressing cells from DIV 7 onwards every four days. DAT is a membrane-spanning protein that pumps dopamine from the synaptic cleft back into the cytosol (Sonders et al. 1997). In the control condition, cells did not express DT-VM, but dopamine was applied to the culture medium of cells. This system was named as cell-based model 2 (**Fig.3.10.F**).

The supernatant and intracellular fraction of cells from each well (250,000 cells) were treated with buffer containing 1:1 ratio of 1% sodium metabisulfite and 2M perchloroacetic acid to stabilize dopamine. The processed supernatant and intracellular fractions were analyzed by HPLC with electrochemical detection of catecholamines. For better representation, the concentration (µM) of catecholamines were represented as the amount (nanograms) of total catecholamines obtained from 10,000 cells.

From cell-based model 1, results indicated that intracellular dopamine (**Fig.3.10.B.C**) peaked up to 0.8-1.0 nanograms (per 10,000 cells) at DIV 19 in the condition where L-DOPA was applied to the medium. In the control group where L-DOPA was not applied, intracellular dopamine, DOPAC, and HVA were not detected at DIV 15 and DIV 19, suggesting a tight control over the system. Unexpectedly, dopamine was detected in the supernatant (**Fig.3.10.D.E**). Furthermore, HVA accumulation was observed in the supernatant. It appears that glutamatergic vesicles presumably sequester the dopamine produced intracellularly and release it into the supernatant (Benoit-Marand 2013; Granger, Wallace, and Sabatini 2017) due to the endogenous electrical activity of cortical neurons (Opitz, De Lima, and Voigt 2002; Ramakers, Corner, and Habets 1990; Sun, Kilb, and Luhmann 2010). Dopamine released into the supernatant is uptaken by the glial cells present in the cortical culture, which degrade it to DOPAC and HVA by monoamine oxygenase-A (MAO-A), aldehyde dehydrogenase, and catechol-O-methyltransferase (COMT) (Liesi et al. 1981; Swahn and Wiesel 1976). Taken together, the results suggested that multiple doses of 10µM L-DOPA in AADC and VMAT2 expressing cells produced dopamine robustly.

From cell-based model 2, results indicated that the intracellular dopamine was drastically enhanced up to 3 nanograms (per 10,000 cells) already at DIV 15

(**Fig.3.10.G**) and up to 5 nanograms (per 10,000 cells) at DIV 19 (**Fig.3.10.H**) when 12.5µM dopamine was applied to the culture medium with cells expressing DAT and VMAT2. In the control condition, where dopamine was applied to the cells that did not express DAT and VMAT2, intracellular dopamine was not detected, therefore establishing a tight control over the system. In the supernatant (**Fig.3.10.I.J**), dopamine, DOPAC and HVA were detected in both the conditions because glial cells uptake dopamine that was applied to the medium, and degrade it to DOPAC and HVA (Liesi et al. 1981). Taken together, the results suggested that the introduction of DAT resulted in the uptake of dopamine into the cytosol of cortical neurons.

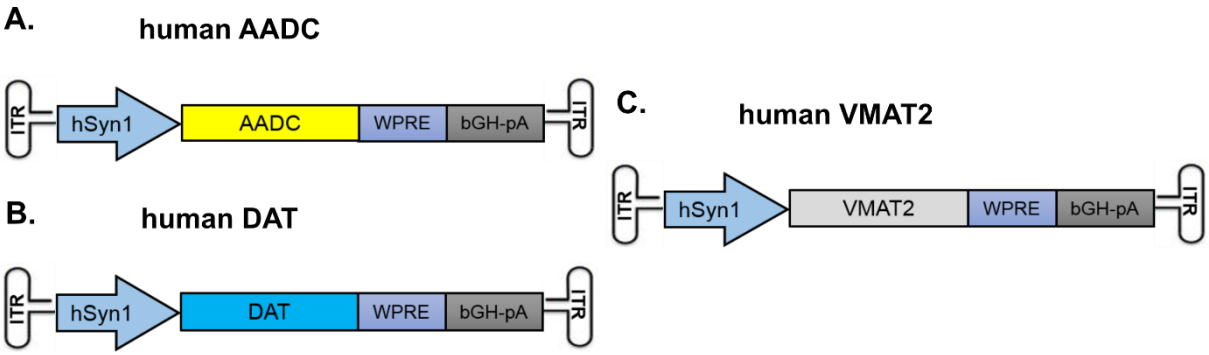

Figure 3.9. Monocistronic AAV vectors introduced into cortical neurons.

Monocistronic AAV vector expressing **(A)** human aromatic L-amino acid decarboxylase (AADC), **(B)** human dopamine transporter (DAT), and **(C)** vesicular monoamine transferase 2 (VMAT2).

hSyn1: human synapsin 1 gene promoter, WPRE: woodchuck hepatitis virus post-transcriptional control element, bGH-pA: bovine growth hormone poly-adenylation site, Int-a: intron, ITR: inverted terminal repeat.

Dr. Sebastian Kügler, Monika Zebski and Sonja Heyroth produced viruses (AAVs). Monika Zebski cloned the AAV vector genomes. Department of Neurology, University Medical Center Goettingen (UMG).

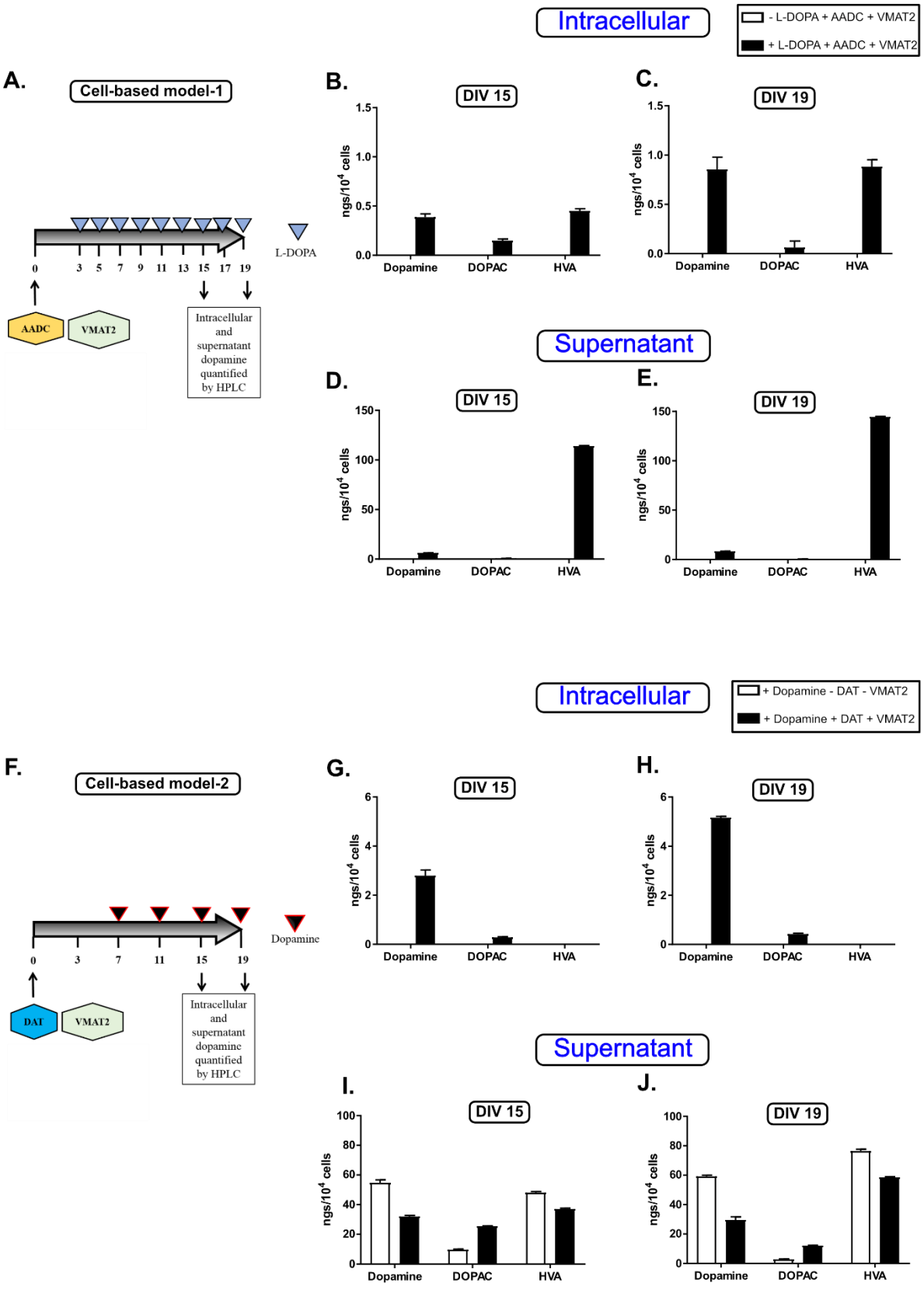

Figure 3.10. The two different cell-based models developed.

Figure 3.10. The two different cell-based models developed.

(A) *Schematic of the cell-model 1.* Cells were transduction with adeno-associated virus vectors expressing aromatic L-amino acid Decarboxylase (AADC) and vesicular monoamine transferase 2 (VMAT2) before seeding at DIV 0. 10µM of L-3,4-dihydroxyphenylalanine (L-DOPA) was applied to the cells from days *in vitro* (DIV) 3 onwards in the intervals of every two days. The levels of intracellular dopamine, 3,4-dihydxroxyphenylacetic acid (DOPAC), and homovanillic acid (HVA) were quantified at DIV 15 and DIV 19.

(B, C) Intracellular dopamine, DOPAC, and HVA detected at **(B)** DIV 15 and **(C)** DIV 19. **(D, E)** Supernatant dopamine, DOPAC, and HVA detected at **(D)** DIV 15 and **(E)** DIV 19.

The group of cells expressing AADC and VMAT2 and not treated with extracellular L-DOPA (white bar) acted as a control for the group expressing AADC and VMAT2 and treated with L-DOPA (black bar). Bars represent nanograms (ngs) of dopamine, DOPAC, and HVA from 10000 cells. Error bars represent the standard deviation of metabolite levels. N=3 independent transductions.

(F) *Schematic of the cell-model 2.* Cells were transduced with AAV vectors expressing dopamine transporter (DAT) and vesicular monoamine transferase 2 (VMAT2) before seeding at DIV 0. 12.5µM of extracellular dopamine was applied to the cells from DIV 7 onwards in the intervals of every four days. The intracellular dopamine, DOPAC, and HVA levels were quantified at DIV 15 and DIV 19.

(G, H) Intracellular dopamine, DOPAC, and HVA detected at **(G)** DIV 15 and **(H)** DIV 19. **(I, J)** Supernatant dopamine, DOPAC, and HVA detected at **(I)** DIV 15 and **(J)** DIV 19. The group of cells not expressing DAT and VMAT2 (white bar) acted as a control for the group of cells expressing DAT and VMAT2 vectors (black bar). Bars represent nanograms (ngs) of dopamine, DOPAC, and HVA from 10000 cells. Error bars represent the standard deviation of metabolite levels. N=3 independent transductions.

Summary: Two cell-based models were established. Introduction of AADC, VMAT2 into cortical neurons and extracellular doses of L-DOPA (cell-model 1) resulted in robust dopamine production. Glutamatergic vesicles presumably sequester the dopamine produced intracellularly and release it into the supernatant (Benoit-Marand 2013; Granger, Wallace, and Sabatini 2017) due to the endogenous electrical activity of cortical neurons (Opitz, De Lima, and Voigt 2002; Ramakers, Corner, and Habets 1990; Sun, Kilb, and Luhmann 2010). Introduction of DAT, VMAT2 into cortical neurons and extracellular doses of dopamine (cell-model 2) resulted in enhanced intracellular dopamine in comparison to cell-model 1. The intracellular dopamine levels detected in both the cell-models after 19 days in culture ranged from 0.8 to 5.0 nanograms (per 10,000 cells).

In this study, I found that the intracellular levels in both the cell-models is the highest-ever achieved in comparison to the existing dopaminergic neuronal cell-models used for PD research. Taken together, both the developed cell-models laid a solid foundation to study and investigate the neurodegeneration induced by ß-synuclein in the context of the neurotransmitter dopamine.

3.2.2 Toxicity of different concentrations of L-DOPA and dopamine

The introduction of AADC-VMAT2 and extracellular L-DOPA or DAT-VMAT2 and extracellular dopamine successfully produced dopamine and enhanced the intracellular dopamine levels. To understand the effect of L-DOPA and dopamine on cortical neurons, the toxicity of different doses of L-DOPA and dopamine was next investigated.

3.2.2. (I) Enzymatic degradation of unmetabolized L-DOPA is toxic to cortical neurons

It was necessary to determine the toxicity of different doses of L-DOPA. This study involved the application of dopamine-degrading enzyme inhibitors tranylcypromine. Tranylcypromine (Tcp) is a small molecule that inhibits MAO-A and MAO-B. Tolcapone (Tol) is another small molecule inhibitor that inhibits COMT. These inhibitors were used to prevent the degradation of L-DOPA by MAO and COMT enzymes.

Cortical neurons were transduced with monocistronic adeno-associated virus vector expressing nuclear mCherry (9 x 10^8 vg of virus/250000 cells) to label the nuclei. 12.5µM, 25µM, and 50µM of L-DOPA was applied to the cell culture medium from DIV 7 onwards in the intervals of every four days. Dopamine-degrading enzyme inhibitors Tcp (4µM/250,000cells) and Tol (5nM/250,000 cells) was applied once to the cell culture supernatant at DIV 7 (**Fig.3.11.A.B**). Cell culture medium that was not treated with L-DOPA acted as a control. Cells were also transduced at DIV 3 with neuron-specific AAV vector expressing nuclear mCherry (NmC) to label the nuclei. The nuclei of the surviving neurons were counted at DIV 11, 15, and 19.

With different concentrations of L-DOPA application to the neurons, results indicated that 50µM doses of L-DOPA were toxic to the cortical neurons at DIV 19 (**Fig.3.11.C.D**) suggesting that it is a very high dose. Interestingly, 25µM L-DOPA doses were toxic to the cells where inhibitors were not applied to the medium (**Fig.3.11.C**), whereas these doses were not toxic to the cells where inhibitors were applied to the medium (**Fig.3.11.D**). This suggested that intracellular L-DOPA is metabolized by COMT to 3-*O*-methyldopa (Kaenmaki et al. 2009), which is further metabolized to vanillactic acid. The metabolite 3-*O*-methyldopa might be toxic to cortical neurons (Lee et al. 2008). 12.5µM doses of L-DOPA were not found to be toxic.

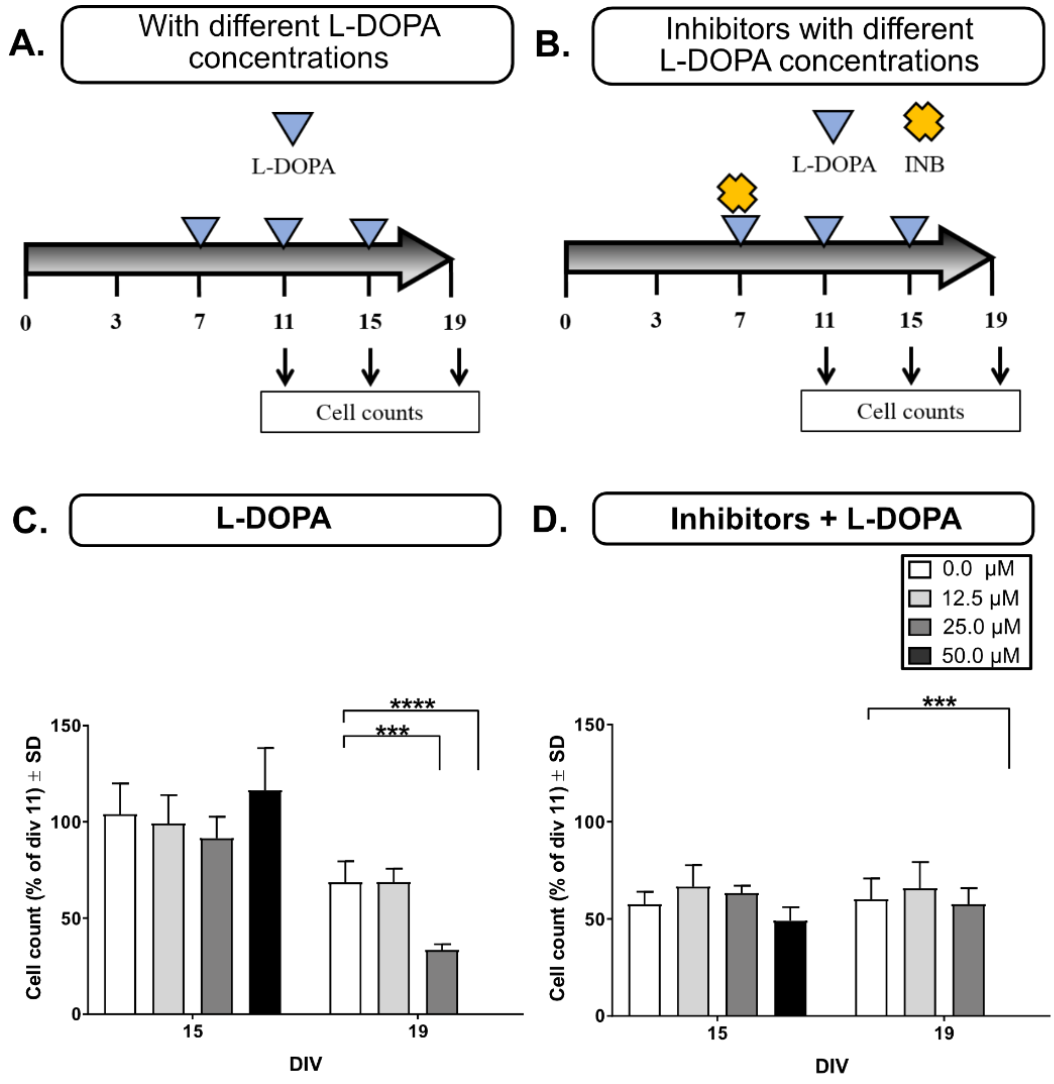

Figure 3.11. Enzymatic degradation of unmetabolized L-DOPA is toxic to cortical neurons.

Figure 3.11. Enzymatic degradation of unmetabolized L-DOPA is toxic to cortical neurons.

(A, B) *Schematic of 2 different experimental set-ups.* Cells were transduced with monocistronic adeno-associated virus vector expressing nuclear mCherry (9 x 10^8 vg/250000 cells) to label the nuclei. 0µM, 12.5µM, 25µM, and 50µM of L-3,4-dihydroxyphenylalanine (L-DOPA) was applied to the cells from days *in vitro* (DIV) 7 onwards in the intervals of every four days. The nuclei of the surviving cells were counted at DIV 11, 15, and 19. **(A)** 0µM, 12.5µM, 25µM, and 50µM of L-DOPA was applied to the cells. **(B)** The inhibitors (INB) of dopamine-degrading enzymes, monoamine oxidase (MAO) and catechol-O-methyltransferase (COMT) were applied to the cells in combination with 0µM, 12.5µM, 25µM, and 50µM of L-DOPA.

(C, D) Cell count was plotted for cells treated with 0µM (control, white), 12.5µM (light grey), 25µM (dark grey), and 50µM (black) of L-DOPA. **(C)** without MAO and COMT inhibitors **(D)** with MAO and COMT inhibitors together.

Bars represent the percentage of surviving cells (normalized to DIV 11). Error bars represent standard deviation (SD) of cell count percentage. Statistics by 1-way analysis of variance/Dunnett's test where light grey, dark grey and black bars were compared against the white bar (control). ***p<0.0002, ****p<0.0001. N=3 independent transductions. Power > 0.90.

3.2.2. (II) Extracellular dose of 10µM L-DOPA every alternate days was not toxic to AADC-VMAT2 expressing cortical neurons

Previous results suggested that dopamine-degrading enzymes might degrade unmetabolized L-DOPA into compounds toxic to cortical neurons. Therefore, the next objective was to determine the toxicity of multiple doses of L-DOPA metabolized to dopamine.

Cells were transduced with AAV-AADC and AAV-VMAT2 vectors (9 x 10^8 vg of each virus/250000 cells) before seeding at DIV 0 (**Fig.3.12.A**). In order to produce dopamine, 10µM of L-DOPA was applied to the neurons in the intervals of every two days from DIV 3 onwards (**Fig.3.12.B**). Neuronal cells were transduced at DIV 3 with monocistronic AAV vectors expressing the enhanced green fluorescent protein (EGFP, 60x10^8 vg of virus/250,000 neurons). Cells were also transduced at DIV 3 with neuron-specific AAV vector expressing nuclear mCherry (NmC) to label the nuclei. The nuclei of the surviving neurons were counted at DIV 11, 15, and 19.

In total, there were three groups of cells:

1. *No L-DOPA (control):* Cells did not express AADC-VMAT2, and no L-DOPA was applied to the culture supernatant.

2. *Metabolized L-DOPA:* Cells expressed AADC-VMAT2, and L-DOPA was applied to the culture supernatant.

3. *Unmetabolized L-DOPA:* Cells did not express AADC-VMAT2, and L-DOPA was applied

Results indicated that the cell counts dropped by 50% in the group of cells where L-DOPA was not unmetabolized (**Fig.3.12.C**) in comparison to the control (**Fig.3.12.A**).

When L-DOPA was metabolized to dopamine (**Fig.3.12.B**), the cell counts did not drop as compared to control. This suggested that multiple doses of 10µM L-DOPA was not toxic to the cortical neurons when metabolized to dopamine.

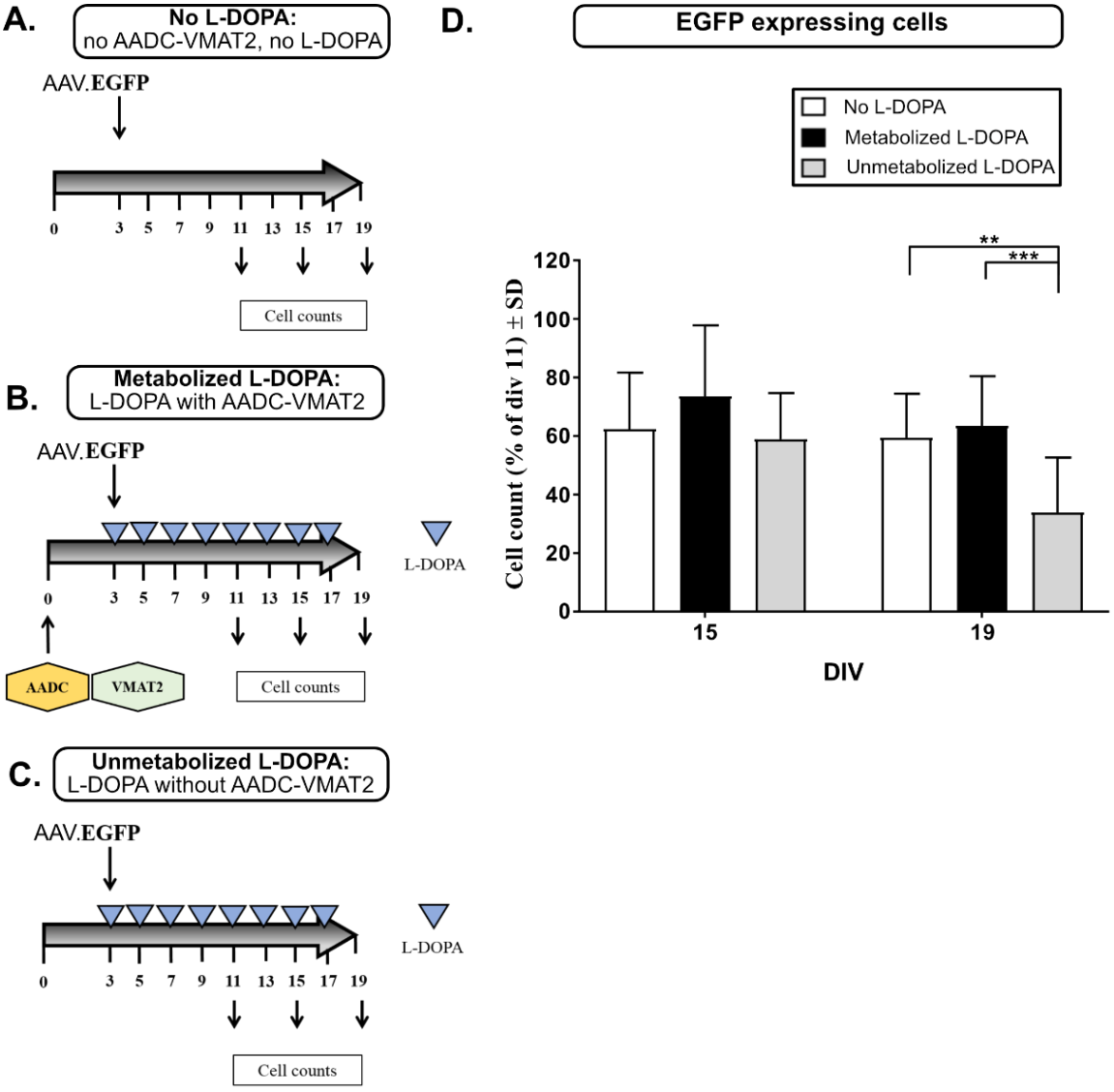

Figure 3.12. Extracellular dose of 10µM L-DOPA every alternate days was not toxic to AADC-VMAT2 expressing cortical neurons.

Figure 3.12. Extracellular dose of 10µM L-DOPA every alternate days was not toxic to AADC-VMAT2 expressing cortical neurons.

(A, B, C) *Schematics of 3 different types of the experimental set-up.* Primary cortical neurons were transduced with adeno-associated virus vectors at 3 days *in vitro* (DIV) expressing the enhanced green fluorescent protein (EGFP) ($60x10^8$ vg/250,000 neurons). Cells were also transduced with AAV vector expressing nuclear mCherry (NmC) to label the nuclei. The nuclei of the surviving cells were counted at DIV 11, 15, and 19. Cells were transduced with AAV-AADC and AAV-VMAT2 vectors before seeding at DIV 0. To produce dopamine, 10µM of L-DOPA was applied to the cell culture supernatant in the intervals of every two days from DIV 3 onwards. **(A)** The experimental set-up lacked the expression AADC-VMAT2 and L-DOPA application. **(B)** The cells expressed AADC-VMAT2 and supernatant was also treated with L-DOPA. AADC metabolized L-DOPA. **(C)** The cells did not express AADC and VMAT2 but supernatant was treated with L-DOPA. Cells were unable to metabolize L-DOPA as they lacked the expression of AADC.

(D) Surviving cells analyzed at DIV 15 and DIV 19. L-DOPA untreated group (white bar) acted as a control for metabolized L-DOPA group (black bar) and unmetabolized L-DOPA group (light grey bar).

Bars represent the percentage of surviving cells (normalized to DIV 11). Error bars represent standard deviation (SD) of cell count. Statistics by 1-way analysis of variance/Dunnett's test where light grey bar (unmetabolized L-DOPA) was compared against controls (white and black bars). **p=0.0021, ***p<0.0002. N=11-12 independent transductions. 5 independent experiments

3.2.2. (III) Extracellular dose of 12.5µM dopamine every 4 days is not toxic to DAT-VMAT2 expressing cortical neurons

As the introduction of DAT and VMAT2 along with the application of extracellular dopamine enhanced the intracellular dopamine levels, it was necessary to determine the toxicity of different doses of dopamine.

Cells were transduced with AAV-DAT and AAV-VMAT2 vectors (9 x 10^8 vg of each virus/250000 cells) before seeding at DIV 0. Cells were treated with 12.5µM, 25µM, and 50µM of dopamine, in the intervals of every 4 days from DIV 7 onwards. Dopamine degrading enzyme inhibitors Tcp (4µM/250,000cells) and Tol (5nM/250,000 cells) was applied once to the cell culture supernatant at DIV 7. Cell culture medium that was not treated with extracellular dopamine acted as a control. Cells were also transduced with monocistronic AAV vector expressing nuclear mCherry (9 x 10^8 vg of virus/250000 cells) to label the nuclei. The nuclei of the surviving neurons were counted at DIV 11, 15, and 19.

Results suggested that 50µM doses of dopamine was toxic (**Fig.3.13.A.E**), whereas the same doses of dopamine in the presence of inhibitors (**Fig.3.13.B.F**) was not toxic to the cortical neurons (without DAT-VMAT2) in which dopamine was not taken up (**Fig.3.13.**). Furthermore, results suggested that 25µM and 50µM dopamine doses were toxic to the cells (with DAT-VMAT2), which can uptake dopamine in the presence of inhibitors (**Fig.3.13.D.H**). Interestingly, in the absence of inhibitors (**Fig.3.13.C.G**), 25µM dopamine doses were not toxic, whereas 50µM dopamine doses were toxic to the cells (with DAT-VMAT2), which can uptake dopamine. The results suggested that dopamine-degrading enzyme inhibitors might have further enhanced the intracellular dopamine levels with 25µM extracellular dopamine doses, resulting in the toxicity of

cortical neurons. The dose of 12.5µM extracellular dopamine every 4 days was not found to be toxic to the cortical neurons expressing DAT and VMAT2.

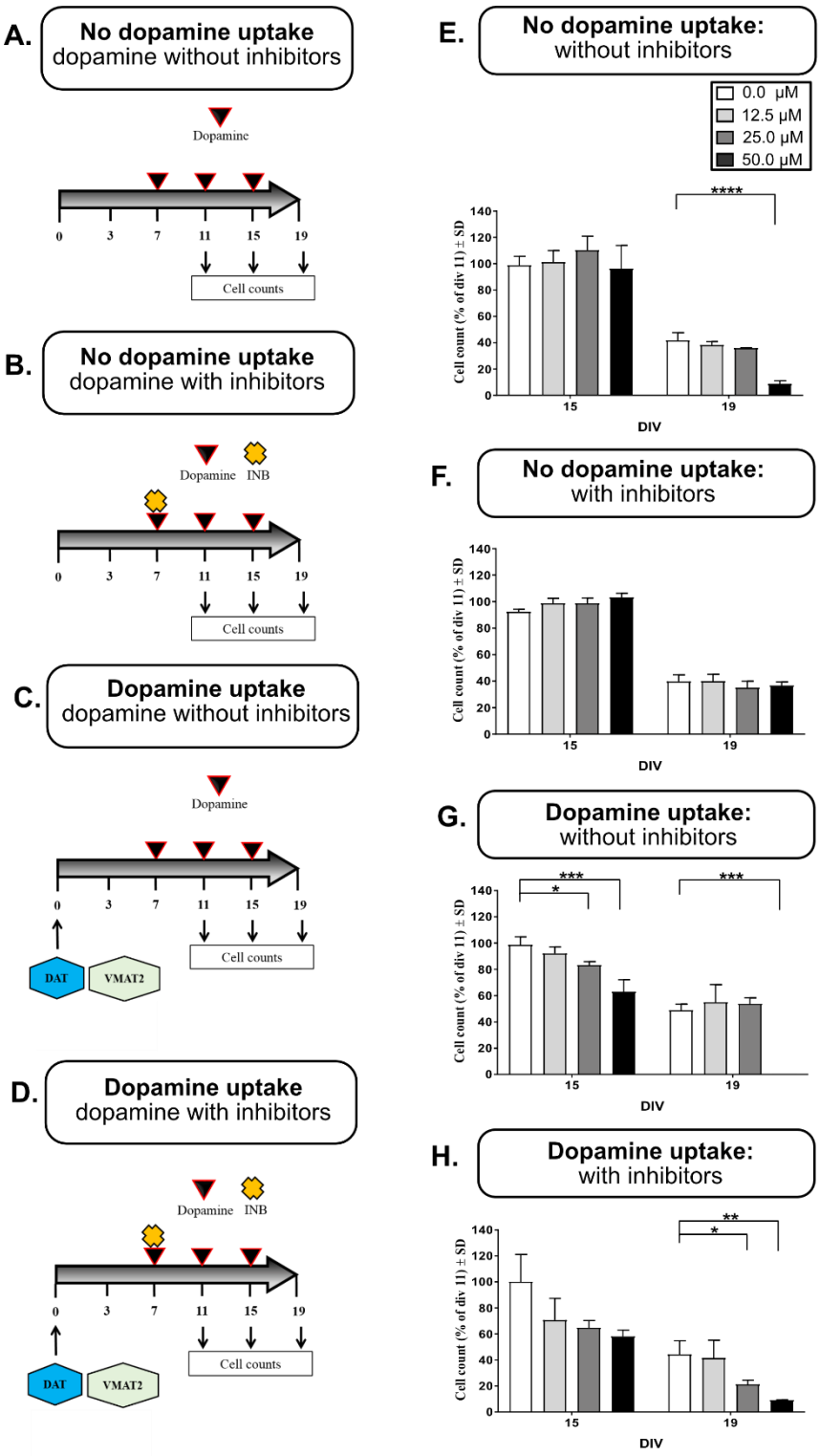

Figure 3.13. Extracellular dose of 12.5µM dopamine every 4 days is not toxic to DAT-VMAT2 expressing cortical neurons.

Figure 3.13. Extracellular dose of 12.5µM dopamine every 4 days is not toxic to DAT-VMAT2 expressing cortical neurons.

(A, B, C, D) *Schematic of 4 different experimental set-ups.* Cells were transduced with AAV-DAT and AAV-VMAT2 vectors before seeding at DIV 0. Cell culture supernatant was treated with 0µM, 12.5µM, 25µM, and 50µM of dopamine, in the intervals of every 4 days from DIV 7 onwards. Cells were also transduced with monocistronic AAV vector expressing nuclear mCherry ($9x10^8$ vg of virus/250000 cells) to label the nuclei. The nuclei of the surviving cells were counted at DIV 11, 15, and 19. **(A, B)** Dopamine was not uptaken in this experimental set-up as DAT and VMAT2 was not expressed by cells. **(C, D)** Dopamine was uptaken intracellularly by the cells in this set-up because the cells expressed DAT and VMAT2. **(B, D)** the inhibitors (INB) of dopamine-degrading enzymes, monoamine oxidase (MAO) and catechol-O-methyltransferase (COMT), were applied to the cell culture supernatant.

(E, F, G, H) Cell count was plotted for all conditions. Cell culture supernatant was treated with 0µM (control, white), 12.5µM (light grey), 25µM (dark grey), and 50µM (black) of dopamine. **(E, G)** without MAO and COMT inhibitors and **(F, H)** with MAO and COMT inhibitors.

Bars represent the percentage of surviving cells (normalized to DIV 11). Error bars represent standard deviation (SD) of cell count percentage. Statistics by 1-way analysis of variance/Dunnett's test where light grey, dark grey and black bars were compared against the white bar (control). *p=0.0332, ***p<0.0002, ****p<0.0001. N=3 independent transductions. Power > 0.80.

Summary: 10µM L-DOPA every alternate days from DIV 3 onwards until DIV 19 was not toxic to cortical neurons expressing AADC and VMAT2. Cortical neurons can tolerate up to 12.5µM of L-DOPA administered every 4 days from DIV 7, whereas the limit of tolerance was increased up to 25µM L-DOPA when coupled with dopamine-degrading enzyme inhibitors. The results suggested that endogenous dopamine-degrading enzymes (COMT) might degrade unmetabolized L-DOPA (Kaenmaki et al. 2009) into compounds that might be toxic to cortical neurons. Furthermore, Mosharov and colleagues reported that different higher doses (200µM to 1000µM) of L-DOPA are toxic to mice midbrain dopaminergic neurons *in vitro*, suggesting that higher intracellular L-DOPA induces toxicity to dopaminergic neurons *in vitro* (Mosharov et al. 2009).

Furthermore, the dose of 12.5µM extracellular dopamine every 4 days from DIV 7 onwards was not toxic to the cortical neurons expressing DAT and VMAT2. Very high intracellular dopamine levels was apparently achieved when 25µM doses were coupled with dopamine-degrading enzyme inhibitors. These cortical neurons were found to be toxic to very high intracellular dopamine levels.

3.3. Neurodegeneration induced by ß-synuclein in the context of dopamine

Our group reported that ß-synuclein induces neurodegeneration of nigral dopaminergic neurons in rodent model of PD (Taschenberger et al. 2013). This study suggested a possible link between dopamine and ß-synuclein. Therefore, it was of interest to study the neurotoxicity induced by ß-synuclein in the context of the neurotransmitter dopamine. The established cell-models with dopaminergic neurotransmitter phenotype were used.

Primary cortical neurons were transduced with AAV vectors (**Fig.3.14**) at DIV 3 expressing enhanced green fluorescent protein (EGFP), and bicistronic AAV vectors coexpressing EGFP + α-synuclein, EGFP + ß-synuclein and EGFP + γ-synuclein ($60x10^8$ vg of virus/250,000 neurons). Cells were also transduced with monocistronic AAV vector expressing nuclear mCherry (NmC) to label the nuclei. The nuclei of the surviving cortical neurons were counted at DIV 11, 15, and 19

3.3.1. Dopamine aggravates ß-synuclein neurotoxicity in cell-model with robust dopamine production: based on AADC, VMAT2, and L-DOPA

In order to study the neurodegeneration induced by ß-synuclein in the context of robust dopamine production, this experiment was divided into 3 groups of cells:

Group – 1 (*control****):*** Untransduced cells with no L-DOPA application to the culture medium (**Fig.3.15.A**)

Group – 2 (*control****):*** Cells transduced by neuron-specific AAV 6 vectors expressing AADC and VMAT2. L-DOPA was not applied to the culture medium (**Fig.3.15.B**).

Group – 3 (*dopamine-producing****):*** Cells transduced by neuron-specific AAV 6 vectors expressing AADC and VMAT2. L-DOPA was applied to the culture medium (**Fig.3.15.C**).

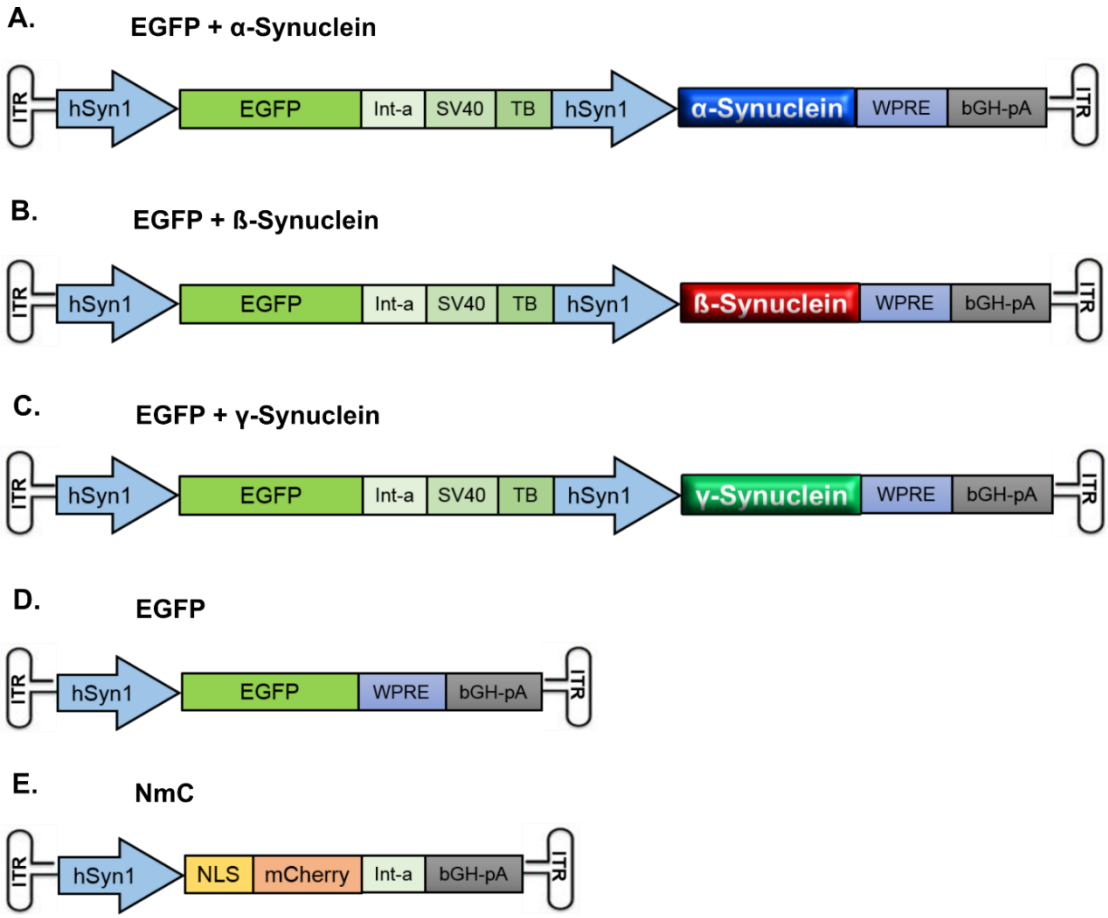

Figure 3.14. Monocistronic and bicistronic AAV vectors to study neurodegeneration

(A, B, C) *Bicistronic AAV vector genomes:* Bicistronic AAV vectors coexpressing **(A)** enhanced green fluorescent protein (EGFP) + α-synuclein, **(B)** EGFP + ß-synuclein, **(C)** EGFP + γ-synuclein. **(D, E)** *Monocistronic AAV vectors genomes:* Monocistronic AAV vectors expressing **(D)** EGFP, and **(E)** Nuclear mCherry (NmC)

hSyn1: human synapsin 1 gene promoter, NLS: nuclear localization signal, WPRE: woodchuck hepatitis virus post-transcriptional control element, bGH-pA: bovine growth hormone fused to poly adenylation site, Int-a: intron, SV40: simian virus 40, TB: transcription blocker, ITR: inverted terminal repeat.

Dr. Sebastian Kügler, Monika Zebski and Sonja Heyroth produced viruses (AAVs). Monika Zebski cloned the AAV vector genomes. Department of Neurology, University Medical Center Goettingen (UMG).

Intriguingly, results further suggested for the first time that dopamine production in ß-synuclein overexpressing cells (**Fig.3.15.D**) aggravated neurodegeneration. Dopamine production in ß-synuclein overexpressing cells exacerbated the degeneration of 25 – 45% more cells in comparison to the controls at DIV 19.

Results suggested that dopamine production in α-synuclein overexpressing cells (**Fig.3.15.E**) aggravated neurodegeneration of 20 - 30% more cells in comparison to the controls at DIV 19.

Dopamine production in γ-synuclein expressing cells (**Fig.3.15.F**) aggravated degeneration of 13% more cells in comparison to the controls at DIV 19. However, the drop in cell-counts was not statistically significant. Dopamine production in EGFP expressing cells (**Fig.3.15.G**) did not aggravate degeneration of cells.

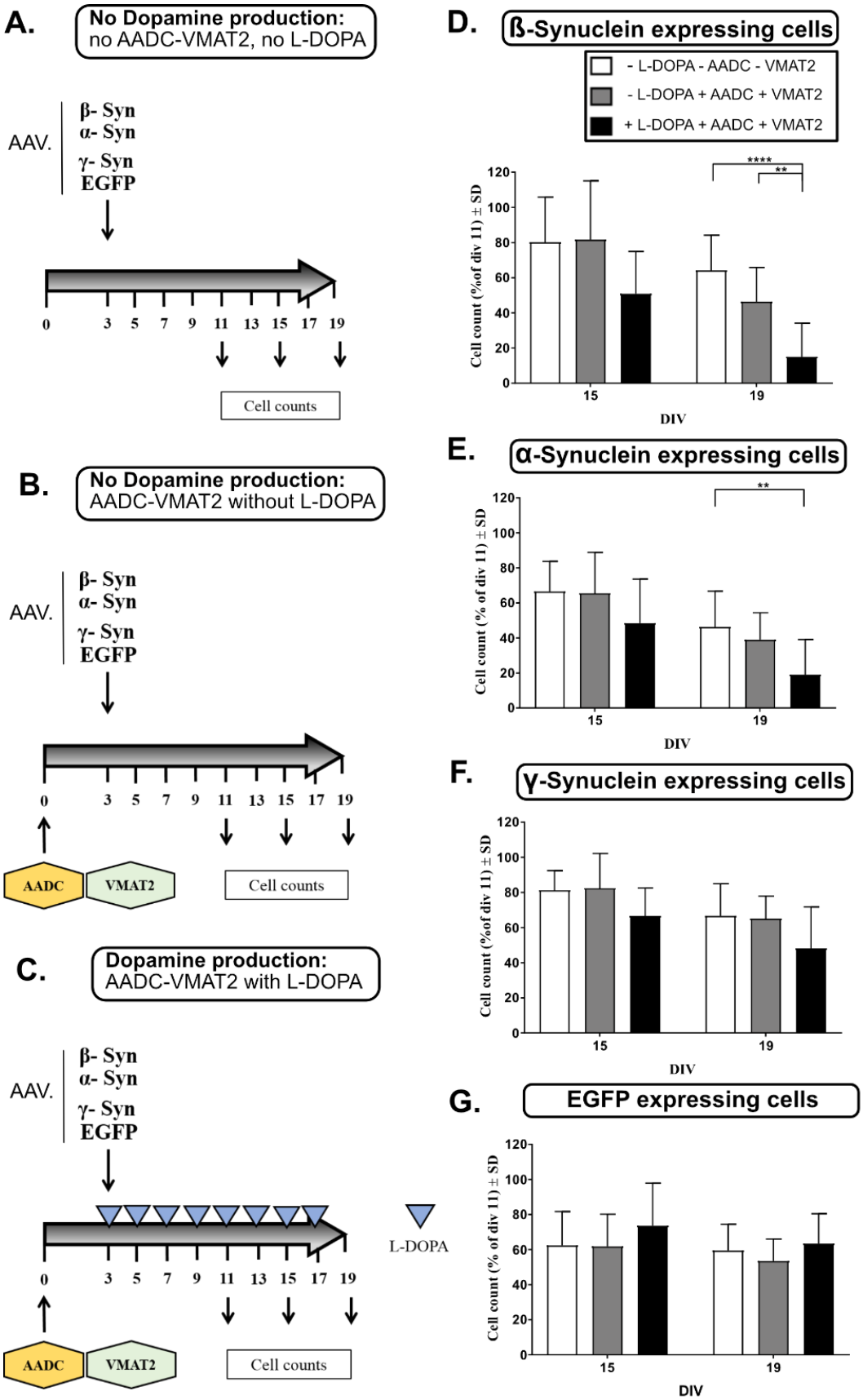

Figure 3.15. Robust dopamine production aggravates neurotoxicity of ß-synuclein, and to similar extent, of α-Synuclein.

Figure 3.15. Robust dopamine production aggravates neurotoxicity of ß-synuclein, and to similar extent, of α-Synuclein.

(A, B, C) *Schematics of 3 different types of the experimental set-up.* Cells were transduced with AAV-AADC and AAV-VMAT2 before seeding at DIV 0. To produce dopamine, 10µM of L-DOPA was applied to the cells in the intervals of every two days from days *in vitro* (DIV) 3 onwards. At DIV 3 cells were transduced with adeno-associated virus vectors at 3 days *in vitro* (DIV) expressing the enhanced green fluorescent protein (EGFP), and bicistronic AAV vectors coexpressing EGFP + α-synuclein, EGFP + ß-synuclein and EGFP + γ-synuclein ($60x10^8$ vg of virus/250,000 neurons). Cells were also transduced with monocistronic AAV vector expressing nuclear mCherry (NmC) to label the nuclei. The nuclei of the surviving cells were counted at DIV 11, 15, and 19. **(A)** Dopamine was not produced in this set-up because it lacked the AADC-VMAT2 and L-DOPA application. **(B)** Although the AADC-VMAT2 was expressed, dopamine was not produced in this set-up because cells were not treated with L-DOPA. **(C)** Dopamine was produced in this set-up because cells expressed AADC-VMAT2 and were also treated with L-DOPA.

(D, E, F, G) Surviving cells expressing ß-synuclein, α-synuclein, γ-synuclein, and EGFP, respectively, analyzed at DIV 15 and DIV 19.

Bars represent the percentage of surviving cells normalized to DIV 11. Error bars represent standard deviation (SD) of cell count. Statistics by 1-way analysis of variance/Dunnett's test where black bar (dopamine-producing neurons) was compared against controls (white and grey bar). **p=0.0021, ****p<0.0001. N=10-13 independent transductions. 5 independent experiments. Power > 0.90.

3.3.2. Dopamine aggravates ß-synuclein neurotoxicity in cell-model with enhanced intracellular dopamine: based on DAT, VMAT2, and dopamine

In order to study the neurodegeneration induced by ß-synuclein in the context of enhanced intracellular dopamine, this experiment was divided into 4 groups of cells:

Group – 1 (*control****):*** Untransduced cells with no dopamine application to the culture medium (**Fig.3.16.A**)

Group – 2 (*control****):*** Cells transduced by neuron-specific AAV 6 vectors expressing DAT and VMAT2. Dopamine was not applied to the culture medium (**Fig.3.16.B**).

Group – 3 (*extracellular dopamine; no uptake****):*** Untransduced cells with dopamine application to the culture medium (**Fig.3.16.C**)

Group – 4 (*intracellular dopamine; uptake****):*** Cells transduced by neuron-specific AAV 6 vectors expressing DAT and VMAT2. Dopamine was applied to the culture medium (**Fig.3.16.D**).

Interestingly, the results from this cell-model supported the results from the dopamine-producing cell-model. It was found that enhanced dopamine levels in ß-synuclein overexpressing cells (**Fig.3.16.E**), aggravated the degeneration of 42% more cells in comparison to the control groups. Moreover, it appeared that the extracellular dopamine in ß-synuclein overexpressing cells, aggravated the degeneration of 20% more cells in comparison to the group of cells without dopamine application in the culture medium.

The enhanced intracellular dopamine levels in α-synuclein overexpressing cells (**Fig.3.16.F**) aggravated the degeneration of 28% more cells in comparison to the control groups. The enhanced intracellular dopamine levels in γ-synuclein (**Fig.3.16.G**)

and EGFP overexpressing cells (**Fig.3.16.H**) did not aggravate the degeneration of cells in comparison to the control groups.

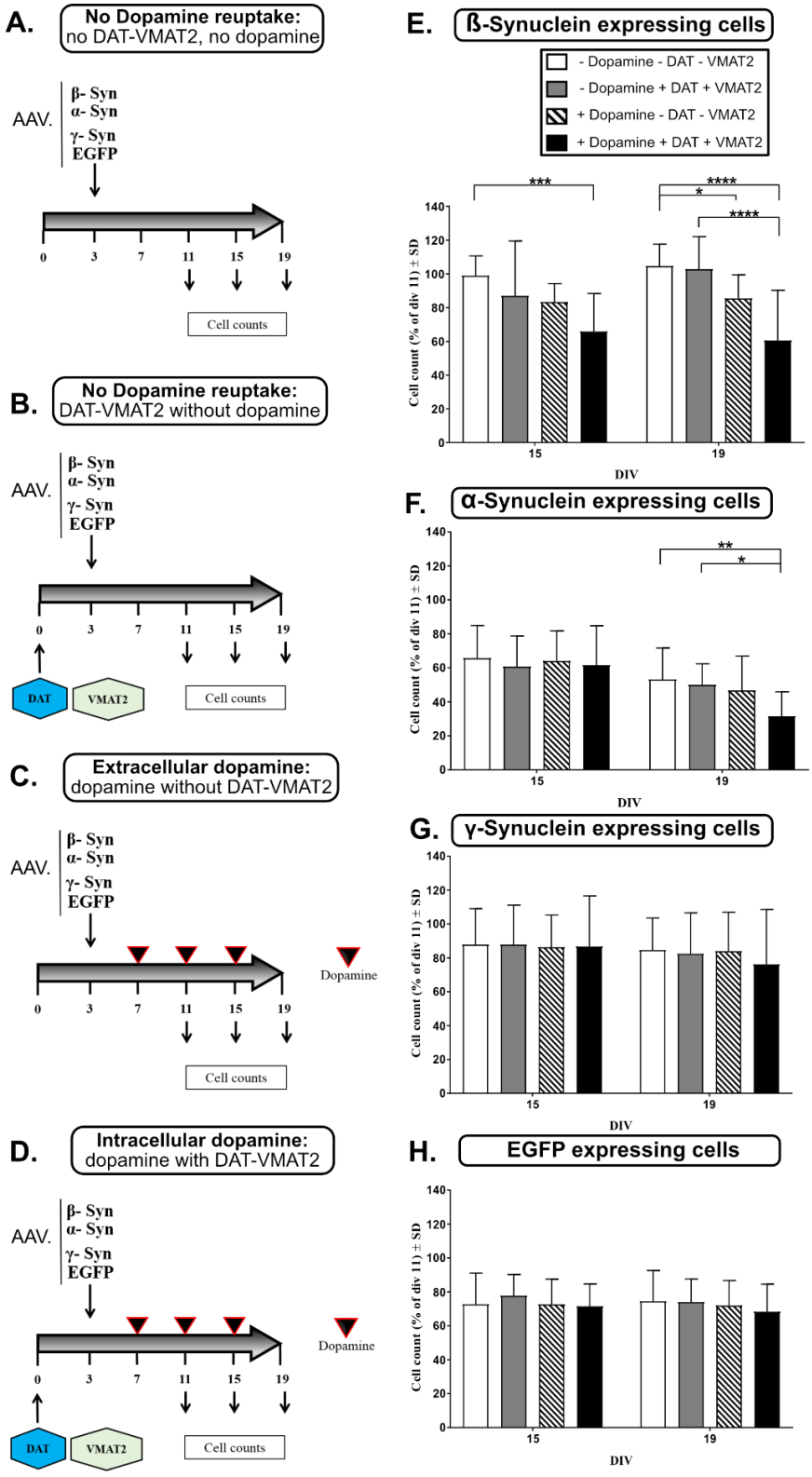

Figure 3.16. Enhanced intracellular dopamine aggravates neurotoxicity of ß-synuclein.

Figure 3.16. Enhanced intracellular dopamine aggravates neurotoxicity of ß-synuclein.

(A, B, C, D) *Schematics of 4 different types of the experimental set-up.* Cells were transduced with AAV-DAT and AAV-VMAT2 vectors before seeding at DIV 0. To take up dopamine, 12.5µM of dopamine was applied to the cell culture supernatant, in the intervals of every 4 days from DIV 7 onwards. Cells were transduced with adeno-associated virus vectors at 3 days *in vitro* (DIV) expressing enhanced green fluorescent protein (EGFP), and bicistronic AAV vectors coexpressing EGFP + α-synuclein, EGFP + ß-synuclein and EGFP + γ-synuclein ($60x10^8$ vg of virus/250,000 neurons). Cells were also transduced with AAV vector expressing nuclear mCherry (NmC) to label the nuclei. The nuclei of the surviving cells were counted at DIV 11, 15, and 19. **(A)** Dopamine was not uptaken in this set-up because it lacked the DAT-VMAT2 and dopamine application. **(B)** Although the DAT-VMAT2 was expressed, dopamine was not uptaken in this set-up because dopamine was not applied to the culture supernatant. **(C)** Dopamine was not uptaken as DAT-VMAT2 was not expressed, but dopamine was applied to the culture supernatant. **(D)** Dopamine was uptaken in this set-up because the cells expressed DAT-VMAT2 and they were also treated with dopamine.

(E, F, G, H) Surviving cells overexpressing ß-synuclein, α-synuclein, γ-synuclein, and EGFP, respectively, analyzed at DIV 15 and DIV 19.

Bars represent the percentage of surviving cells (normalized to DIV 11). Error bars represent standard deviation (SD) of cell count. Statistics by 1-way analysis of variance/Dunnett's test where black bar (intracellular dopamine) was compared against controls (white and grey bar), and patterned bar (extracellular dopamine) was compared against the controls. *p=0.0332, **p=0.0021, ***p<0.0002, ****p<0.0001. N=11-13 independent transductions. 5 independent experiments. Power > 0.90.

Summary: Robust dopamine production and enhanced intracellular dopamine aggravates the neurotoxic properties of ß-synuclein, and to a similar extent, of α-synuclein. Dopamine did not aggravate cell loss in EGFP and γ-synuclein expressing cells.

3.4. Dopamine does not modulate the endogenous network activity in ß-synuclein and α-synuclein overexpressing cells

The spontaneous network activity is impaired in several psychiatric and neurodegenerative diseases like depression, Alzheimer´s and Parkinson´s disease (Mohan et al. 2016; Tessitore et al. 2012). Our group reported that α-synuclein impairs endogenous network activity by decreasing the action potential frequency (Tolo et al. 2018). Therefore, it was important to study the modulation in endogenous network activity by ß-synuclein in the presence of dopamine.

This experiment was divided into 2 groups of cells:

Group – 1 (*control****):*** Untransduced cells with no L-DOPA application to the culture medium (**Fig.3.18.A**).

Group – 2 (*dopamine-producing****):*** Cells transduced by neuron-specific AAV 6 vectors expressing AADC and VMAT2. L-DOPA was applied to the culture medium (**Fig.3.18.B**)

Primary cortical neurons (with and without AADC-VMAT2 expression) were transduced at DIV 2 with AAV6 vectors expressing calcium sensor (GCaMP) and anti-apoptotic factor (Bcl-xL). Bcl-xL maintained the neuronal viable cell counts until the end of DIV 23. Primary cortical neurons were later transduced with bicistronic AAV6 vectors at DIV 3 coexpressing NmC + α-synuclein, NmC + ß-synuclein and NmC + γ-synuclein ($60x10^8$ vg of virus/250,000 neurons).

Each event of synchronized depolarization of 10% of neurons was defined as a burst. The frequency of bursts (per minute) was counted at DIV 15 and 19. The average percentage of neurons involved in a single synchronous depolarization was defined as

the percentage of network participation, which was calculated at DIV 15 and 19. The nuclei of the surviving cortical neurons were counted at DIV 15, and 19.

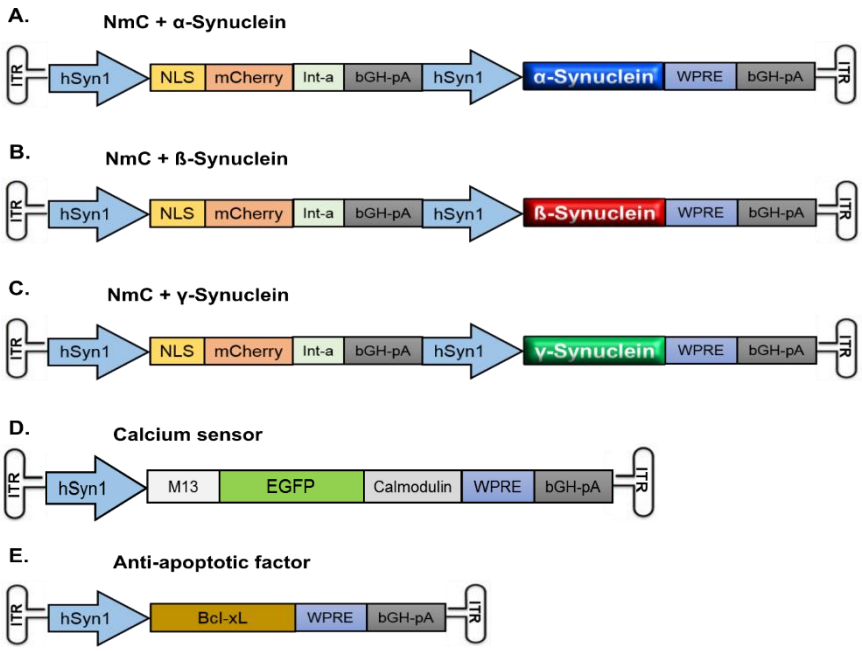

Fig. 3.17. Bicistronic and monocistronic AAV vectors to study modulation in endogenous network activity

(A, B, C) *Bicistronic AAV vector genomes:* Bicistronic AAV vectors coexpressing **(A)** nuclear localized mCherry (NmC) + α-synuclein, **(B) NmC** + ß-synuclein, **(C) NmC** + γ-synuclein. **(D, E)** *Calcium sensor and anti-apoptotic factor:* Monocistronic AAV vectors expressing **(D)** GCaMP, calcium sensor, and **(E)** BcL-xL, an anti-apoptotic factor.

hSyn1: human synapsin 1 gene promoter, NLS: nuclear localization signal, WPRE: woodchuck hepatitis virus post-transcriptional control element, bGH-pA: bovine growth hormone poly-adenylation site, Int-a: intron, M13: a peptide sequence from myosin light-chain kinsae, ITR: inverted terminal repeat.

Dr. Sebastian Kügler, Monika Zebski and Sonja Heyroth produced viruses (AAVs). Monika Zebski cloned the AAV vector genomes. Department of Neurology, University Medical Center Goettingen (UMG).

Results suggested that dopamine production did not impair the frequency of action potentials and the percentage of network participation in ß-synuclein, α-synuclein, and γ-synuclein overexpressing cells (**Fig.3.18.D.E.F**). Bcl-xL maintained constant cell counts in the control and the dopamine-producing group of neurons (**Fig.3.18.C**).

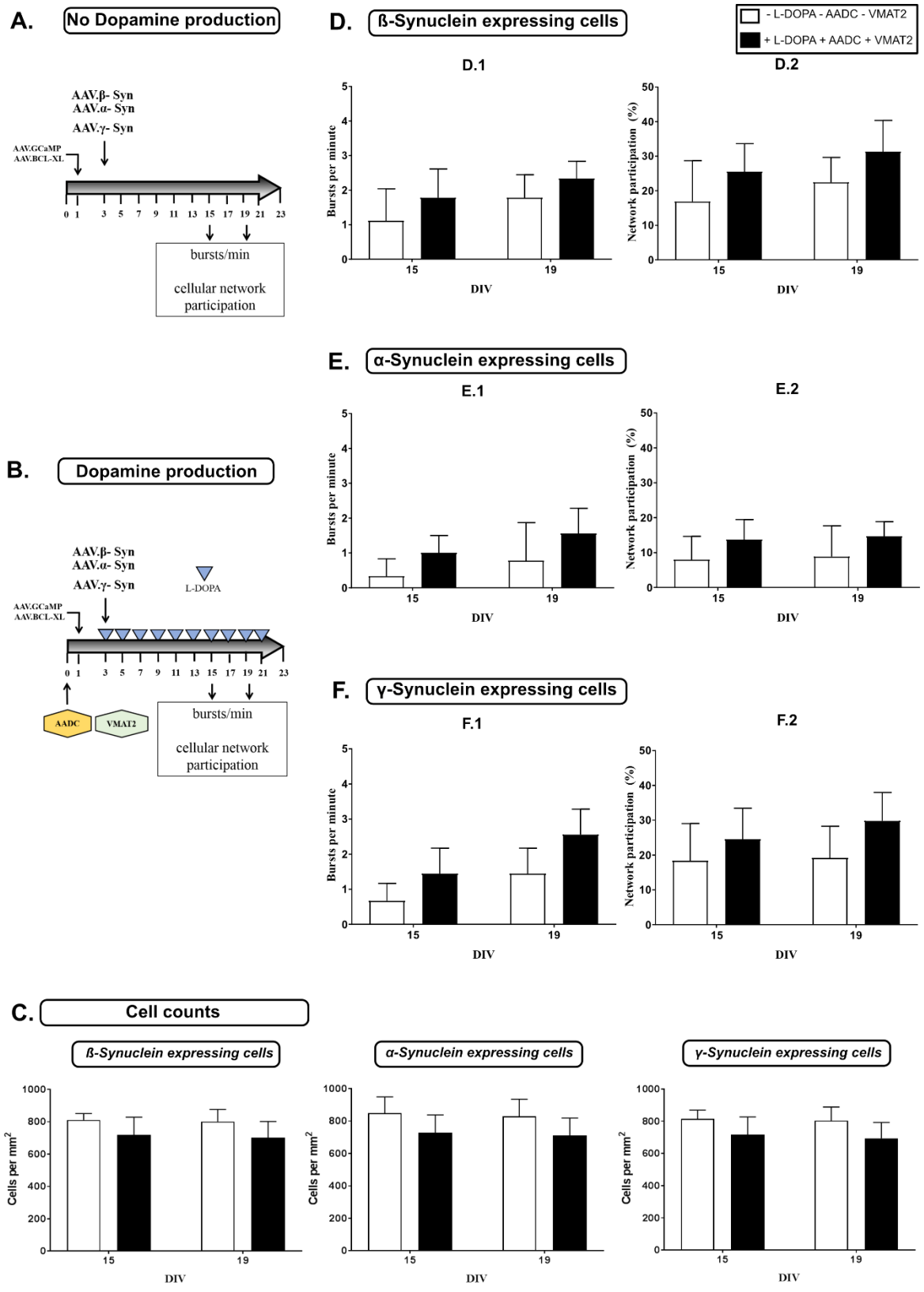

Figure 3.18. Dopamine does not modulate the endogenous network activity in ß-synuclein and α-synuclein expressing cells.

Figure 3.18. Dopamine does not modulate the endogenous network activity in ß-synuclein and α-synuclein expressing cells.

(A, B) *Schematics of 2 different types of the experimental set-up.* Cells were transduced with AAV-AADC and AAV-VMAT2 vectors before seeding at DIV 0. To produce dopamine, 10µM of L-DOPA was applied to the cells in the intervals of every two days from DIV 3 onwards. Cells were transduced at DIV 2 with adeno-associated virus vectors expressing calcium sensor (GCaMP) and anti-apoptotic factor (Bcl-xL). At DIV 3, cells were transduced with bicistronic AAV vectors coexpressing nuclear mCherry (NmC) + α-synuclein, NmC + ß-synuclein, and NmC + γ-synuclein ($60x10^8$ vg/250,000 neurons). **(A)** Dopamine was not produced in this set-up because neurons lacked the AADC-VMAT2 and L-DOPA application. **(B)** Dopamine was produced in this set-up because cells expressed AADC-VMAT2 and L-DOPA was applied to the cell culture supernatant. Each event of synchronized depolarization of 10% of cells was defined as a burst.

The frequency of bursts per minute was counted at DIV 15 and 19. The average percentage of cells involved in a single synchronous depolarization was defined as the percentage of network participation, which was calculated at DIV 15 and 19.

(D.1, E.1, F.1) Burst frequency and **(D.2, E.2, F.2)** network participation of cells expressing ß-synuclein **(D)**, α-synuclein **(E)**, and γ-synuclein **(F)**, analyzed at DIV 15 and DIV 19. **(C)** Number of surviving cells expressing ß-synuclein, α-synuclein, and γ-synuclein.

Bars represent the burst frequency **(D.1, E.1, F.1)** and the network participation of cells **(D.2, E.2, F.2)**. Error bars represent standard deviation (SD) of burst frequency, network participation percentage, and cell counts. Statistics by unpaired 2-tailed t-test with Welch´s correction, where black bar (dopamine-producing neurons) was compared against white bar (non-dopamine producing neurons). N=9 independent transductions. 3 independent experiments. Power > 0.90.

Kristian Leite performed the experiment, generated data, and assisted to prepare figure legends. Anupam Raina analyzed and plotted the data, identified trends from the plots to derive conclusion, and generated the figure with legends. Department of Neurology, University Medical Center Goettingen (UMG).

Summary: Results suggest that dopamine does not impair the endogenous network activity in α-synuclein and ß-synuclein overexpressing cortical neurons. The impact of α-synuclein and ß-synuclein on electrical activity is mechanistically not well characterized. In the absence of dopamine production, Tolo and colleagues reported that α-synuclein impairs endogenous network activity of cortical neurons *in vitro* (Tolo et al. 2018). To speculate, dopamine production might itself enhance the burst frequency in these cell-models in such a way that impairments in network activity by α-synuclein and ß-synuclein is completely masked or not detected. However, this needs to be further studied.

3.5. Dopamine interacts with ß-synuclein

Dopamine interacts with α-synuclein at ^{125}YEMPS^{129} motif in the C-terminus and alters its aggregation properties by increasing total steady-state levels of α-synuclein oligomers (Mor et al. 2017). In this thesis, it was found that dopamine aggravated the neurotoxicity of ß-synuclein, and to a similar extent, of α-synuclein. Therefore, it was of interest to study the interaction of dopamine to ß-synuclein.

The NMR spectra were collected and recorded on a Bruker 800MHz spectrometer at 10°C in 20mM sodium phosphate buffer (pH 6.0), 2mM TCEP (tris(2-carboxyethyl)phosphine), and 10% D_2O (deuterated water). Two-dimensional ^{1}H -^{15}N heteronuclear single quantum coherence (HSQC) spectrum was recorded to study the interaction of dopamine with β-synuclein. 100μM of β-synuclein were titrated against different concentrations of dopamine ranging from 0.02mM to 2mM. Chemical shift perturbations (CSP) were calculated using the formula $CSP = [(\delta H)^2 + (0.1\ \delta N)^2]^{1/2}$, where δN and δH are chemical shift differences (parts per million (ppm) of nitrogen and proton, respectively.

The NMR spectra (CSP > 0.35 ppm) results of β-synuclein and dopamine studies (**Fig. 3.19.A**) indicated that dopamine interacted all over β-synuclein with a dissociation constant (ß.K_d) value of 2.10 ± 0.16 mM (**Fig. 3.19.B**). In the N-terminal domain (NTD) of β-synuclein, dopamine interacted with K6, A17, V49, Q50, and K60 (**Fig. 3.19.C**). In the non-amyloid beta component (NAC) domain of β-synuclein, dopamine interacted with I77. In the C-terminal domain (CTD) of β-synuclein, dopamine interacted with E87, M112, and Y127 (**Fig. 3.19.D**). The K_d value of dopamine´s interaction with α-synuclein is reported (using surface plasmon resonance (SPR)) to be 10-100 fold less than ß.K_d (Jha et al. 2017), suggesting a weak binding of dopamine to ß-synuclein in comparison to the binding of dopamine to α-synuclein.

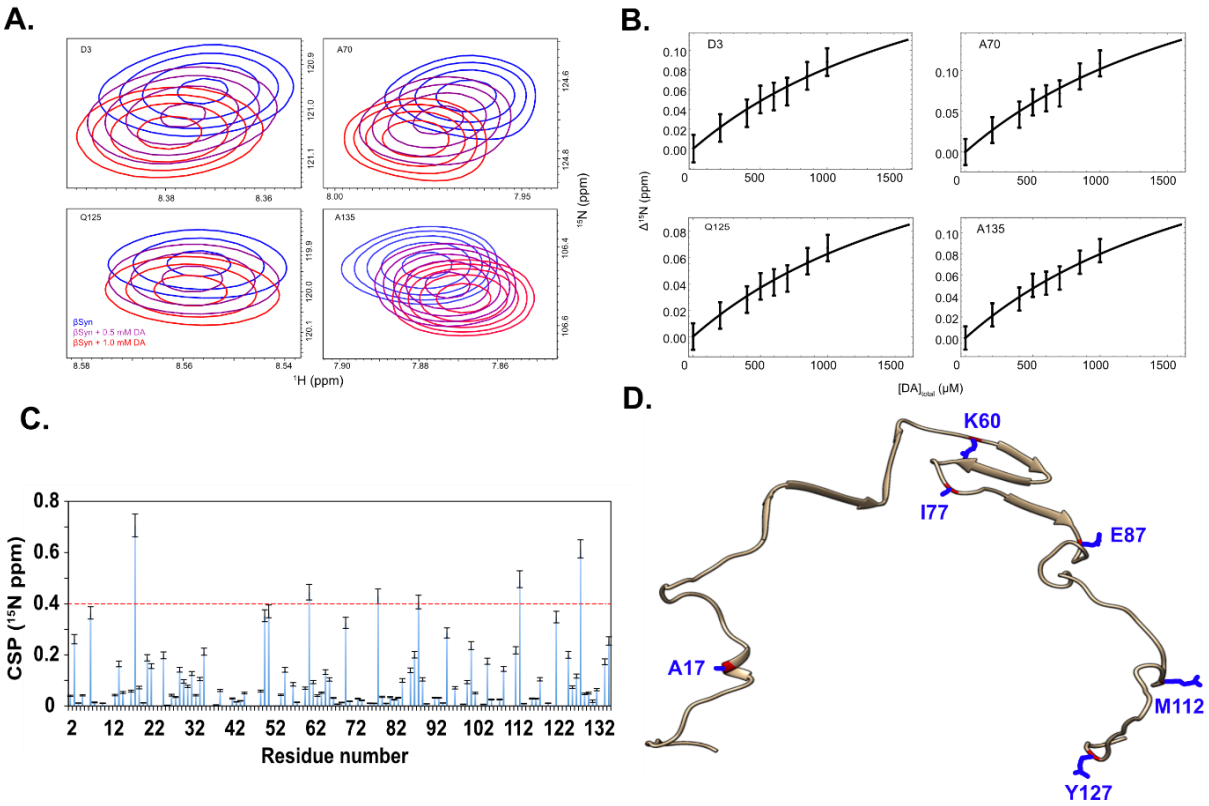

Figure 3.19. Dopamine interacts with ß-synuclein.

Figure 3.19. Dopamine interacts with ß-synuclein.

(A) A large number of residues of ß-synuclein show chemical shift perturbations (CSP) upon binding dopamine. Overlay of the NMR spectra of the representative residues D3, A70, Q125, and A135 are shown. The spectra are shown using the color scheme: free ß-synuclein (blue), 0.5 mM dopamine bound to ß-synuclein (magenta) and 1.0mM dopamine bound to ß-synuclein (red).

(B) All the residues of ß-synuclein that showed significant ^{15}N CSP (Δδ) were fitted simultaneously to determine the K_d = 2.10 + 0.16 mM (standard error of fitting). The error bar on the data points for a residue was calculated from repeat measurement of ß-synuclein peak positions at 1 mM dopamine concentration.

(C) The residue-wise difference of the ^{15}N chemical shifts between free and bound ß-synuclein in solution (Δδ). The error bars represent standard error of fitting.

(D) The full-length ß-synuclein modeled based on its homology with α-synuclein using the Swiss-Model program. The residues with CSP values in the ^{15}N dimension, i.e., Δδ > 0.4 ppm, (in red; shown in stick representation) were mapped onto the modeled structure of ß-synuclein (in golden). For modeling, the full-length α-synuclein structure from its pathogenic fibrils was used as the template (PDB 2n0a; Tuttle et al. 2015).

Dr. Kalyan Chakrabarti analyzed NMR spectra and plotted data to determine the K_d. Modeled full-length ß-synuclein. Generated the figure with legends. Dr. Stefan Becker kindly provided the purified α-synuclein and ß-synuclein. Department of NMR-based Structural Biology, Max Planck Institute for Biophysical Chemistry, Goettingen.

Anupam Raina performed the experiment under the supervision of Dr. Kalyan Chakrabarti, generated the data, and identified trends from the plots to derive conclusion. Department of Neurology, University Medical Center Goettingen (UMG).

Summary: Dopamine interacted all over β-synuclein. The ß.K_d value was found to be 2.10mM, which is 10-100 fold more than the reported (using SPR) α.K_d value. This suggests that it is probably not ß-synuclein-dopamine binding directly responsible for aggravated neurotoxicity.

3.6 Summary of Results – II

Two different *in vitro* cell-based models with dopaminergic neurotransmitter phenotype were established using glutamatergic cortical neurons, which demonstrated robust dopamine production, and enhanced intracellular dopamine levels. Both the cell-models acted as valuable research tools to study the neurodegeneration induced by ß-synuclein in the context of dopamine.

Dopamine aggravated the neurotoxic properties of ß-synuclein, and to a similar extent, of α-synuclein. Dopamine does not impair the endogenous network activity in ß-synuclein and α-synuclein expressing cells. Dopamine interacted all over ß-synuclein with binding affinity of 10-100 fold lower in comparison to α-synuclein and dopamine interaction.

Discussion

4. Discussion

So far, the potential neurotoxicity of ß-synuclein had not been linked to a dopaminergic neurotransmitter phenotype, and dopamine had not been known to aggravate neurotoxic properties of ß-synuclein. Rather, α-synuclein is linked to dopaminergic neurotransmitter phenotype because studies revealed that dopamine stabilized potentially toxic α-synuclein oligomers *in vitro* by interaction with $_{125}$YEMPS$_{129}$ motif in C-terminus of α-synuclein (Conway et al. 2001; Mazzulli et al. 2007; Mazzulli et al. 2006; Norris et al. 2005), and dopamine increased total steady-state levels of α-synuclein oligomers and promoted larger oligomer conformations *in vivo* (Mor et al. 2017). Furthermore, ß-synuclein aggregates and induces neurodegeneration of dopaminergic neurons *in vivo* (Taschenberger et al. 2013). Therefore, it was important to investigate the link between ß-synuclein and dopamine, which might explain the neurodegeneration of mostly dopaminergic neurons in Parkinson´s disease. The results of this study provide new perspectives on neurodegeneration induced by ß-synuclein in the context of the neurotransmitter dopamine.

A therapeutic intervention for Parkinson´s disease (PD) is desperately needed. PD is a progressive neurodegenerative disorder that affects more than 7 million people around the globe, and the number is expected to double, with over 14 million cases by 2040 (Dorsey and Bloem 2018). The motor symptoms include tremor at rest, rigidity, bradykinesia or akinesia, and non-motor symptoms include depression, cognitive decline, and sleep disturbances (Jellinger 2012). The pathophysiological features of PD include progressive degeneration of dopaminergic neurons in the substantia nigra and accumulation of Lewy bodies and Lewy neurites in substantia nigra and other regions of brain, which are protein rich intracellular inclusions majorly comprised of aggregated form of protein α-synuclein (Spillantini et al. 1997; Goedert et al. 2013).

The studies indicate a relationship between α-synuclein and the neurotransmitter phenotype dopamine.

The interaction of dopamine with α-synuclein conferring neurodegeneration or neuroprotection is heavily debated. Cytosolic dopamine (DA) oxidizes to electrophilic dopamine-quinone (DAQ) and reactive oxygen species which may interact with cytosolic dopamine or cytosolic proteins to form neurotoxic products (Cubells et al. 1994; Graham 1978; Jenner and Olanow 1996; Sulzer and Zecca 2000). α-synuclein oligomerizes to protofibrils, which further oligomerize to form fibrils (Lashuel et al. 2013). The intermediate α-synuclein protofibrils are suggested to be most neurotoxic. Lansbury and colleagues suggest that in a cell-free solution, DAQ or dopamine might interact with α-synuclein to form DAQ-α-synuclein (DAQ-αS) or DA-α-synuclein (DA-αS) adduct which stabilizes toxic protofibrils, thereby promoting neurodegeneration (Conway et al. 2001; Sulzer 2001). Even though α-synuclein and dopamine adducts are known to be cytotoxic in vitro, not much is known about how α-synuclein and dopamine adducts and DAQs can impair dopaminergic neurons *in vivo*. Using 3 different mice systems with enhanced dopamine production (by more than 50%), wild-type mice (control), A53T mice, and human α-synuclein expressing A53T mice, Giasson, Mor and colleagues demonstrated that enhanced dopamine production (by more than 50%) in A53T mice expressing human α-synuclein resulted in the loss of dopaminergic synapses (by 62%) and the number of cell bodies in the substantia nigra (by 25%) after 5 months post injection (mpi) (Mor et al. 2017; Giasson et al. 2002). They further reported that the striatal dopamine levels were reduced by 37% from 2.5 mpi to 5 mpi in human α-synuclein expressing A53T mice (Mor et al. 2017). However, the striatal dopamine levels did not drop significantly in A53T mice as compared to the wild-type mice (Mor et al. 2017). Mor and colleagues further reported that enhanced dopamine levels increased the total steady-state levels of α-synuclein oligomers and

boosted larger oligomeric conformations by performing *in vitro* assays from oligomers isolated from the substantia nigra of A53T mice with enhanced dopamine production and control mice (Mor et al. 2017). The studies so far, provide a link between the neurotransmitter phenotype dopamine and α-synuclein aggregation.

Interestingly, non-amyloidogenic ß-synuclein might confer neuroprotection against α-synuclein (Hashimoto et al. 2001; Park and Lansbury 2003; Hashimoto, Rockenstein, et al. 2004); however, the neurodegenerative and neuroprotective role of ß-synuclein is still disputed. In 2010, Fujita and colleagues demonstrated that P123H ß-synuclein, one of the mutants of ß-synuclein associated with familial dementia with Lewy bodies (DLB), stimulated neurodegeneration, and might seed the aggregation of α-synuclein *in vivo* (Fujita et al. 2010). It was in 2013 that Taschenberger and colleagues were the first to report that ß-synuclein aggregates, and induces neurodegeneration in dopaminergic neurons to a similar extent as α-synuclein *in vivo* (Taschenberger et al. 2013). The evidence that ß-synuclein aggregates in dopaminergic neurons, strongly suggests a link between ß-synuclein and the neurotransmitter phenotype dopamine that was not investigated so far.

In order to investigate the link between ß-synuclein and neurotransmitter phenotype dopamine, a better cell-model with dopaminergic neurotransmitter phenotype is highly demanded. Dopaminergic neurons isolated from rodent midbrain embryos contain only a minority of dopaminergic neurons in a majority of GABAergic neuronal culture. Additionally, the midbrain cultures are difficult to prepare, and are short-lived (Yan, Studer, and McKay 2001; Prasad et al. 1994). Dopaminergic neurons can be generated from human midbrain neural stem cells (Ribeiro et al. 2013), human fibroblasts (Caiazzo et al. 2011), or human induced pluripotent stem cells (iPSCs) (Kriks et al. 2011); however, the yield of dopaminergic neurons is not sufficient, greatly

variable, a robust dopamine production in the generated dopaminergic neurons is highly questionable (Marton and Ioannidis 2018). In contrast, the cortical neurons from rodent embryos can be readily isolated in very large amounts, and thus are valuable research tools. These neurons survive in culture for several weeks, show endogenous non-stimulated neuronal network activity, and are a reliable cellular model for neurobiological studies. It has not been investigated so far, if postnatal cortical neurons can be experimentally (*in vitro*) prompted to switch their neurotransmitter phenotype to another neurotransmitter phenotype of interest. The approach of experimentally switching readily available cortical neurons to the desired neurotransmitter phenotype would deliver the advantage that neuronal morphology and all functionalities have already been established, and a large number of neurons with the desired neurotransmitter phenotype could be achieved.

4.1. Project 1: Transdifferentiation of primary cortical neurons towards dopaminergic neurotransmitter phenotype

4.1.1. Important transcription factors for inducing dopaminergic neurotransmitter phenotype: Lmx1a, Nurr1, Pitx3, and Ascl1

I investigated transcription factors known to be important for patterning and differentiation into dopaminergic neurons for their potential to induce dopaminergic neurotransmitter phenotype in cortical neurons isolated from E18 embryonal rat brain. Transcription factors Nurr1 (nuclear receptor 4a2), Lmx1a (LIM homeobox transcription factor 1a), and Pitx3 (pituitary homeobox 3) are known to be important for patterning and differentiation into dopaminergic neurons (Arenas, Denham, and Villaescusa 2015). Shh specifies the floor plate by upregulating Foxa2 at E8 in mice

(Ang et al. 1993). Moreover, one of the major events in the patterning of midbrain floor plate is the upregulation of Lmx1a/b by Foxa2 and Wnt1/ß-catenin (Chung et al. 2009). Foxa2 (Lin et al. 2009) together with Otx2 (Ono et al. 2007) regulate the expression of Lmx1a/b. ß-catenin upregulates Lmx1a and Otx2, and on the other hand, Lmx1a upregulates Wnt1 and Msx1, thus forming an Lmx1a-Wnt1-ß-catenin autoregulatory loop together with Foxa2 and Otx2 (Chung et al. 2009). Furthermore, Lmx1a upregulate Nurr1 and Pitx3 which are necessary for the differentiation and survival of midbrain dopaminergic neurons (Arenas, Denham, and Villaescusa 2015). Interestingly, studies revealed that the deletion of both Lmx1a and Lmx1b leads to almost complete loss of midbrain dopaminergic neurons (Yan et al. 2011). Addionally, Nurr1 and Pitx3 regulate each other (Volpicelli et al. 2012). Nurr1 upregulates En1, which in turn regulates Pitx3, TH (tyrosine hydroxylase), VMAT2 (vesicular monoamine transporter 2), DAT (dopamine transporter), therefore inducing the expression of dopaminergic battery of genes (Veenvliet et al. 2013). In summary, the studies suggested that Lmx1a is one of the most essential transcription factor for specification into midbrain dopaminergic neurons. Furthermore, Nurr1 and Pitx3 are crucial for terminal differentiation, and survival of midbrain dopaminergic neurons, and maintenance of dopaminergic neurotransmitter phenotype.

I also investigated a pan-neuronal transcription factor Ascl1 that was used with Brn1 and Myt1l to transdifferentiate fibroblasts into induced neurons (Vierbuchen et al. 2010). Ascl1 along with Nurr1 and Lmx1a transdifferentiated fibroblasts to dopaminergic neurons (Caiazzo et al. 2011). Wapinski and colleagues revealed that Ascl1 alone was able to push the fate of fibroblasts to induced neurons, suggesting that Ascl1 plays a key role in the process of transdifferentiation (Wapinski et al. 2013). Therefore, we also introduced Ascl1, along with Lmx1a, Nurr1, and Pitx3 to transdifferentiate cortical neurons towards dopaminergic neurotransmitter phenotype.

4.1.2. Ascl1, Nurr1, and Lmx1a (“ANL”) induce dopaminergic neurotransmitter phenotype in a subpopulation of cortical neurons

Cortical neurons can be isolated in large amounts from rat pups at embryonic day of development 15 – 19 (E15 - E19). These neurons survive in culture for several weeks, show endogenous non-stimulated neuronal network activity, and are a reliable cellular model for neurobiological studies. The majority of cortical neurons are glutamatergic, while GABAergic neurons make up 5-20%, and catecholaminergic neurons are present in very low amounts (Dichter 1978, 1980; Herrero et al. 1998; Stichel and Muller 1991). The relative percentage of catecholaminergic (TH+) neurons depends on the time of isolation of cells. Cortical neurons isolated at E13 contained large amounts of TH+ neurons, which lose their phenotype over time, while cortical neurons isolated at E18 contain only very minor amounts of TH+ neurons from the time of seeding (Iacovitti et al. 1987).

The cortical cultures were isolated at E18 and maintained in the presence of glial cells, which at later stages constitute 40-50% of all cells. The transcription factors were expressed in these neurons by adeno-associated viral (AAV) vectors from the time of seeding onwards. Transcription factors were driven by hSyn1 promoter that restricts the expression of transcription factors strictly to neurons (Kugler et al. 2003). Moreover, each transcription factor, Nurr1, Lmx1a, and Pitx3, when overexpressed alone in human iPSCs, was capable to pattern and differentiate human iPSCs to 50% of dopaminergic neurons, suggesting that Nurr1, Lmx1a, and Pitx3 are functional (Mahajani et al. unpublished data).

Results suggested that Ascl1, Nurr1, and Lmx1a (“ANL”) overexpression induced the expression of TH in a subpopulation (15-22%) of cortical neurons. The cortical

dopaminergic neuron-like cells (cDNs) expressed all classical dopaminergic markers, TH, AADC, DAT, and VMAT2 that are necessary for producing dopamine, suggesting an induction of dopaminergic neurotransmitter phenotype. The results further suggest that Ascl1 alone cannot induce dopaminergic neurotransmitter phenotype; however, Nurr1 alone can induce dopaminergic neurotransmitter phenotype in a small number (< 2.5%) of cortical neurons already at DIV 7 but their numbers did not increase over time. Combining Nurr1 expression with Lmx1a did not increase the overall TH+ cell numbers. Intriguingly, Nurr1 when combined with Ascl1 significantly enhanced the yield of dopaminergic neuron-like cells (12%), and the yield was insignificantly improved by coexpression of Lmx1a with Ascl1 and Nurr1.

Currently, it is unclear how Ascl1 together with Nurr1 induces dopaminergic neurotransmitter phenotype in a subpopulation of cortical neurons. Studies with Ascl1 suggest that Ascl1 is a pioneer transcription factor, which may access the silent sites directly on the nucleosomes to initiate transdifferentiation (Bertrand, Castro, and Guillemot 2002; Iwafuchi-Doi and Zaret 2014; Wapinski et al. 2013).

In conclusion, results demonstrated that the concerted action of Ascl1, Nurr1, and Lmx1a (“ANL”) induced dopaminergic neurotransmitter phenotype in a subpopulation of cortical neurons, however the mechanism remains to be elucidated.

4.1.3. Cortical GABAergic neurons transdifferentiate to dopaminergic neuron-like cells (cDNs)

The transduction efficacy of AAV6 vectors in cortical neuron culture is sufficient to reach > 90% of all neurons (Taschenberger et al. 2013; Tolo et al. 2018). Therefore, I wondered why the percentage of transdifferentiated cortical neurons was limited to 15%. Immunocytochemical analyses of cDNs (identified as TH), GABAergic neurons

(identified as GAD 65), and glutamatergic neurons (identified as CaMKIIß) revealed that TH expression was induced in GABAergic neurons because TH and GAD65 colocalize. At DIV 7, cDNs coexpressing TH and GAD65 amounted to 55%, which at DIV 14 and 21 dropped significantly. Furthermore, results suggested GAD 65 marker in GABAergic neurons diminishes by DIV 21 suggesting a transdifferentiation to dopaminergic neurotransmitter phenotype. Results further revealed that "ANL" overexpression specifically caused degeneration of glutamatergic neurons already at DIV 7, resulting in drop of overall number of neurons. As it was found that GABAergic neurons are the source of cDNs, the drop in the number of GABAergic neurons can be accounted by an increase in the number of cDNs (TH+) from DIV 7 to DIV 21 and diminishing of GAD65 marker from DIV 7 to DIV 21.

In light of the published data, the results are novel because I demonstrated for the first time that postnatal cortical GABAergic neurons could be transdifferentiated to dopaminergic neuron-like cells by Ascl1, Nurr1, and Lmx1a *in vitro*. In the context of cortical neurons, it is reported that Fezf2 could reprogram the postnatal callosal projection neurons to its subtype corticofugal projection neurons (Arlotta et al. 2008; De la Rossa et al. 2013). The recently published data (September 2018) by Niu and colleagues revealed that striatal GABAergic neurons could be reprogrammed to dopaminergic neuron-like cells by Sox2, Nurr1, Lmx1a, Foxa2 and valproic acid *in vivo* (Niu et al. 2018). They reported that this combination yielded 1,700 TH+ cells per injection in an adult mouse striatum after 36 weeks post injection (Niu et al. 2018).

In conclusion, I have shown that cortical GABAergic neurons can be transdifferentiated to dopaminergic neurotransmitter phenotype at the cost of significant loss of glutamatergic neurons in cortical culture.

4.1.4. Midbrain GABAergic neurons cannot transdifferentiate into dopaminergic neurotransmitter phenotype

In order to improve the yield of dopaminergic neurons, I next hypothesized that “ANL” overexpression in rat E14.5 midbrain neurons might enhance the yield of dopaminergic neurons; as it is reported that the GABAergic neurons (GAD+ cells) are predominantly present in a midbrain culture along with a minority of TH+ neurons (Gaven, Marin, and Claeysen 2014). I thus overexpressed “ANL” in neurons isolated from rat E14.5 midbrain.

To my surprise, I found that there was no increase in the amount of TH+ neurons, because the midbrain GABAergic neurons did not transdifferentiate into dopaminergic neurotransmitter phenotype.

Cortical GABAergic neurons (cGNs) primarily originate from medial ganglionic eminence (MGE) and caudal ganglionic eminence (CGE), and a minority from lateral ganglionic eminence (Pleasure et al. 2000; Butt et al. 2005; Wonders and Anderson 2006). Transcription factors Nkx2.1 and Lhx6 are majorly involved in the specification of cGNs originating from MGE (Azim et al. 2009; Zhao et al. 2008), whereas Gsx1/2 and Ascl1 along with Dlx1/2/5/6 are majorly involved in the specification of cGNs originating from CGE (Casarosa, Fode, and Guillemot 1999; Wang et al. 2010; Xu et al. 2010). Ascl1 upregulates Dlx1/2 which upregulates Dlx5/6 in CGE precursors (Long et al. 2009). Ectopic overexpression of Dlx2/5 can induce the expression of GAD65/67 in forebrain and midbrain slice cultures (Colasante et al. 2008; Stuhmer et al. 2002).

The development and specification of midbrain GABAergic neurons (mGNs) are not well understood. The mGNs originate from ventral hindbrain and require transcription factors Tal2 and GATA2 to upregulate Tal1 and GATA3 for the maintenance of

GABAergic phenotype (Achim et al. 2012; Joshi et al. 2009). Mutation in GATA2 leads to a switch in the fate of mGNs to glutamatergic neurons (Achim, Salminen, and Partanen 2014; Kala et al. 2009).

Due to the indirect involvement of Ascl1 in the upregulation of GAD65 through Dlx2 in CGE-derived precursor cells, might be cGNs, which pattern and differentiate from CGE-derived precursor cells, are more amenable to fate change than mGNs upon ectopic overexpression of Ascl1, Nurr1, and Lmx1a ("ANL"). I demonstrated that GAD65 marker expression is diminished upon "ANL" overexpression in cortical neurons. In light of the published data, my results suggest that Ascl1 may act as a switch, which controls the expression of GAD65 in cooperation with the ectopic overexpression of Nurr1 and Lmx1a in CGE precursor cells derived postnatal cortical neurons.

In conclusion, midbrain GABAergic neurons did not transdifferentiate into dopaminergic neurotransmitter phenotype because it appears that the cortical GABAergic postnatal cells may undergo patterning, differentiation, and migration in a different microenvironment than midbrain GABAergic postnatal cells. However, the mechanism remains to be elucidated.

4.2. Project 2: Creating a dopaminergic cell-model by the introduction of AADC, VMAT, and extracellular L-DOPA or DAT, VMAT2, and extracellular dopamine into cortical neurons

Transdifferentiation of cortical neurons using transcription factors resulted in low yield of dopaminergic neurons, and led to profound loss of neurons that were unable to transdifferentiate. Therefore, an alternate strategy was employed in which aromatic amino acid decarboxylase (AADC), vesicular monoamine transferase 2 (VMAT2), and extracellular L-3,4-dihydroxyphenylalanaine (L-DOPA) or dopamine transporter (DAT), VMAT2 and extracellular dopamine were introduced into the cortical neurons. Dopamine is produced when L-DOPA is decarboxylated by AADC, and cytosolic dopamine is sequestered into synaptic vesicles by VMAT2 (Cartier et al. 2010).

The cortical neurons isolated from rat pups on embryonic day of development 18 (E18) consist of a majority (80-95%) of glutamatergic neurons and a minority (5-20%) of GABAergic neurons (Dichter 1980; Herrero et al. 1998; Stichel and Muller 1991). Cortical neurons are maintained with glial cells that grow up to 40-50% of all cells in later stages.

Two cell-based models were established. Introduction of AADC, VMAT2 into cortical neurons and extracellular doses of L-DOPA resulted in robust dopamine production. Introduction of DAT, VMAT2 into cortical neurons and extracellular doses of dopamine resulted in enhanced intracellular dopamine levels.

4.2.1. Comparison with the existing cell-models

One of the *in vitro* dopaminergic cell-models routinely used are Lund Human Mesencephalic cells (LUHMES) and human iPSCs derived dopaminergic neurons.

Both, LUHMES (Scholz et al. 2011) and iPSCs (Chambers et al. 2009; Kriks et al. 2011; Theka et al. 2013) are human derived cells which are differentiated into dopaminergic neurons. Even though both the cell-models are human derived and exhibit endogenous electrical activity, the intracellular dopamine levels reported for LUHMES derived dopaminergic neurons are less than 0.2 nanograms (per 10,000 cells) (Scholz et al. 2011). The intracellular dopamine levels in iPSCs derived dopaminergic neurons are not reported. The released dopamine is 2.25 nanograms/ml, however they do not report the total cell-count present at the time-point of dopamine quantification from the supernatant (Kriks et al. 2011). Some of the other *in vitro* cell-models still used are neuroblastoma cell-line SH-SY5Y and pheochromocytoma cell-line PC12 (Chutna et al. 2014; Hasegawa et al. 2004; Kim et al. 2015; Roberti, Jovin, and Jares-Erijman 2011). Although primary midbrain neurons contain only a minority (5 – 10%) of dopamine producing neurons, they are also used to study molecular mechanisms in the context of Parkinson´s disease (Aksenova et al. 2005; Tonges et al. 2014). In this thesis, I found that the developed cell-models mimicking the dopaminergic neurotransmitter phenotype, resulted in robust dopamine production and enhanced intracellular dopamine levels reaching up to 5.0 nanograms (per 10,000 cells), which is the highest-ever achieved in comparison to the existing dopaminergic neuronal cell-models used for PD research.

4.2.2. Multi-transmitter phenotype: A boon or a drawback?

It is reported that dopaminergic neurons in the substantia nigra also release GABA (Tritsch, Ding, and Sabatini 2012). It was found that VMAT2 can sequester GABA into vesicles and release it in the striatum and nucleus accumbens (Tritsch, Ding, and Sabatini 2012). Sabatini and colleagues propose that all dopaminergic neurons from the substantia nigra release GABA. In another report, a subset of dopaminergic

neurons in the ventral tegmental area express vesicular glutamate transporter 2, which also release glutamate in the striatum and nucleus accumbens (Howe and Dombeck 2016). These reports suggest that the release of GABA and glutamate by dopaminergic neurons is a physiological phenomenon. In the developed cell-based models, glutamatergic or GABAergic neurotransmitter phenotype was not eliminated. Glutamatergic vesicles presumably sequester the dopamine produced intracellularly and release it into the supernatant due to the endogenous electrical activity of cortical neurons (Opitz, De Lima, and Voigt 2002; Ramakers, Corner, and Habets 1990; Sun, Kilb, and Luhmann 2010), thereby mimicking the same physiological process demonstrated by midbrain dopaminergic neurons. In conclusion, based on the reports published and the studies performed in this thesis, I can say that having a multi-transmitter phenotype in the developed cell-models is a boon and thus, an important ingredient for making this cell-based model more valuable for PD research.

4.2.3. Dopamine aggravates neurotoxicity of ß-synuclein

Our group reported that when ß-synuclein is overexpressed in substantia nigra of rodent model of PD, ß-synuclein induces neurodegeneration of dopaminergic neurons (Taschenberger et al. 2013). This report suggested a link between ß-synuclein and dopamine, which was not investigated so far. Therefore, it was of interest to study the neurotoxicity induced by ß-synuclein in the context of the neurotransmitter dopamine. After the cell-models with dopaminergic neurotransmitter phenotype were established, the neurotoxicity of ß-synuclein was investigated in the developed cell-models. Intriguingly, results suggested for the first time that dopamine production and enhanced intracellular dopamine aggravated the neurotoxic properties of ß-synuclein and α-synuclein.

As discussed in the introduction, dopamine is known to interact with ^{125}YEMPS^{129} motif present in the C-terminal domain of α-synuclein (Conway et al. 2001; Norris et al. 2005). This interaction leads to kinetic stabilization of α-synuclein oligomers and inhibits their fibrillization (Conway et al. 2001). Dopamine aggravates neurodegeneration of dopaminergic neurons in human α-synuclein A53T transgenic mice by binding to ^{125}YEMPS^{129} motif and increasing the steady state levels of α-synuclein oligomers (Mor et al. 2017). As a result, the toxic α-synuclein oligomeric species may result in several cellular dysfunctions. The dissociation constant (α.K_d) of dopamine binding to α-synuclein using NMR is not yet studied.

Interestingly, from the results it appears that dopamine binds all over ß-synuclein, and to Y127, E87, M112 on the C-terminus with a dissociation constant (ß.K_d) of 2.10 mM. Comparing ß.K_d with α.K_d (as reported) indicates that the binding affinity of dopamine to α-synuclein is much weaker than the binding affinity of dopamine to α-synuclein. On comparing the C-terminal regions of α-synuclein and ß-synuclein, the ^{125}YEMPS^{129} motif of α-synuclein is different by ^{119}YEDPP^{123} on ß-synuclein, suggesting that the lack of ^{125}YEMPS^{129} motif on ß-synuclein might be the reason of poor affinity of dopamine to ß-synuclein (**Fig. 4.1**). This suggests that it is probably not ß-synuclein-dopamine binding directly responsible for aggravated neurotoxicity.

Next, I scrutinized potentially toxic metabolites known to be involved in dopamine metabolism. One of the metabolites that is known to be involved in α-synuclein aggregation is 3,4-dihydroxyphenylacetaldehyde (DOPAL). DOPAL is generated by the enzyme MAO. It is highly unstable and a toxic product of dopamine (DA) metabolism. Reports suggest that DOPAL:DA ratios are higher in PD brains as compared to the healthy control brains (Goldstein et al. 2011). It has been reported that DOPAL can covalently modify the lysine residues (**shown in figure 4.1**) in cell-

models (HEK293T and primary cortical neurons) and cell-free solution (Plotegher et al. 2017). DOPAL can oligomerize α-synuclein, and α-synuclein-DOPAL oligomers are reported to permeabilize lipid membranes, thus affects the structural and functional integrity of synaptic vesicles (Plotegher et al. 2017).

When I analyzed the structural similarities of ß-synuclein and α-synuclein, I found that ß-synuclein contains 8 lysine residues (out of 11 possible binding sites) at the same position found in α-synuclein to which DOPAL is known to bind covalently. In conclusion, considering the existing reports about DOPAL, the results from this my thesis provides a clue about the possible role of toxic DOPAL, and not dopamine directly, in aggravating the neurotoxicity of ß-synuclein.

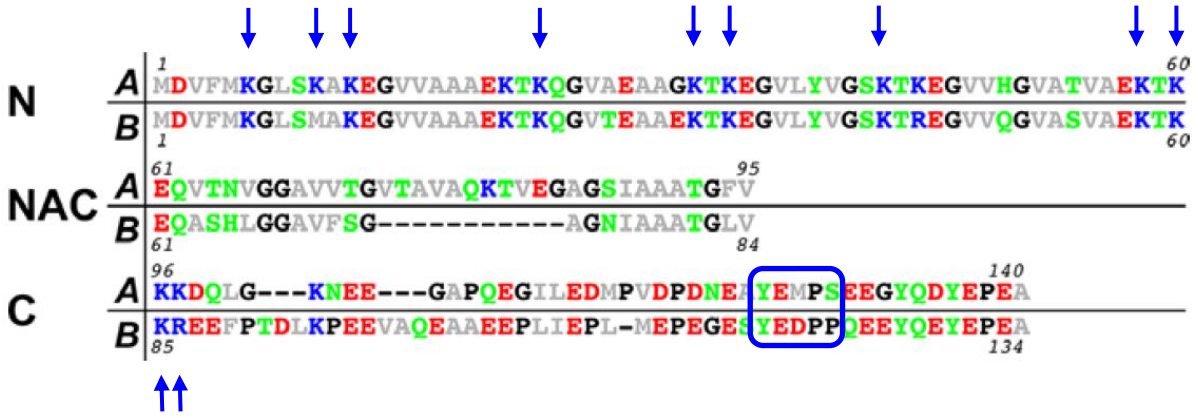

Figure 4.1 Comparison of α-synuclein and ß-synuclein sequences

A – α-synuclein, B – ß-synuclein, N – N-terminal region, NAC – NAC domain, C – C-terminal region

Hydrophobic residues (gray), positively charged residues (blue), negatively charged residues (red), uncharged-polar residues (green) (Williams, Yang, and Baum 2018).

Blue box: dopamine binding site on α-synuclein and the corresponding site on ß-synuclein.

Blue arrows: reported binding sites of DOPAL on α-synuclein and the corresponding site on ß-synuclein.

Conclusion and perspectives

5. Conclusion and perspectives

The results of this thesis demonstrate for the first time that dopamine aggravates the neurotoxic properties of ß-synuclein. It has been reported that α-synuclein impairs endogenous network activity by decreasing the action potential frequency (Tolo et al. 2018). However, in this study, it was found that dopamine production in α-synuclein and ß-synuclein expressing cells, does not impair the endogenous network activity *in vitro*. Furthermore, NMR studies revealed that dopamine interacted all over ß-synuclein and the binding of ß-synuclein-dopamine was weak in comparison with α-synuclein-dopamine binding (reported in literature using surface plasmon resonance). This suggested that ß-synuclein-dopamine binding might not be directly responsible for aggravated neurodegeneration. Taken all together, this study provides new perspectives on the neurodegeneration induced by ß-synuclein in the context of the neurotransmitter dopamine.

The results of my thesis demonstrate that probably it is not ß-synuclein-dopamine binding directly responsible for aggravated neurotoxicity of ß-synuclein. Digging further deep into dopamine metabolism, an unstable and a toxic intermediate, 3,4-dihydroxyphenylacetaldehyde (DOPAL), came into picture. DOPAL is produced by the oxidation of dopamine by monoamine oxygenase. It is known to bind to lysine residues on α-synuclein and promote its aggregation forming DOPAL-α-synuclein oligomers that can permeabilize synaptic vesicles (Plotegher et al. 2017). ß-synuclein contains 8 lysine residues (out of 11 possible binding sites) at the same position found in α-synuclein to which DOPAL is known to bind covalently. This suggests that DOPAL might also bind to ß-synuclein with almost same binding affinity. If this holds true, DOPAL-ß-synuclein binding, might play a role in aggravating the neurotoxic properties

of ß-synuclein. Investigating neurotoxicity of ß-synuclein in the context of DOPAL might open new frontiers to unravel the enigma of Parkinson´s disease.

Materials and Methods

6. Materials and Methods

6.1. Animal procedures

All experiments were performed with female Wistar rats (Janvier labs). All the procedures involving Wistar rats were performed according to the local regulation and the Directive 2010/63/EU of the European Parliament and of the Council on the protection of animals used for scientific purposes.

The female Wistar rats were housed in cages in groups of 5 with 12 hour/12 hour dark/light cycle, providing access to water and food *ad libitum*.

6.2. Primary neuronal culture

Primary cortical cell cultures were prepared from embryonic development day E17.5 from rat pups as described (Zahur et al. 2017). Primary midbrain cell cultures were prepared from embryonic development day E14.5 from rat pups as previously described (Weinert et al. 2015; Roser et al. 2018). The cortical plate or the ventral midbrain was isolated from the rat embryos. 0.25% Trypsin (Gibco;15090-046) was used to dissect the isolated tissue into single cells, and incubated at 37°C for 15 mins. The cells were either seeded in 24-well plate (on 12mm coverslips for immunocytochemistry) pre-coated with poly-L-ornithine (50µg/ml; Sigma; P-3655) and laminin (2µg/ml; Sigma; L2020), or cells were pre-treated with viral vectors for 30 mins. at 37°C incubator in Neurobasal medium (750µL/well; Invitrogen; 21103-049) with 1% Penicillin-Streptomycin-Neomycin (PSN; Gibco; 15640-055), L-Glutamine (0.5mM; Invitrogen; 25030-081), 0.5% transferrin (Applichem; A3124-0250), and 2% B27 serum (Invitrogen; 10889-038), until further analyzed. Cell density of 250,000 was plated for Western blots and cell density of 150,000 was plated for immunocytochemistry per

well. Transduction with viral vectors was performed at DIV 0 (Ascl1, Lmx1a, Nurr1, Pitx3) and immunocytochemistry was performed at DIV 7, 14, and 21. Pre-treatment of cells was performed with AAV vectors AADC and VMAT2. AAV vectors with transgene as α-synuclein, ß-synuclein γ-synuclein, GCaMP3.1, BcL-xL, EGFP, NmC were introduced into the cells at DIV 3.

6.3. Construction and propagation of viral vectors

Adeno-associated viral vectors (recombinant) were prepared by transient transfection of vector plasmids (**Fig.3.1, 3.9, 3.14, 3.17**) in HEK293 cells with DP6 helper plasmid. Heparin affinity chromatography and iodixanol gradient centrifugation were used to purify viral particles from cell lysates. These AAV viral vectors overexpressed the transgene under the control of human synapsin 1 promoter, as described (Kugler et al. 2003; Kugler et al. 2007). Dialysis against PBS was performed and 20µL were frozen in -80°C. Genome titer was quantified by qPCR and purity was determined by SDS-PAGE (>98%).

6.4. Immunocytochemistry

Immunocytochemistry was performed as previously described (Mahajani et al. 2017) with minor modifications as given: 0.1% Triton X-100 in PBS was used as a washing solution. Cells were blocked and membraned were permeabilized by 5% neonatal goat serum (Genetex; GTX73206). Coverslips were incubated with primary antibody at 4°C overnight (16hrs.) and with secondary antibody for 1 hr. After washing, cells were coated with DAPI for 2 mins. After that, washing and mounted on Mowiol medium (Sigma, 81381). Zeiss Axioplan2 microscope (automated) with Zeiss AxioCam ERc5s camera and 20x or 40x – Plan NEOFLUAR objective and Zeiss Axiovision software

was used to take fluorescent images ImageJ was used to quantify cell counts manually, and also automatically using an algorithm designed (Kristian Leite 2018).

6.5 Antibodies

Anti-Tyrosine hydroxylase (rabbit, AB152, 1:500)

Anti-DOPA decarboxylase (rabbit, ab3905, 1:500)

Anti-VMAT2 (goat, Everest, 1:500)

Anti-GAD65 (mouse, MAB351, 1:500)

Anti-DAT (rat, MAB369, 1:500)

Anti-CaMKIIß (rabbit, ab34703, 1:1000)

Anti-Nurr1 (mouse, ab41917, 1:500)

Anti-Ascl1 (rabbit, ab74065, 1:1000)

Secondary antibodies conjugated with cy2/cy3 (Dianova1:500)

4´, 6´ diamidino-2-phenylindole (DAPI, 2µg/ml, D3571)

For Western blot, anti-mouse-HRP (Dianova, 1:4000)

Anti-rabbit-HRP (Dianova, 1:3000)

Anti-ß-Tubulin (Sigma, T4026, 1:500)

6.6. Western Blot

Western blot was performed as described in a recent publication from our group (Tolo et al. 2018) with minor modifications as given. PVDF membranes were washed briefly

twice in 1x TBS-T and then again washed twice in 1x TBS-T after 5 mins incubation. Anti-Nurr1, anti-Lmx1a, anti-Pitx3, anti-Ascl1, and anti-AU1 tag antibody was used to detect desired protein. Chemoluminescent detectin was performed on BioRad ChemiDoc XRS+ Imager.

6.7. HPLC

HPLC analysis of dopamine, DOPAC, and HVA was performed as previously described (Tereshchenko et al. 2014) with minor modifications as given. Supernatant samples (400µL) were diluted in 1:1 ratio of sodium metabisulfite (NaMBS) and 2M perchloroacetic acid (PCA, 100µL) an incubated in ice for at least 10 mins. Cells were treated with 3% trichloroacetic acid (200µL), and incubated for 10 mins. at 37°C incubator. 180µL was added to 1:1 mixture of NaMBS and PCA. Processed samples were spun at 4° for 30 mins. and filteres through 0.2µm filter, and loaded onto HPLC.

6.8. NMR

ß-synuclein was purified as described (Taschenberger et al. 2013; Hoyer et al. 2002). The NMR spectra were collected and recorded on a Bruker 800MHz spectrometer at 10°C in 20mM sodium phosphate buffer (pH 6.0), 2mM TCEP, and 10% D_2O. Two-dimensional ^{1}H -^{15}N heteronuclear single quantum coherence (HSQC) spectrum was recorded to study the interaction of dopamine with α-synuclein and β-synuclein (Mori et al. 1995). 100µM of α-synuclein and β-synuclein were titrated against different concentrations of dopamine ranging from 0.02mM to 2mM. Chemical shift perturbations (CSP) were calculated using the formula $CSP = [(\delta H)^2 + (0.1\ \delta N)^2]^{1/2}$, where δN and δH are chemical shift differences (parts per million (ppm) of nitrogen and proton, respectively.

6.9. Statistical analysis

The data from experiments were analyzed for significant differences (statistically) between groups by 1-way ANOVA with Dunnet´s *posthoc* test. Statistical power between groups were computed by G*Power3.1 (Faul et al. 2009) with the settings as previously described (Tolo et al. 2018).

7. References

Achim, K., P. Peltopuro, L. Lahti, J. Li, M. Salminen, and J. Partanen. 2012. 'Distinct developmental origins and regulatory mechanisms for GABAergic neurons associated with dopaminergic nuclei in the ventral mesodiencephalic region', *Development*, 139: 2360-70.

Achim, K., M. Salminen, and J. Partanen. 2014. 'Mechanisms regulating GABAergic neuron development', *Cell Mol Life Sci*, 71: 1395-415.

Aksenova, M. V., M. Y. Aksenov, C. F. Mactutus, and R. M. Booze. 2005. 'Cell culture models of oxidative stress and injury in the central nervous system', *Curr Neurovasc Res*, 2: 73-89.

Alim, M. A., Q. L. Ma, K. Takeda, T. Aizawa, M. Matsubara, M. Nakamura, A. Asada, T. Saito, H. Kaji, M. Yoshii, S. Hisanaga, and K. Ueda. 2004. 'Demonstration of a role for alpha-synuclein as a functional microtubule-associated protein', *J Alzheimers Dis*, 6: 435-42; discussion 43-9.

Andersson, E., U. Tryggvason, Q. Deng, S. Friling, Z. Alekseenko, B. Robert, T. Perlmann, and J. Ericson. 2006. 'Identification of intrinsic determinants of midbrain dopamine neurons', *Cell*, 124: 393-405.

Ang, S. L., A. Wierda, D. Wong, K. A. Stevens, S. Cascio, J. Rossant, and K. S. Zaret. 1993. 'The formation and maintenance of the definitive endoderm lineage in the mouse: involvement of HNF3/forkhead proteins', *Development*, 119: 1301-15.

Arenas, E., M. Denham, and J. C. Villaescusa. 2015. 'How to make a midbrain dopaminergic neuron', *Development*, 142: 1918-36.

Arlotta, P., B. J. Molyneaux, D. Jabaudon, Y. Yoshida, and J. D. Macklis. 2008. 'Ctip2 controls the differentiation of medium spiny neurons and the establishment of the cellular architecture of the striatum', *J Neurosci*, 28: 622-32.

Azim, E., D. Jabaudon, R. M. Fame, and J. D. Macklis. 2009. 'SOX6 controls dorsal progenitor identity and interneuron diversity during neocortical development', *Nat Neurosci*, 12: 1238-47.

Barker, R. A., and C. H. Williams-Gray. 2016. 'Review: The spectrum of clinical features seen with alpha synuclein pathology', *Neuropathol Appl Neurobiol*, 42: 6-19.

Benoit-Marand, M. 2013. 'Dopamine neurons are multi-neurotransmitter neurons', *Mov Disord*, 28: 1211.

Bertoncini, C. W., R. M. Rasia, G. R. Lamberto, A. Binolfi, M. Zweckstetter, C. Griesinger, and C. O. Fernandez. 2007. 'Structural characterization of the intrinsically unfolded protein beta-synuclein, a natural negative regulator of alpha-synuclein aggregation', *J Mol Biol*, 372: 708-22.

Bertrand, N., D. S. Castro, and F. Guillemot. 2002. 'Proneural genes and the specification of neural cell types', *Nat Rev Neurosci*, 3: 517-30.

Biedler, J. L., L. Helson, and B. A. Spengler. 1973. 'Morphology and growth, tumorigenicity, and cytogenetics of human neuroblastoma cells in continuous culture', *Cancer Res*, 33: 2643-52.

Brown, J. W., A. K. Buell, T. C. Michaels, G. Meisl, J. Carozza, P. Flagmeier, M. Vendruscolo, T. P. Knowles, C. M. Dobson, and C. Galvagnion. 2016. 'beta-Synuclein suppresses both the initiation and amplification steps of alpha-synuclein aggregation via competitive binding to surfaces', *Sci Rep*, 6: 36010.

Burre, J., M. Sharma, T. Tsetsenis, V. Buchman, M. R. Etherton, and T. C. Sudhof. 2010. 'Alpha-synuclein promotes SNARE-complex assembly in vivo and in vitro', *Science*, 329: 1663-7.

Butt, S. J., M. Fuccillo, S. Nery, S. Noctor, A. Kriegstein, J. G. Corbin, and G. Fishell. 2005. 'The temporal and spatial origins of cortical interneurons predict their physiological subtype', *Neuron*, 48: 591-604.

Caiazzo, M., M. T. Dell'Anno, E. Dvoretskova, D. Lazarevic, S. Taverna, D. Leo, T. D. Sotnikova, A. Menegon, P. Roncaglia, G. Colciago, G. Russo, P. Carninci, G. Pezzoli, R. R. Gainetdinov, S. Gustincich, A. Dityatev, and V. Broccoli. 2011. 'Direct generation of functional dopaminergic neurons from mouse and human fibroblasts', *Nature*, 476: 224-7.

Campion, D., C. Martin, R. Heilig, F. Charbonnier, V. Moreau, J. M. Flaman, J. L. Petit, D. Hannequin, A. Brice, and T. Frebourg. 1995. 'The NACP/synuclein gene: chromosomal assignment and screening for alterations in Alzheimer disease', *Genomics*, 26: 254-7.

Cartier, E. A., L. A. Parra, T. B. Baust, M. Quiroz, G. Salazar, V. Faundez, L. Egana, and G. E. Torres. 2010. 'A biochemical and functional protein complex involving dopamine synthesis and transport into synaptic vesicles', *J Biol Chem*, 285: 1957-66.

Casarosa, S., C. Fode, and F. Guillemot. 1999. 'Mash1 regulates neurogenesis in the ventral telencephalon', *Development*, 126: 525-34.

Chambers, S. M., C. A. Fasano, E. P. Papapetrou, M. Tomishima, M. Sadelain, and L. Studer. 2009. 'Highly efficient neural conversion of human ES and iPS cells by dual inhibition of SMAD signaling', *Nat Biotechnol*, 27: 275-80.

Chandra, S., F. Fornai, H. B. Kwon, U. Yazdani, D. Atasoy, X. Liu, R. E. Hammer, G. Battaglia, D. C. German, P. E. Castillo, and T. C. Sudhof. 2004. 'Double-knockout mice for alpha- and beta-synucleins: effect on synaptic functions', *Proc Natl Acad Sci U S A*, 101: 14966-71.

Choi, B. K., M. G. Choi, J. Y. Kim, Y. Yang, Y. Lai, D. H. Kweon, N. K. Lee, and Y. K. Shin. 2013. 'Large alpha-synuclein oligomers inhibit neuronal SNARE-mediated vesicle docking', *Proc Natl Acad Sci U S A*, 110: 4087-92.

Choi, H. K., L. Won, J. D. Roback, B. H. Wainer, and A. Heller. 1992. 'Specific modulation of dopamine expression in neuronal hybrid cells by primary cells from different brain regions', *Proc Natl Acad Sci U S A*, 89: 8943-7.

Chung, S., A. Leung, B. S. Han, M. Y. Chang, J. I. Moon, C. H. Kim, S. Hong, J. Pruszak, O. Isacson, and K. S. Kim. 2009. 'Wnt1-lmx1a forms a novel autoregulatory loop and controls midbrain dopaminergic differentiation synergistically with the SHH-FoxA2 pathway', *Cell Stem Cell*, 5: 646-58.

Chutna, O., S. Goncalves, A. Villar-Pique, P. Guerreiro, Z. Marijanovic, T. Mendes, J. Ramalho, E. Emmanouilidou, S. Ventura, J. Klucken, D. C. Barral, F. Giorgini, K. Vekrellis, and T. F. Outeiro. 2014. 'The small GTPase Rab11 co-localizes with alpha-synuclein in intracellular inclusions and modulates its aggregation, secretion and toxicity', *Hum Mol Genet*, 23: 6732-45.

Colasante, G., P. Collombat, V. Raimondi, D. Bonanomi, C. Ferrai, M. Maira, K. Yoshikawa, A. Mansouri, F. Valtorta, J. L. Rubenstein, and V. Broccoli. 2008. 'Arx is a direct target of Dlx2 and thereby contributes to the tangential migration of GABAergic interneurons', *J Neurosci*, 28: 10674-86.

Conway, K. A., J. C. Rochet, R. M. Bieganski, and P. T. Lansbury, Jr. 2001. 'Kinetic stabilization of the alpha-synuclein protofibril by a dopamine-alpha-synuclein adduct', *Science*, 294: 1346-9.

Cubells, J. F., S. Rayport, G. Rajendran, and D. Sulzer. 1994. 'Methamphetamine neurotoxicity involves vacuolation of endocytic organelles and dopamine-dependent intracellular oxidative stress', *J Neurosci*, 14: 2260-71.

Danzer, K. M., D. Haasen, A. R. Karow, S. Moussaud, M. Habeck, A. Giese, H. Kretzschmar, B. Hengerer, and M. Kostka. 2007. 'Different species of alpha-synuclein oligomers induce calcium influx and seeding', *J Neurosci*, 27: 9220-32.

De la Rossa, A., C. Bellone, B. Golding, I. Vitali, J. Moss, N. Toni, C. Luscher, and D. Jabaudon. 2013. 'In vivo reprogramming of circuit connectivity in postmitotic neocortical neurons', *Nat Neurosci*, 16: 193-200.

Dichter, M. A. 1978. 'Rat cortical neurons in cell culture: culture methods, cell morphology, electrophysiology, and synapse formation', *Brain Res*, 149: 279-93.

———. 1980. 'Physiological identification of GABA as the inhibitory transmitter for mammalian cortical neurons in cell culture', *Brain Res*, 190: 111-21.

Dorsey, E. R., and B. R. Bloem. 2018. 'The Parkinson Pandemic-A Call to Action', *JAMA Neurol*, 75: 9-10.

Drew, Liam. 2016. 'Two hundred steps', *Nature*, 538: S2.

Faul, F., E. Erdfelder, A. Buchner, and A. G. Lang. 2009. 'Statistical power analyses using G*Power 3.1: tests for correlation and regression analyses', *Behav Res Methods*, 41: 1149-60.

Fujita, M., S. Sugama, K. Sekiyama, A. Sekigawa, T. Tsukui, M. Nakai, M. Waragai, T. Takenouchi, Y. Takamatsu, J. Wei, E. Rockenstein, A. R. Laspada, E. Masliah, S. Inoue, and M. Hashimoto. 2010. 'A beta-synuclein mutation linked to dementia produces neurodegeneration when expressed in mouse brain', *Nat Commun*, 1: 110.

Galvin, J. E., K. Uryu, V. M. Lee, and J. Q. Trojanowski. 1999. 'Axon pathology in Parkinson's disease and Lewy body dementia hippocampus contains alpha-, beta-, and gamma-synuclein', *Proc Natl Acad Sci U S A*, 96: 13450-5.

Gaven, F., P. Marin, and S. Claeysen. 2014. 'Primary culture of mouse dopaminergic neurons', *J Vis Exp*: e51751.

Giasson, B. I., J. E. Duda, S. M. Quinn, B. Zhang, J. Q. Trojanowski, and V. M. Lee. 2002. 'Neuronal alpha-synucleinopathy with severe movement disorder in mice expressing A53T human alpha-synuclein', *Neuron*, 34: 521-33.

Goedert, M., M. G. Spillantini, K. Del Tredici, and H. Braak. 2013. '100 years of Lewy pathology', *Nat Rev Neurol*, 9: 13-24.

Goldstein, D. S., P. Sullivan, C. Holmes, I. J. Kopin, M. J. Basile, and D. C. Mash. 2011. 'Catechols in post-mortem brain of patients with Parkinson disease', *Eur J Neurol*, 18: 703-10.

Graham, D. G. 1978. 'Oxidative pathways for catecholamines in the genesis of neuromelanin and cytotoxic quinones', *Mol Pharmacol*, 14: 633-43.

Granger, A. J., M. L. Wallace, and B. L. Sabatini. 2017. 'Multi-transmitter neurons in the mammalian central nervous system', *Curr Opin Neurobiol*, 45: 85-91.

Greene, L. A., and A. S. Tischler. 1976. 'Establishment of a noradrenergic clonal line of rat adrenal pheochromocytoma cells which respond to nerve growth factor', *Proc Natl Acad Sci U S A*, 73: 2424-8.

Hasegawa, T., M. Matsuzaki, A. Takeda, A. Kikuchi, H. Akita, G. Perry, M. A. Smith, and Y. Itoyama. 2004. 'Accelerated alpha-synuclein aggregation after differentiation of SH-SY5Y neuroblastoma cells', *Brain Res*, 1013: 51-9.

Hashimoto, M., K. Kawahara, P. Bar-On, E. Rockenstein, L. Crews, and E. Masliah. 2004. 'The Role of alpha-synuclein assembly and metabolism in the pathogenesis of Lewy body disease', *J Mol Neurosci*, 24: 343-52.

Hashimoto, M., E. Rockenstein, M. Mante, L. Crews, P. Bar-On, F. H. Gage, R. Marr, and E. Masliah. 2004. 'An antiaggregation gene therapy strategy for Lewy body disease utilizing beta-synuclein lentivirus in a transgenic model', *Gene Ther*, 11: 1713-23.

Hashimoto, M., E. Rockenstein, M. Mante, M. Mallory, and E. Masliah. 2001. 'beta-Synuclein inhibits alpha-synuclein aggregation: a possible role as an anti-parkinsonian factor', *Neuron*, 32: 213-23.

Hashimoto, M., T. Takenouchi, M. Mallory, E. Masliah, and A. Takeda. 2000. 'The role of NAC in amyloidogenesis in Alzheimer's disease', *Am J Pathol*, 156: 734-6.

Herrera, F. E., A. Chesi, K. E. Paleologou, A. Schmid, A. Munoz, M. Vendruscolo, S. Gustincich, H. A. Lashuel, and P. Carloni. 2008. 'Inhibition of alpha-synuclein fibrillization by dopamine is mediated by interactions with five C-terminal residues and with E83 in the NAC region', *PLoS One*, 3: e3394.

Herrero, M. T., M. J. Oset-Gasque, S. Canadas, S. Vicente, and M. P. Gonzalez. 1998. 'Effect of various depolarizing agents on endogenous amino acid neurotransmitter release in rat cortical neurons in culture', *Neurochem Int*, 32: 257-64.

Howe, M. W., and D. A. Dombeck. 2016. 'Rapid signalling in distinct dopaminergic axons during locomotion and reward', *Nature*, 535: 505-10.

Hoyer, W., T. Antony, D. Cherny, G. Heim, T. M. Jovin, and V. Subramaniam. 2002. 'Dependence of alpha-synuclein aggregate morphology on solution conditions', *J Mol Biol*, 322: 383-93.

Hsu, L. J., Y. Sagara, A. Arroyo, E. Rockenstein, A. Sisk, M. Mallory, J. Wong, T. Takenouchi, M. Hashimoto, and E. Masliah. 2000. 'alpha-synuclein promotes mitochondrial deficit and oxidative stress', *Am J Pathol*, 157: 401-10.

Hyman, A. H., and K. Simons. 2011. 'The new cell biology: Beyond HeLa cells', *Nature*, 480: 34.

Iacovitti, L., J. Lee, T. H. Joh, and D. J. Reis. 1987. 'Expression of tyrosine hydroxylase in neurons of cultured cerebral cortex: evidence for phenotypic plasticity in neurons of the CNS', *J Neurosci*, 7: 1264-70.

Iwafuchi-Doi, M., and K. S. Zaret. 2014. 'Pioneer transcription factors in cell reprogramming', *Genes Dev*, 28: 2679-92.

Jellinger, K. A. 2012. 'Neuropathology of sporadic Parkinson's disease: evaluation and changes of concepts', *Mov Disord*, 27: 8-30.

Jenner, P., and C. W. Olanow. 1996. 'Oxidative stress and the pathogenesis of Parkinson's disease', *Neurology*, 47: S161-70.

Jha, N. N., R. Kumar, R. Panigrahi, A. Navalkar, D. Ghosh, S. Sahay, M. Mondal, A. Kumar, and S. K. Maji. 2017. 'Comparison of alpha-Synuclein Fibril Inhibition by Four Different Amyloid Inhibitors', *ACS Chem Neurosci*, 8: 2722-33.

Joshi, K., S. Lee, B. Lee, J. W. Lee, and S. K. Lee. 2009. 'LMO4 controls the balance between excitatory and inhibitory spinal V2 interneurons', *Neuron*, 61: 839-51.

Kaenmaki, M., A. Tammimaki, J. A. Garcia-Horsman, T. Myohanen, N. Schendzielorz, M. Karayiorgou, J. A. Gogos, and P. T. Mannisto. 2009. 'Importance of membrane-bound catechol-O-methyltransferase in L-DOPA metabolism: a

pharmacokinetic study in two types of Comt gene modified mice', *Br J Pharmacol*, 158: 1884-94.

Kahle, P. J., M. Neumann, L. Ozmen, V. Muller, H. Jacobsen, A. Schindzielorz, M. Okochi, U. Leimer, H. van Der Putten, A. Probst, E. Kremmer, H. A. Kretzschmar, and C. Haass. 2000. 'Subcellular localization of wild-type and Parkinson's disease-associated mutant alpha -synuclein in human and transgenic mouse brain', *J Neurosci*, 20: 6365-73.

Kala, K., M. Haugas, K. Lillevali, J. Guimera, W. Wurst, M. Salminen, and J. Partanen. 2009. 'Gata2 is a tissue-specific post-mitotic selector gene for midbrain GABAergic neurons', *Development*, 136: 253-62.

Kawamoto, Y., I. Akiguchi, S. Nakamura, Y. Honjyo, H. Shibasaki, and H. Budka. 2002. '14-3-3 proteins in Lewy bodies in Parkinson disease and diffuse Lewy body disease brains', *J Neuropathol Exp Neurol*, 61: 245-53.

Kim, C., E. Rockenstein, B. Spencer, H. K. Kim, A. Adame, M. Trejo, K. Stafa, H. J. Lee, S. J. Lee, and E. Masliah. 2015. 'Antagonizing Neuronal Toll-like Receptor 2 Prevents Synucleinopathy by Activating Autophagy', *Cell Rep*, 13: 771-82.

Kriks, S., J. W. Shim, J. Piao, Y. M. Ganat, D. R. Wakeman, Z. Xie, L. Carrillo-Reid, G. Auyeung, C. Antonacci, A. Buch, L. Yang, M. F. Beal, D. J. Surmeier, J. H. Kordower, V. Tabar, and L. Studer. 2011. 'Dopamine neurons derived from human ES cells efficiently engraft in animal models of Parkinson's disease', *Nature*, 480: 547-51.

Kruger, R., W. Kuhn, T. Muller, D. Woitalla, M. Graeber, S. Kosel, H. Przuntek, J. T. Epplen, L. Schols, and O. Riess. 1998. 'Ala30Pro mutation in the gene encoding alpha-synuclein in Parkinson's disease', *Nat Genet*, 18: 106-8.

Kugler, S., R. Hahnewald, M. Garrido, and J. Reiss. 2007. 'Long-term rescue of a lethal inherited disease by adeno-associated virus-mediated gene transfer in a mouse model of molybdenum-cofactor deficiency', *Am J Hum Genet*, 80: 291-7.

Kugler, S., P. Lingor, U. Scholl, S. Zolotukhin, and M. Bahr. 2003. 'Differential transgene expression in brain cells in vivo and in vitro from AAV-2 vectors with small transcriptional control units', *Virology*, 311: 89-95.

Lashuel, H. A., C. R. Overk, A. Oueslati, and E. Masliah. 2013. 'The many faces of alpha-synuclein: from structure and toxicity to therapeutic target', *Nat Rev Neurosci*, 14: 38-48.

Lavedan, C., E. Leroy, A. Dehejia, S. Buchholtz, A. Dutra, R. L. Nussbaum, and M. H. Polymeropoulos. 1998. 'Identification, localization and characterization of the human gamma-synuclein gene', *Hum Genet*, 103: 106-12.

Lee, E. S., H. Chen, J. King, and C. Charlton. 2008. 'The role of 3-O-methyldopa in the side effects of L-dopa', *Neurochem Res*, 33: 401-11.

Lee, S. J., H. Jeon, and K. V. Kandror. 2008. 'Alpha-synuclein is localized in a subpopulation of rat brain synaptic vesicles', *Acta Neurobiol Exp (Wars)*, 68: 509-15.

Leitao, A., A. Bhumkar, D. J. B. Hunter, Y. Gambin, and E. Sierecki. 2018. 'Unveiling a Selective Mechanism for the Inhibition of alpha-Synuclein Aggregation by beta-Synuclein', *Int J Mol Sci*, 19.

Liesi, P., A. Paetau, L. Rechardt, and D. Dahl. 1981. 'Glial uptake of monoamines in primary cultures of rat median raphe nucleus and cerebellum. A combined monoamine fluorescence and glial fibrillary acidic protein immunofluorescence study', *Histochemistry*, 73: 239-50.

Lin, W., E. Metzakopian, Y. E. Mavromatakis, N. Gao, N. Balaskas, H. Sasaki, J. Briscoe, J. A. Whitsett, M. Goulding, K. H. Kaestner, and S. L. Ang. 2009. 'Foxa1 and Foxa2 function both upstream of and cooperatively with Lmx1a and Lmx1b in a feedforward loop promoting mesodiencephalic dopaminergic neuron development', *Dev Biol*, 333: 386-96.

Long, J. E., I. Cobos, G. B. Potter, and J. L. Rubenstein. 2009. 'Dlx1&2 and Mash1 transcription factors control MGE and CGE patterning and differentiation through parallel and overlapping pathways', *Cereb Cortex*, 19 Suppl 1: i96-106.

Lotharius, J., J. Falsig, J. van Beek, S. Payne, R. Dringen, P. Brundin, and M. Leist. 2005. 'Progressive degeneration of human mesencephalic neuron-derived cells triggered by dopamine-dependent oxidative stress is dependent on the mixed-lineage kinase pathway', *J Neurosci*, 25: 6329-42.

Mahajani, S., C. Giacomini, F. Marinaro, D. De Pietri Tonelli, A. Contestabile, and L. Gasparini. 2017. 'Lamin B1 levels modulate differentiation into neurons during embryonic corticogenesis', *Sci Rep*, 7: 4897.

Martinez-Vicente, M., Z. Talloczy, S. Kaushik, A. C. Massey, J. Mazzulli, E. V. Mosharov, R. Hodara, R. Fredenburg, D. C. Wu, A. Follenzi, W. Dauer, S. Przedborski, H. Ischiropoulos, P. T. Lansbury, D. Sulzer, and A. M. Cuervo. 2008. 'Dopamine-modified alpha-synuclein blocks chaperone-mediated autophagy', *J Clin Invest*, 118: 777-88.

Marton, R. M., and J. P. A. Ioannidis. 2018. 'A Comprehensive Analysis of Protocols for Deriving Dopaminergic Neurons from Human Pluripotent Stem Cells', *Stem Cells Transl Med*.

Mazzulli, J. R., M. Armakola, M. Dumoulin, I. Parastatidis, and H. Ischiropoulos. 2007. 'Cellular oligomerization of alpha-synuclein is determined by the interaction of oxidized catechols with a C-terminal sequence', *J Biol Chem*, 282: 31621-30.

Mazzulli, J. R., A. J. Mishizen, B. I. Giasson, D. R. Lynch, S. A. Thomas, A. Nakashima, T. Nagatsu, A. Ota, and H. Ischiropoulos. 2006. 'Cytosolic catechols inhibit alpha-synuclein aggregation and facilitate the formation of intracellular soluble oligomeric intermediates', *J Neurosci*, 26: 10068-78.

Mohan, A., A. J. Roberto, A. Mohan, A. Lorenzo, K. Jones, M. J. Carney, L. Liogier-Weyback, S. Hwang, and K. A. Lapidus. 2016. 'The Significance of the Default Mode Network (DMN) in Neurological and Neuropsychiatric Disorders: A Review', *Yale J Biol Med*, 89: 49-57.

Mor, D. E., E. Tsika, J. R. Mazzulli, N. S. Gould, H. Kim, M. J. Daniels, S. Doshi, P. Gupta, J. L. Grossman, V. X. Tan, R. G. Kalb, K. A. Caldwell, G. A. Caldwell, J. H. Wolfe, and H. Ischiropoulos. 2017. 'Dopamine induces soluble alpha-synuclein oligomers and nigrostriatal degeneration', *Nat Neurosci*, 20: 1560-68.

Mori, F., K. Tanji, M. Yoshimoto, H. Takahashi, and K. Wakabayashi. 2002. 'Immunohistochemical comparison of alpha- and beta-synuclein in adult rat central nervous system', *Brain Res*, 941: 118-26.

Mori, S., C. Abeygunawardana, M. O. Johnson, and P. C. van Zijl. 1995. 'Improved sensitivity of HSQC spectra of exchanging protons at short interscan delays using a new fast HSQC (FHSQC) detection scheme that avoids water saturation', *J Magn Reson B*, 108: 94-8.

Moriarty, G. M., M. P. Olson, T. B. Atieh, M. K. Janowska, S. D. Khare, and J. Baum. 2017. 'A pH-dependent switch promotes beta-synuclein fibril formation via glutamate residues', *J Biol Chem*, 292: 16368-79.

Mosharov, E. V., K. E. Larsen, E. Kanter, K. A. Phillips, K. Wilson, Y. Schmitz, D. E. Krantz, K. Kobayashi, R. H. Edwards, and D. Sulzer. 2009. 'Interplay between cytosolic dopamine, calcium, and alpha-synuclein causes selective death of substantia nigra neurons', *Neuron*, 62: 218-29.

Ninkina, N., O. Peters, S. Millership, H. Salem, H. van der Putten, and V. L. Buchman. 2009. 'Gamma-synucleinopathy: neurodegeneration associated with overexpression of the mouse protein', *Hum Mol Genet*, 18: 1779-94.

Niu, W., T. Zang, L. L. Wang, Y. Zou, and C. L. Zhang. 2018. 'Phenotypic Reprogramming of Striatal Neurons into Dopaminergic Neuron-like Cells in the Adult Mouse Brain', *Stem Cell Reports*, 11: 1156-70.

Norris, E. H., B. I. Giasson, R. Hodara, S. Xu, J. Q. Trojanowski, H. Ischiropoulos, and V. M. Lee. 2005. 'Reversible inhibition of alpha-synuclein fibrillization by dopaminochrome-mediated conformational alterations', *J Biol Chem*, 280: 21212-9.

Ohtake, H., P. Limprasert, Y. Fan, O. Onodera, A. Kakita, H. Takahashi, L. T. Bonner, D. W. Tsuang, I. V. Murray, V. M. Lee, J. Q. Trojanowski, A. Ishikawa, J. Idezuka, M. Murata, T. Toda, T. D. Bird, J. B. Leverenz, S. Tsuji, and A. R. La Spada. 2004. 'Beta-synuclein gene alterations in dementia with Lewy bodies', *Neurology*, 63: 805-11.

Ono, Y., T. Nakatani, Y. Sakamoto, E. Mizuhara, Y. Minaki, M. Kumai, A. Hamaguchi, M. Nishimura, Y. Inoue, H. Hayashi, J. Takahashi, and T. Imai. 2007. 'Differences in neurogenic potential in floor plate cells along an anteroposterior location: midbrain dopaminergic neurons originate from mesencephalic floor plate cells', *Development*, 134: 3213-25.

Opitz, T., A. D. De Lima, and T. Voigt. 2002. 'Spontaneous development of synchronous oscillatory activity during maturation of cortical networks in vitro', *J Neurophysiol*, 88: 2196-206.

Park, J. Y., and P. T. Lansbury, Jr. 2003. 'Beta-synuclein inhibits formation of alpha-synuclein protofibrils: a possible therapeutic strategy against Parkinson's disease', *Biochemistry*, 42: 3696-700.

Payton, J. E., R. J. Perrin, W. S. Woods, and J. M. George. 2004. 'Structural determinants of PLD2 inhibition by alpha-synuclein', *J Mol Biol*, 337: 1001-9.

Pleasure, S. J., S. Anderson, R. Hevner, A. Bagri, O. Marin, D. H. Lowenstein, and J. L. Rubenstein. 2000. 'Cell migration from the ganglionic eminences is required for the development of hippocampal GABAergic interneurons', *Neuron*, 28: 727-40.

Plotegher, N., G. Berti, E. Ferrari, I. Tessari, M. Zanetti, L. Lunelli, E. Greggio, M. Bisaglia, M. Veronesi, S. Girotto, M. Dalla Serra, C. Perego, L. Casella, and L. Bubacco. 2017. 'DOPAL derived alpha-synuclein oligomers impair synaptic vesicles physiological function', *Sci Rep*, 7: 40699.

Polymeropoulos, M. H., C. Lavedan, E. Leroy, S. E. Ide, A. Dehejia, A. Dutra, B. Pike, H. Root, J. Rubenstein, R. Boyer, E. S. Stenroos, S. Chandrasekharappa, A. Athanassiadou, T. Papapetropoulos, W. G. Johnson, A. M. Lazzarini, R. C.

Duvoisin, G. Di Iorio, L. I. Golbe, and R. L. Nussbaum. 1997. 'Mutation in the alpha-synuclein gene identified in families with Parkinson's disease', *Science*, 276: 2045-7.

Prasad, K. N., E. Carvalho, S. Kentroti, J. Edwards-Prasad, C. Freed, and A. Vernadakis. 1994. 'Establishment and characterization of immortalized clonal cell lines from fetal rat mesencephalic tissue', *In Vitro Cell Dev Biol Anim*, 30a: 596-603.

Ramakers, G. J., M. A. Corner, and A. M. Habets. 1990. 'Development in the absence of spontaneous bioelectric activity results in increased stereotyped burst firing in cultures of dissociated cerebral cortex', *Exp Brain Res*, 79: 157-66.

Ribeiro, D., R. Laguna Goya, G. Ravindran, R. Vuono, C. L. Parish, C. Foldi, T. Piroth, S. Yang, M. Parmar, G. Nikkhah, J. Hjerling-Leffler, O. Lindvall, R. A. Barker, and E. Arenas. 2013. 'Efficient expansion and dopaminergic differentiation of human fetal ventral midbrain neural stem cells by midbrain morphogens', *Neurobiol Dis*, 49: 118-27.

Rick, C. E., A. Ebert, T. Virag, M. C. Bohn, and D. J. Surmeier. 2006. 'Differentiated dopaminergic MN9D cells only partially recapitulate the electrophysiological properties of midbrain dopaminergic neurons', *Dev Neurosci*, 28: 528-37.

Roberti, M. J., T. M. Jovin, and E. Jares-Erijman. 2011. 'Confocal fluorescence anisotropy and FRAP imaging of alpha-synuclein amyloid aggregates in living cells', *PLoS One*, 6: e23338.

Roser, A. E., L. Caldi Gomes, R. Halder, G. Jain, F. Maass, L. Tonges, L. Tatenhorst, M. Bahr, A. Fischer, and P. Lingor. 2018. 'miR-182-5p and miR-183-5p Act as GDNF Mimics in Dopaminergic Midbrain Neurons', *Mol Ther Nucleic Acids*, 11: 9-22.

Salemi, S., P. Baktash, B. Rajaei, M. Noori, H. Amini, M. Shamsara, and M. Massumi. 2016. 'Efficient generation of dopaminergic-like neurons by overexpression of Nurr1 and Pitx3 in mouse induced Pluripotent Stem Cells', *Neurosci Lett*, 626: 126-34.

Sampaio-Maia, B., M. P. Serrao, and P. Soares-da-Silva. 2001. 'Regulatory pathways and uptake of L-DOPA by capillary cerebral endothelial cells, astrocytes, and neuronal cells', *Am J Physiol Cell Physiol*, 280: C333-42.

Scholz, D., D. Poltl, A. Genewsky, M. Weng, T. Waldmann, S. Schildknecht, and M. Leist. 2011. 'Rapid, complete and large-scale generation of post-mitotic neurons from the human LUHMES cell line', *J Neurochem*, 119: 957-71.

Scott, D. A., I. Tabarean, Y. Tang, A. Cartier, E. Masliah, and S. Roy. 2010. 'A pathologic cascade leading to synaptic dysfunction in alpha-synuclein-induced neurodegeneration', *J Neurosci*, 30: 8083-95.

Sonders, M. S., S. J. Zhu, N. R. Zahniser, M. P. Kavanaugh, and S. G. Amara. 1997. 'Multiple ionic conductances of the human dopamine transporter: the actions of dopamine and psychostimulants', *J Neurosci*, 17: 960-74.

Spillantini, M. G., A. Divane, and M. Goedert. 1995. 'Assignment of human alpha-synuclein (SNCA) and beta-synuclein (SNCB) genes to chromosomes 4q21 and 5q35', *Genomics*, 27: 379-81.

Spillantini, M. G., M. L. Schmidt, V. M. Lee, J. Q. Trojanowski, R. Jakes, and M. Goedert. 1997. 'Alpha-synuclein in Lewy bodies', *Nature*, 388: 839-40.

Stichel, C. C., and H. W. Muller. 1991. 'Dissociated cell culture of rat cerebral cortical neurons in serum-free, conditioned media: GABA-immunopositive neurons', *Brain Res Dev Brain Res*, 64: 145-54.

Stuhmer, T., L. Puelles, M. Ekker, and J. L. Rubenstein. 2002. 'Expression from a Dlx gene enhancer marks adult mouse cortical GABAergic neurons', *Cereb Cortex*, 12: 75-85.

Sulzer, D. 2001. 'alpha-synuclein and cytosolic dopamine: stabilizing a bad situation', *Nat Med*, 7: 1280-2.

Sulzer, D., and L. Zecca. 2000. 'Intraneuronal dopamine-quinone synthesis: a review', *Neurotox Res*, 1: 181-95.

Sun, J. J., W. Kilb, and H. J. Luhmann. 2010. 'Self-organization of repetitive spike patterns in developing neuronal networks in vitro', *Eur J Neurosci*, 32: 1289-99.

Surguchov, A. 2013. 'Synucleins: are they two-edged swords?', *J Neurosci Res*, 91: 161-6.

Swahn, C. G., and F. A. Wiesel. 1976. 'Determination of conjugated monoamine metabolites in brain tissue', *J Neural Transm*, 39: 281-90.

Takahashi, K., and S. Yamanaka. 2006. 'Induction of pluripotent stem cells from mouse embryonic and adult fibroblast cultures by defined factors', *Cell*, 126: 663-76.

Taschenberger, G., J. Toloe, J. Tereshchenko, J. Akerboom, P. Wales, R. Benz, S. Becker, T. F. Outeiro, L. L. Looger, M. Bahr, M. Zweckstetter, and S. Kugler. 2013. 'beta-synuclein aggregates and induces neurodegeneration in dopaminergic neurons', *Ann Neurol*, 74: 109-18.

Tereshchenko, J., A. Maddalena, M. Bahr, and S. Kugler. 2014. 'Pharmacologically controlled, discontinuous GDNF gene therapy restores motor function in a rat model of Parkinson's disease', *Neurobiol Dis*, 65: 35-42.

Tessitore, A., F. Esposito, C. Vitale, G. Santangelo, M. Amboni, A. Russo, D. Corbo, G. Cirillo, P. Barone, and G. Tedeschi. 2012. 'Default-mode network connectivity in cognitively unimpaired patients with Parkinson disease', *Neurology*, 79: 2226-32.

Theka, I., M. Caiazzo, E. Dvoretskova, D. Leo, F. Ungaro, S. Curreli, F. Manago, M. T. Dell'Anno, G. Pezzoli, R. R. Gainetdinov, A. Dityatev, and V. Broccoli. 2013. 'Rapid generation of functional dopaminergic neurons from human induced pluripotent stem cells through a single-step procedure using cell lineage transcription factors', *Stem Cells Transl Med*, 2: 473-9.

Tolo, J., G. Taschenberger, K. Leite, M. A. Stahlberg, G. Spehlbrink, J. Kues, F. Munari, S. Capaldi, S. Becker, M. Zweckstetter, C. Dean, M. Bahr, and S. Kugler. 2018. 'Pathophysiological Consequences of Neuronal alpha-Synuclein Overexpression: Impacts on Ion Homeostasis, Stress Signaling, Mitochondrial Integrity, and Electrical Activity', *Front Mol Neurosci*, 11: 49.

Tonges, L., E. M. Szego, P. Hause, K. A. Saal, L. Tatenhorst, J. C. Koch, D. Hedouville Z, V. Dambeck, S. Kugler, C. P. Dohm, M. Bahr, and P. Lingor. 2014. 'Alpha-synuclein mutations impair axonal regeneration in models of Parkinson's disease', *Front Aging Neurosci*, 6: 239.

Tritsch, N. X., J. B. Ding, and B. L. Sabatini. 2012. 'Dopaminergic neurons inhibit striatal output through non-canonical release of GABA', *Nature*, 490: 262-6.

Ueda, K., H. Fukushima, E. Masliah, Y. Xia, A. Iwai, M. Yoshimoto, D. A. Otero, J. Kondo, Y. Ihara, and T. Saitoh. 1993. 'Molecular cloning of cDNA encoding an unrecognized component of amyloid in Alzheimer disease', *Proc Natl Acad Sci U S A*, 90: 11282-6.

Ulmer, T. S., A. Bax, N. B. Cole, and R. L. Nussbaum. 2005. 'Structure and dynamics of micelle-bound human alpha-synuclein', *J Biol Chem*, 280: 9595-603.

Uryu, K., C. Richter-Landsberg, W. Welch, E. Sun, O. Goldbaum, E. H. Norris, C. T. Pham, I. Yazawa, K. Hilburger, M. Micsenyi, B. I. Giasson, N. M. Bonini, V. M. Lee, and J. Q. Trojanowski. 2006. 'Convergence of heat shock protein 90 with

ubiquitin in filamentous alpha-synuclein inclusions of alpha-synucleinopathies', *Am J Pathol*, 168: 947-61.

Uversky, V. N. 2008. 'Amyloidogenesis of natively unfolded proteins', *Curr Alzheimer Res*, 5: 260-87.

Veenvliet, J. V., M. T. Dos Santos, W. M. Kouwenhoven, L. von Oerthel, J. L. Lim, A. J. van der Linden, M. J. Koerkamp, F. C. Holstege, and M. P. Smidt. 2013. 'Specification of dopaminergic subsets involves interplay of En1 and Pitx3', *Development*, 140: 3373-84.

Vierbuchen, T., A. Ostermeier, Z. P. Pang, Y. Kokubu, T. C. Sudhof, and M. Wernig. 2010. 'Direct conversion of fibroblasts to functional neurons by defined factors', *Nature*, 463: 1035-41.

Volpicelli, F., R. De Gregorio, S. Pulcrano, C. Perrone-Capano, U. di Porzio, and G. C. Bellenchi. 2012. 'Direct regulation of Pitx3 expression by Nurr1 in culture and in developing mouse midbrain', *PLoS One*, 7: e30661.

Wakabayashi, K., S. Engelender, M. Yoshimoto, S. Tsuji, C. A. Ross, and H. Takahashi. 2000. 'Synphilin-1 is present in Lewy bodies in Parkinson's disease', *Ann Neurol*, 47: 521-3.

Wang, Y., C. A. Dye, V. Sohal, J. E. Long, R. C. Estrada, T. Roztocil, T. Lufkin, K. Deisseroth, S. C. Baraban, and J. L. Rubenstein. 2010. 'Dlx5 and Dlx6 regulate the development of parvalbumin-expressing cortical interneurons', *J Neurosci*, 30: 5334-45.

Wapinski, O. L., T. Vierbuchen, K. Qu, Q. Y. Lee, S. Chanda, D. R. Fuentes, P. G. Giresi, Y. H. Ng, S. Marro, N. F. Neff, D. Drechsel, B. Martynoga, D. S. Castro, A. E. Webb, T. C. Sudhof, A. Brunet, F. Guillemot, H. Y. Chang, and M. Wernig. 2013. 'Hierarchical mechanisms for direct reprogramming of fibroblasts to neurons', *Cell*, 155: 621-35.

Weinert, M., T. Selvakumar, T. S. Tierney, and K. N. Alavian. 2015. 'Isolation, culture and long-term maintenance of primary mesencephalic dopaminergic neurons from embryonic rodent brains', *J Vis Exp*.

Williams, J. K., X. Yang, and J. Baum. 2018. 'Interactions between the Intrinsically Disordered Proteins beta-Synuclein and alpha-Synuclein', *Proteomics*: e1800109.

Wonders, C. P., and S. A. Anderson. 2006. 'The origin and specification of cortical interneurons', *Nat Rev Neurosci*, 7: 687-96.

Xie, H. R., L. S. Hu, and G. Y. Li. 2010. 'SH-SY5Y human neuroblastoma cell line: in vitro cell model of dopaminergic neurons in Parkinson's disease', *Chin Med J (Engl)*, 123: 1086-92.

Xu, Q., L. Guo, H. Moore, R. R. Waclaw, K. Campbell, and S. A. Anderson. 2010. 'Sonic hedgehog signaling confers ventral telencephalic progenitors with distinct cortical interneuron fates', *Neuron*, 65: 328-40.

Yan, C. H., M. Levesque, S. Claxton, R. L. Johnson, and S. L. Ang. 2011. 'Lmx1a and lmx1b function cooperatively to regulate proliferation, specification, and differentiation of midbrain dopaminergic progenitors', *J Neurosci*, 31: 12413-25.

Yan, J., L. Studer, and R. D. McKay. 2001. 'Ascorbic acid increases the yield of dopaminergic neurons derived from basic fibroblast growth factor expanded mesencephalic precursors', *J Neurochem*, 76: 307-11.

Zahur, M., J. Tolo, M. Bahr, and S. Kugler. 2017. 'Long-Term Assessment of AAV-Mediated Zinc Finger Nuclease Expression in the Mouse Brain', *Front Mol Neurosci*, 10: 142.

Zarranz, J. J., J. Alegre, J. C. Gomez-Esteban, E. Lezcano, R. Ros, I. Ampuero, L. Vidal, J. Hoenicka, O. Rodriguez, B. Atares, V. Llorens, E. Gomez Tortosa, T. del Ser, D. G. Munoz, and J. G. de Yebenes. 2004. 'The new mutation, E46K, of alpha-synuclein causes Parkinson and Lewy body dementia', *Ann Neurol*, 55: 164-73.

Zhang, L., C. Zhang, Y. Zhu, Q. Cai, P. Chan, K. Ueda, S. Yu, and H. Yang. 2008. 'Semi-quantitative analysis of alpha-synuclein in subcellular pools of rat brain neurons: an immunogold electron microscopic study using a C-terminal specific monoclonal antibody', *Brain Res*, 1244: 40-52.

Zhao, Y., P. Flandin, J. E. Long, M. D. Cuesta, H. Westphal, and J. L. Rubenstein. 2008. 'Distinct molecular pathways for development of telencephalic interneuron subtypes revealed through analysis of Lhx6 mutants', *J Comp Neurol*, 510: 79-99.

8. Abbreviations

ANL – Ascl1, Nurr1, and Lmx1a

Ascl1 - Achaete-scute homolog 1

Lmx1a - LIM homeobox transcription factor 1, alpha

Nurr1 - Nuclear Receptor Related 1

Pitx3: Pituitary homeobox 3

cDNs – cortical dopaminergic neuron-like cells

cGNs – cortical GABAergic neurons

mGNs – midbrain GABAergic neurons

TH – Tyrosine hydroxylase

AADC - L-amino acid decarboxylase

L-DOPA - L-3,4-dihydroxyphenylalanine

VMAT2 - vesicular monoamine transferase 2

DAT - dopamine transporter

AAV – Adeno-associated viral vectors

NTD – N-terminal domain

CTD – C-terminal domain

DIV - days *in vitro*

ICC – immunocytochemistry

UT – untreated

AD-VM – AADC+VMAT2

DT-VM – DAT+VMAT2

DOPAC – 3,4-dihydroxyphenylacetic acid

HVA – homovanillic acid

HPLC – high-performance liquid chromatography

MAO-A - monoamine oxygenase-A

COMT - catechol-O-methyltransferase

hSyn1 – human synapsin 1

WPRE - woodchuck hepatitis virus post-transcriptional control element

bGH-pA - bovine growth hormone poly-adenylation site

Int-a - intron

ITR - inverted terminal repeat

ngs – nanograms

PD – Parkinson´s disease

Tol - Tolcapone

Tcp – Tranylcypromine

EGFP - enhanced green fluorescent protein

NmC – nuclear mCherry

SD – standard deviation

vg – viral genomes

INB – dopamine-degrading enzyme inhibitors

α-synuclein – alpha-synuclein

ß-synuclein – beta –synuclein

γ-synuclein – gamma-synuclein

NLS – nuclear localization sequence

M13 - a peptide sequence from myosin light-chain kinsae

ITR inverted terminal repeat

HSQC - heteronuclear single quantum coherence

CSP - Chemical shift perturbations

Ppm – parts per million

K_d - Dissociation constant

PDB – protein Data Bank

NMR – Nuclear Magnetic Resonance

E18 - embryonic day of development 18

iPSCs – induced pluripotent stem cells

MGE - medial ganglionic eminence

CGE - caudal ganglionic eminence

LUHMES - Lund Human Mesencephalic cells

PC12 - pheochromocytoma cell-line

GABA – γ-aminobutyricacid

DOPAL - 3,4-dihydroxyphenylacetaldehyde

Dopamine – DA

HRP – Horseradish peroxidase

PVDF - Polyvinylidene fluoride

ANOVA – Analysis of variance

9. Acknowledgements

It has already given me immense pleasure that I finally reached this page of my thesis. What a journey!

First of all, I want to thank Dr. Sebastian Kügler for mentoring me throughout my PhD. I want to thank him for having patience to deal with me (people usually need it ☺). He has taught me to do Science. To be honest, when I started my PhD, I was far away from being independent in terms of planning work. After failing many times, actually, many many many times, I have learned doing good Science. I also want to acknowledge his efforts to help me improve my presentation skills. These skills will always stick to me for the rest of my life. Thank you, Sebastian!

Next, I want to thank my colleagues for being a nice company. I want to especially thank Dr. Sameehan Mahajani, for always motivating me and being around whenever I needed help. He has been supportive all throughout my PhD, staring from learning new techniques, to eating pizza after every Friday seminar until making/offering delicious food when I used to skip food sometimes. Thank you, Sam! I also want to thank Maryna, Shi, Pauline, Sofia, Dodo, Sonja, Barbara, Uwe, Monika for having fun at work. Thank you!

Next, I want to thank my friends, Parth Joshi, Salim Ansari, Aman Arora for being such a wonderful people. I will remember our King-size lunch after badminton and football, and new year tour to Croatia! Thank you for being such good friends!

I want to thank my Dad who supported me throughout my different career moves. He is rather surprised how I managed to achieve what I achieved until now. This already

says that he got more than he expected ☺. I also want to thank DAAD for being my DAD in Germany.

Getting married to Sneha Bhat during my PhD was another achievement in its own ☺ However, the distances have kept us away, she is the one, who supported me through ups and downs in life. She gives her best to condition my brain, so that I can focus more on work, and work, and work, and work. Life would have been difficult without her support.

Achieving a PhD is an achievement for our mentors, and near and dear ones. I will give my best in whatever I will do in future, and I will always cherish the memories of Waldweg 33, of Göttingen weekend parties, and Waldweg October fest!

Thank you for making me, what I have become!

Cheers!

Anupam ☺